COUPLED BIOGEOCHEMICAL CYCLING OF MERCURY AND IRON: IMPLICATIONS FOR MERCURY REMOVAL FROM AQUEOUS EFFLUENTS AND BIOTRANSFORMATION IN SEDIMENTARY ENVIRONMENTS

By

JULIANNE D. VERNON

A DISSERTATION PRESENTED TO THE GRADUATE SCHOOL
OF THE UNIVERSITY OF FLORIDA IN PARTIAL FULFILLMENT
OF THE REQUIREMENTS FOR THE DEGREE OF
DOCTOR OF PHILOSOPHY

UNIVERSITY OF FLORIDA

2010

© 2010 Julianne Vernon

To my loving husband

ACKNOWLEDGMENTS

I thank my advisor, Dr. Jean-Claude J. Bonzongo, for his guidance, support, and humor that has helped me through my journey at the University of Florida. I thank my committee members, Dr. Angela S. Linder, Dr. Joseph J.Delfino, and Dr. Roy Rhue, for their valuable expertise, advice, and support. My special thanks go to NSF Graduate Assistance in Areas of National Needs, HDR Engineering Inc., Progress Energy Foundation and the UF Graduate Minority Office for supporting me in my research. I thank all members of my research group for their help and support. Finally, special thanks go to my family and friends. I greatly appreciate their love, support, and encouragement. Lastly, I thank my husband for his encouragement, patience, and support.

TABLE OF CONTENTS

page

LIST OF TABLES

LIST OF FIGURES

LIST OF ABBREVIATIONS

AC	Activated carbon
As	Arsenic
BET	Braunauer Emmett Teller
CMC	Carboxyl methyl cellulose
Cr	Chromium
DI	Deionized water
DOC	Dissolved organic carbon
Hg	Mercury
HgS	Mercury sulfide
IRB	Iron reducing bacteria
MeHg	Methyl mercury
NM	Nano materials
nZVI	Nano zero valent iron
OM	Organic matter
PRB	Permeable reactive barriers
SR1	Suwannee River 1
SR2	Suwannee River 2
SR3	Suwannee River 3
SRB	Sulfate reducing bacteria
SSA	Specific surface area
THg	Total mercury
US EPA	Unites States Environmental Protection Agency
WW	Wastewater effluent
VOC	Volatile Organic Carbon

ZVI	Zero Valent Iron

Abstract of Dissertation Presented to the Graduate School
of the University of Florida in Partial Fulfillment of the
Requirements for the Degree of Doctor of Philosophy

COUPLED BIOGEOCHEMICAL CYCLING OF MERCURY AND IRON: IMPLICATIONS FOR MERCURY REMOVAL FROM AQUEOUS EFFLUENTS AND BIOTRANSFORMATION IN SEDIMENTARY ENVIRONMENTS

By

Julianne Vernon

December 2010

Chair: Jean Claude J. Bonzongo
Major: Environmental Engineering

The toxic effects of mercury (Hg) on the environment and human health have led the US regulatory agencies to set stringent guidelines for Hg levels in gaseous and aqueous waste effluents. With regard to Hg contaminated waters, which is the focus of this proposed research, Hg levels in the concentration range of 12-15 ng/L, parts per trillion (ppt) are targeted for wastewater effluents. Several treatment methods for Hg remediation of contaminated waters and sediments/soils exist. Unfortunately, the above-mentioned low ppt levels set forth by federal and state agencies remain out of reach by any of the treatment technologies that are currently available. In addition to these remediation issues, the conversion of inorganic Hg into methyl mercury (MeHg) compounds, primarily in anoxic aquatic compartments has led to concerns over the cycling of Hg in the environment due to the toxicity of MeHg as it readily accumulates in living tissues and biomagnifies in food chains.

In this study, interactions between metallic iron and dissolved aqueous Hg were investigated with the ultimate goal to evaluate the potential for use of zero-valent iron

(ZVI) in the treatment of Hg-contaminated effluents on one hand, and for controlling MeHg formation in sediments on the other.

First, the increase in surface area and the decrease in kinetic reaction time favored by nanosize particles could allow the removal of Hg from aqueous effluents through the combination of (i) ionic Hg (Hg^{2+}) reduction to elemental Hg and volatilization, and (ii) Hg adsorption onto the oxyhydroxide coating that develops over time around the iron particles. To verify the above hypothesis, laboratory batch and column experiments were conducted to investigate the interaction between either bulk ZVI or nano-sized ZVI (nZVI) and Hg dissolved in aqueous solutions; and the resulting efficiency for Hg removal. The results of these investigations can be summarized as follows:

- nZVI particles have a much higher maximum adsorption capacity and a faster adsorption rate than ZVI
- The removal of dissolved Hg under dynamic conditions using column studies show that flow rate, Hg speciation, and mass of iron particles used play a significant role in the efficiency of Hg removal by iron particles.
- Further studies are needed to obtain conditions that favor the removal of Hg down to ppt level.

Second, the methylation of Hg in aquatic sediments depends on the interaction of a wide variety of indigenous microorganisms and the intimate coupling of such actions to key geochemical factors such as Hg speciation and availability, temperature, pH, the quantity and types of organic compounds available. However, previous research points to dominant microbial processes and Hg speciation and availability as the main criteria for Hg methylation, with microbial sulfate reduction being the most important microbial-catalyzed geochemical reaction linked to Hg bio-methylation. Accordingly, the presence of metallic iron as a source of dissolved Fe(II) under anoxic conditions in a sulfate-rich

anoxic sediments would lead to Hg sequestration through co-precipitation with iron sulfide minerals, and therefore, a reduced fraction of bio-available Hg. Microcosm studies using anoxic sediment slurries were conducted by varying the Fe to sulfate ratios in Hg-rich sediments in the absence (controls) or presence (treatments) of metallic iron particles. The main findings can be summarized as follows:

- The relationship between the different solid phase Hg fractions (easily exchangeable, ‘humic acid’ soluble, organo chelated, elemental Hg, and mercuric sulfide) and MeHg production show that Hg speciation plays a significant role in controlling Hg methylation.
- MeHg production is impacted by two main mechanisms, (i) adsorption of inorganic Hg on oxyhydroxide layers and/or (ii) co-precipitation of inorganic Hg iron sulfide complexes. This reduces the availability of ionic Hg and its subsequent methylation.

Overall, the results obtained from this study establish the ability of ZVI and nZVI to remove Hg from aqueous effluents and interfere with ionic Hg methylation in sediments. Therefore, the obtained results constitute a foundation for further research on validating the use of nZVI in the remediation of Hg contaminated systems.

CHAPTER 1
INTRODUCTION

In a paper entitled “A Silent Epidemic of Environmental Metal Poisoning” published over two decades ago, Nriagu (1988) rang the bell on potential health effects of increasing levels of heavy metals introduced into natural systems by anthropogenic activities. The outcry was driven primarily by the increasing pressure on natural resources and waste generation associated with the exponential growth of human populations. Since, a large numbers of papers focusing on the investigation of both the environmental fate and impacts of heavy metals and the remediation of metal-contaminated systems have been published (e.g. see review by (Cundy et al. 2008; Mulligan et al. 2001; Noubactep 2008).

Heavy metals are introduced to aquatic systems from both anthropogenic and natural sources. However, unlike organic pollutants, metals released to the environment are not biodegradable and their persistence, transformation, and transfer to the food chain lead to negative effects on living organisms. Although much is now known on the biogeochemistry of several trace metals including mercury (Hg) in water and soil/sediment, research on the development of cost-effective and environmentally-friendly remediation techniques remains challenging. Current methods for remediation of metal-contaminated liquid and solid matrices include physical separation, thermal processes, biological decontamination, phytoremediation, electro-kinetics, washing, stabilization, and solidification techniques. Unfortunately, only a few of these techniques have been tested commercially and their use remains limited due to factors such as their prohibitive costs and more recently, their inability to meet some of the new limits imposed by federal and state regulatory agencies. Overall, the remediation of metal-

contaminated environments remains one of the most intractable problems of environmental restoration and this is both a national and international issue. It also requires the development of remedial approaches that remove or immobilize metals while avoiding adverse effects on treated systems.

Concerns over the cycling of Hg in the environment have been driven primarily by the toxicity of methyl-Hg (MeHg) as it accumulates in living tissues and biomagnifies in food chains. Since anthropogenic activities (e.g. combustion of fossil fuels, incineration of wastes, industrial activities, gold mining by Hg amalgamation techniques, etc) constitute the primary cause of anomalously high Hg levels found in aquatic systems. The recently developed Clean Air Mercury Rule requires control of Hg emissions by electric power generators by 2020, which would have an estimated annual cost of about $1 billion annually by 2020 (US.EPA 2005). However, despite the above projected high costs, the benefits of the proposed preventive/remedial measures can not be fully guaranteed. The reason is that the link between atmospheric emission of Hg and the bioaccumulation of MeHg in aquatic biota involves a complex series of biogeochemical processes. This includes the poorly studied response of soil/sediment stored-Hg within watersheds to land use changes, the delivery of inorganic Hg species to areas that act as primary loci for Hg methylation, and the presence of both biological and geochemical parameters necessary for MeHg production and accumulation. In addition, despite the overwhelming literature on Hg in aquatic systems, several gaps exist in our current knowledge of the different processes involved in in-situ transformation of inorganic Hg species to MeHg. Due to site-specific changes in both geochemical parameters and the microbial community composition, the assumption of sulfur reducing bacteria (SRB) as

major Hg methylators in all aquatic systems could lead to erroneous model predictions of Hg bioaccumulation in fish and risks for human exposure. Therefore, an approach that takes into account all key environmental parameters in a simultaneous manner and focuses on Hg naturally present in the sediment/soil is needed.

The first objective of this proposed research program is to comparatively investigate the potential use of zero valent iron (ZVI) and nano-zero valent iron (nZVI) as sorbents for Hg removal from aqueous effluents and investigate the mechanisms involved in Hg immobilization. The interaction of ZVI with other metals and organic pollutants can involve several mechanisms including (i) reduction, (ii) sorption on oxidized iron surfaces, and (iii) coupled reduction and sorption as seen in Figure 1-1 (Cundy et al. 2008; Li et al. 2006a; Mulligan et al. 2001; Noubactep 2008).

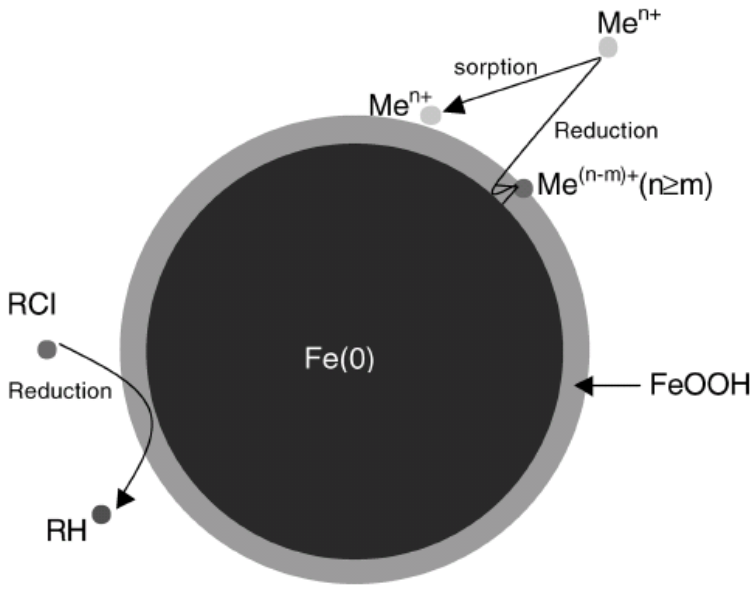

Figure 1-1. Interaction of zero valent iron with pollutants in aqueous solutions. Me=metal, RCl=chlorinated organic pollutant (Li et al. 2006b).

It is hypothesized that: the increase in surface area and the decrease in kinetic reaction time favored by nanosized iron particles will allow a faster removal of Hg from

aqueous effluents through the combination of (i) ionic Hg reduction to elemental Hg and volatilization, and (ii) Hg^{n+} adsorption onto the oxyhydroxide coating layer that develops over time around the solid particles. This study investigated the efficiency of Hg removal by both ZVI and nano-ZVI and assessed their potentials to bring Hg levels from contaminated effluents to levels that are targeted by regulation agencies such as the EPA's 12 to15 ng/L range.

In natural aquatic compartments such as sediments, the presence of solid iron particles could, depending on redox conditions, impact the cycling of metal and organic pollutants as well. Therefore, besides the above described three types of interactions that could lead to the remediation of Hg-contaminated effluents, the second objective of this study was to determine the effect of iron on Hg availability and methylation by sediment microorganisms. In contrast to the common practice that consists of spiking sediments with inorganic or organic Hg compounds to determine potential rates of Hg methylation and MeHg degradation, this study investigated the effect of iron particle addition to sediments historically contaminated with Hg (i.e., not spiked with Hg in the laboratory) in comparison with sediments from the source but spiked with Hg-salt. This approach used here intends to determine the fate of "*old*" versus "*newly added*" Hg in sediments containing iron particles. It was hypothesized that the addition of iron particles in Hg-contaminated sediments would limit Hg bioavailability through a combination of its sorption onto oxyhydroxide layers and co-precipitation with iron sulfide species, depending on redox conditions. The methylation of Hg in aquatic sediments depends on the activity of a wide variety of indigenous microorganisms, primarily the sulfate reducing bacteria (SRB), and key geochemical factors such

availability of specific terminal electron acceptors (TEAs), the quantity/quality of organic substrates, temperature, pH and Hg speciation. However, the availability of Hg to methylating agents constitutes the primary limitation for methylmercury (MeHg) production, even in Hg-contaminated systems. Accordingly, iron particles could depress MeHg production in sediments.

In this dissertation, a review of relevant literature on Hg in the environment, its environmental and health implications, and different techniques that are used for the remediation of Hg contaminated are discussed in Chapter 2. This review is then followed by chapters investigating the interactions of iron particles with aqueous Hg (Chapter 3), as well as the potential of such particles to remove Hg from wastewater effluents using column studies (Chapter 4). The potential impact of iron particles on Hg present in sediments with regard to its bioavailability and transformation to MeHg is presented in Chapter 5. Finally, Chapter 6 gives a summary of the major contributions of this research effort to current knowledge on the biogeochemistry of Hg and its interaction with Fe.

CHAPTER 2
MERCURY IN AQUATIC SYSTEMS AND CURRENT REMEDIATION TECHNIQUES

Mercury

Mercury (Hg) introduced into the environment by most anthropogenic activities are primarily in the inorganic form (e.g., Hg^0 and Hg^{n+}). When released into the atmosphere, Hg can be subject to long range transport leading to the contamination of remote and often pristine environments through both dry and wet precipitations onto terrestrial and aquatic systems. In addition to Hg introduced directly into aquatic systems, Hg deposited on soils can later reach aquatic systems through infiltration (contamination of groundwater) and/or via surface runoff (contamination of rivers, lakes, and coastal waters).

Mercury in Aquatic Systems

Inorganic Hg undergoes a number of bio-chemical and physical transformations in aquatic systems. For instance, the oxidation of metallic mercury (Hg^0) produces ionic species which are then methylated by sedimentary microorganisms (e.g., (Bonzongo et al. 1996; Compeau and Bartha 1985; Gilmour and Henry 1992). Methyl mercury (MeHg) that accumulates in the environment and in living organisms comes primarily from the net balance of the concurrent processes of microbial inorganic Hg methylation and demethylation of produced MeHg (US.EPA 1997). Indeed, nearly all Hg found in biological tissues tend to be present as MeHg (Bloom 1992; Kim 1995; Watras et al. 1995). Unfortunately, exposure to MeHg and other Hg species lead to adverse effects on living organisms including a reduced reproductive capacity, an impaired growth and development, behavioral abnormalities and death. These impacts of Hg on human health depend on several pathways related to toxicokinetic mechanisms of its major

chemical forms present including Hg^0, inorganic Hg salts (e.g., $HgCl_2$), and organic Hg compounds such as MeHg (W.H.O. 1990; W.H.O. 1991) in different environmental media. Depending on the chemical form of Hg, the combination of these toxicokinetic mechanisms (absorption, distribution, metabolism, and excretion) will determine the risk associated with human exposure to Hg and its compounds. For most of the above-mentioned adverse effects, the process of Hg methylation appears to be an important part of the contamination and response processes (US.EPA 1997).

Health Impacts

MeHg is classified as a possible human carcinogen. It is rapidly and extensively absorbed through the gastrointestinal tract (Aberg et al. 1969; Boffetta et al. 1998; Boffetta et al. 1993; US.EPA 1997; W.H.O. 1990). Epidemics of Hg poisoning following exposure to MeHg in Japan and Iraq have demonstrated that neurotoxicity is the health effect of greatest concern when a developing fetus is exposed to MeHg (US.EPA 1997). The disaster in Minamata, Japan, where mass poisonings involving Hg attracted the attention of the world scientific community in late 1950s, is still fresh in memories. The inhabitants of fishing villages along Minamata Bay suffered an epidemic of neurological disorders, visual constriction, brain damage, impairment of speech and hearing, numbness of extremities, impairment of gait, and several death cases. The above aforementioned epidemic was afterward all attributed to Hg poisoning (now known as “Minamata disease’) due to fish consumption from the bay.

In the past two decades, there have been reports of symptoms of the “Minamata disease” in Brazil, due to the use of Hg^0 in artisanal gold mining (AGM) (Hylander et al. 2006). In this case, miners who burn gold (Au)-Hg amalgams show signs of mercurialism due primarily to the inhalation of Hg vapor released during Au-Hg

amalgam burning. In addition fish-eating people living within the mining impacted areas show high Hg concentrations in blood and other tissues (Hinton et al. 2003; Hylander et al. 2006). Hg^0 in the lungs oxidizes to ionic Hg and forms complexes which are quite soluble in body fluids and lipids, allowing for rapid diffusion through cell membranes and reaching vital tissues such as those of the brain. A chronic exposure to Hg vapor results in symptoms like depression, exaggerated emotional response, gingivitis, muscular tremors and ultimately death, while acute exposure produces dysfunction of kidneys and urinary tract, vomiting, and potentially death too (Hinton et al. 2003; Valenzuela and Ftyas 2002).

High levels of Hg are also detected in the blood and other tissues of indigenous people from the Arctic Region. Here, atmospheric deposition of Hg transported from lower latitude industrialized regions is the main source of Hg in both terrestrial and aquatic systems. In fact, the Arctic is a recognized sink of Hg released to the atmosphere in lower latitude and warmer regions (Boening 2000; Givelet et al. 2004; Steffen et al. 2008; Ullrich et al. 2001). Diet, primarily the consumption of fish and other aquatic organisms, is the main exposure pathway for the indigenous Arctic people. Over time, the accumulation of Hg in the Arctic has resulted in increased average Hg levels in the cord blood of newborns and widespread child development problems (e.g. speech, walking, and loss of IQ) (Hylander et al. 2006).

The above listed effects of Hg on humans have led the US regulatory agencies to set stringent guidelines for Hg levels in waste gaseous and aqueous effluents. With regard to Hg contaminated waters which is the focus of this proposed research, Hg

levels in concentration range of 12-15 ng/L are targeted for wastewater effluents (Hanlon 2007).

Common Techniques Used in Remediation of Mercury Contaminated Aqueous Effluents

Several treatment methods for Hg removal from water and Hg removal from and immobilization in sediments/soils exist (Atwood and Zaman 2006; Wang et al. 2004). These treatments include phytoremediation, microbial remediation, constructed wetlands and sorption materials. A brief description is given below.

Phytoremediation

It is defined as the use of living green plants to remove pollutants from environmental compartments or to render them harmless. Phytoremediation has emerged as a promising, cost-effective, and environmentally friendly alternative to most engineering-based remediation techniques. This technology can be applied to either organic and inorganic pollutants present in soil, sludge, sediment, water, or the air. Phytoremediation is divided into the following five sub-categories: (i) phytoextraction, which uses hyper-accumulators to transport and concentrate contaminants from contaminated media to the above-ground parts for subsequent harvesting and removal from the site (Adams et al. 2000; Schnoor 1997); (ii) phytofiltration relies on plant roots or seedlings to sorb contaminants; (iii) phytostabilization uses plants to reduce the mobility and bioavailability of contaminants in the environment; (iv) phytovolatilization where plants volatilize contaminants; and (v) phytodegradation where plants and associated microorganisms are used to degrade organic contaminants. In addition to problems associated with the disposal of metal loaded plants, one of the main disadvantages of this remediation approach is the long time that is required in

comparison to the other available methods (Alkorta and Garbisu 2001; Mulligan et al. 2001; Zavoda et al. 2001).

Different plants have been used in experimental settings to remove Hg from contaminated waters. Kamal et.al (2004) found that plants such as the parrot feather, creeping primrose, and water mint could reduce Hg in an aqueous system to levels as low as 0.15, 1.3, and 0.02 μg/L, respectively in a 21 day remediation experiment. Bennicelli et. al (2004) found that the fern Azolla Caroliniana could reduce the dissolved Hg levels to 20 μg/L in a12 day-experiment. Finally, Skinner et.al (2007) reported on the ability of four different aquatic plants, namely, the water hyacinth, the water lettuce, the zebra brush and the taro to lower Hg from aqueous solutions, but the analytical technique used in this study limited the true assessment of the efficiency of these plants as the instrument detection limit was in mg/L range. Overall, plants are low cost materials. However, the long time required for the removal of the pollutant down to acceptable levels and the fate of Hg-loaded plants are two of the main disadvantages of this technology.

Microbial Bioremediation

Biodegradation refers generally to the breakdown of organic contaminants by microbial population. Metals cannot be biodegraded; however, they can be bio-transformed into compounds with different chemical speciation to reduce the mobility, bioavailability and/or toxicity. Microbial-driven remediation are dependent on site specific and environmental conditions such as pH, temperature, oxygen, nutrients, and soil moisture, (Alvarez and Illman 2006). Some of the limitations are related to the fact that certain microorganisms need specific conditions to be effective, unpleasant odors

can be produced due to the release of volatile organic carbon compounds and reduced sulfur containing gases. Furthermore, nutrient additions to sustain bacterial growth could lead to water contamination via surface runoff and/or infiltration. With regard to Hg, its removal through bioremediation occurs by either microbial catalyzed conversion of ionic Hg to elemental mercury which is then vaporized into the air. Or by precipitation of ionic Hg through binding to reduced sulfur produced by sulfur reducing bacteria (SRB) under reducing conditions. The genetically engineered microorganism, *Pseudomonas putida KT 2442::mer 73*, reduced Hg^{2+} from 200 mg/l to 2.4 mg/L via conversion to elemental Hg (Leonhauser et al. 2006). The natural isolate of *Pseudomonas putida SP3* reduced Hg^{2+} from 192 mg/L to 3.1 mg/L (Leonhauser et al. 2006). The removal of Hg through this method is not sufficient to meet the new requirements that are in the range of ng/L. Also volatilization of Hg does not solve the pollution problem because vaporized mercury will undergo deposition and contaminate pristine systems at both regional and global scales.

Constructed Wetlands

Wetlands are low lying ecosystems where the water table is near or at the surface. Constructed wetlands are manmade and are used for a variety purposes. Some are used as rehabilitating areas, for wastewater treatment, as buffer zones to protect downstream aquatic systems, treatment of metals, etc. These wetlands have been effective in the removal of metals from wastewater and acid mine drainage areas (Hawkins et al. 1997). Some of the principles used for removal of pollutants in wetlands are microbial bioremediation, phytoremediation, adsorption, sedimentation and precipitation. King et al. (2002) found that constructed wetlands can adequately remove low-level Hg to produce an effluent concentration in the range of 18.0 – 28.8 ng/L, but

over a one year-period. Gustin et al. (2006) also found that four experimental designs of constructed wetlands proved to remove Hg. All the designs contained vegetation of 70% cattails (Typha sp.) and the remaining comprised of rushes (Juncus sp.) and duckweed (Lemna sp.). The designs were (1) Hg contaminated water and Hg contaminated sediments, (2) Hg contaminated water and clean sediments, (3) clean water and Hg contaminated sediments, and (4) clean water and clean sediments. The inflow of designs (1) and (2) came from Steamboat Creek, Nevada. The inflow of designs (3) and (4) came from the Truckee Meadows Water Reclamation Facility, Nevada USA. The mean concentration of total Hg for the inflow of design (1) and (2) was 71 ng/L and the outflow was 32 and 25 ng/L, respectively. The mean concentration of total Hg for the inflow of design (3) and (4) was 6.4 ng/L and the outflow was 7.2 and 5.0 ng/L, respectively (Gustin et al. 2006). Design (3) gave a higher total Hg concentration in the outflow than the inflow because there were natural levels present in the wetland.

It has been shown that wetlands can be constructed at low cost and require little maintenance. However, if rigorous experimental examination is lacking, then predicting the effluent characteristics of the wetlands is extremely difficult. This is due to the diversity and complexity of these systems. Wetlands were built to reduce phosphorus loading runoff from the Everglades Agricultural Area and downstream eutrophication. The major concern was that the wetlands would unintentionally worsen the mercury problem. Cell one of three had surface water mercury concentrations reach 32 ng/L of total Hg and 20 ng/L of methyl Hg from about 4 ng/l and 0 ng/l, respectively. By controlling the flow rate and water depth mercury methylation may be reduced. Cell one

met the requirements of not being significantly greater than the average inflow, 1.34 ng/L of total Hg and 0.29 ng/L of MeHg, after four months (Rumbold and Fink 2006).

Sorption Materials

Activated carbon adsorption

Activated carbon (AC) has proven to remove a wide range of pollutants in aqueous systems (Yin et al. 2007). This is due to a number of characteristics such as a high specific surface area which ranges from 500 to 1500 m^2g^{-1}, an internal micro-porosity configuration, and the presence of diverse surface functional groups (Chingombe et al. 2005). Modified AC with sulfur has been used to remove Hg from aqueous effluents, with an increased adsorption capacity of approximately 1.4 times higher than the one obtained with the use of virgin AC (Gomez-Serrano et al. 1998). The basic principle may be explained by Pearson's principle of hard and soft acids and bases (Pearson 1963). Based on this classification, Hg, a soft acid would react readily with sulfur, a soft base to form highly covalent bonds. Overall, the use of both virgin and modified AC allows Hg removal to reach values in the range of 460 – 150 mg/g from 750 mg/g (Nabais et al. 2006). Unfortunately, these values are far above the target action limits mentioned earlier.

Ion exchange resins

Ion exchange resins are insoluble structures created from organic polymer beads. In this technology, the trapping and removal of pollutants from the aqueous phase is done through ion exchange. The resin type' and fabrication methods are very diverse and allow resins to be manipulated to remove specific ions. Resins without specified functional groups have been shown not to remove targeted metals. For instance, thiol-functionalized resins, have been designed for specific removal of ionic Hg species,

decreasing Hg levels in aqueous effluents from approximately 10,000 μg/L to concentrations below 5 μg/L (Dujardin et al. 2000). The use of mercaptan-amine chelating resins showed a Hg removal capacity of 621 μg/ kg (Atia et al. 2005). A cation exchange resin made from banana stems, an abundant lignocellulosic biomass waste, was able to remove Hg from aqueous solutions to about 70 μg/L, but the removal efficiency seemed to decrease with the increase in initial solution concentration (Anirudhan et al. 2007). Although this technology is effective to reduce Hg levels from aqueous effluents, it is apparent that its ability to reduce Hg levels below the target level of 12 ng/L is so far out of reach. It is worth to note that with regard to Hg removal by ion-exchange resins, ongoing research focuses on: (i) understanding the removal mechanisms, (ii) increasing the efficiency of Hg removal in the presence of competitive ions; and (iii) developing efficient recycling methods to guarantee the reuse of exhausted resins.

Other low-cost adsorbents

A wide variety of natural materials are classified as low-cost adsorbents due to their low cost and local availability. These low cost adsorbents are potential candidates to replace expensive adsorbents such as AC. Examples include chitosan and certain waste products from industrial or agricultural operations. Chitosan, a product of the deacetylation of chitin, which is the structural element in the exoskeleton of crustaceans, has excellent metal binding capacity. Penichecovas et al. (1992) found that chitosan has the ability to remove Hg with an adsorption capacity of 430 mg /g. On the other hand, DiNatale et al. (2006) found that three natural materials (i.e. char of South African coal, pozzolana, and yellow tuff) had higher ratios of Hg captured to

amount of adsorbent when compared to AC. Most of these low cost adsorbents are still in the investigative phase and more research is needed to establish their efficiencies, and ultimately, their use in full scale water treatment operations.

Zero valent iron (ZVI), which is the focus of this study, has been used to treat organic and inorganic contaminates from a variety of effluents like wastewater, storm water runoff, industrial, and groundwater. A detailed review of the use of ZVI for remediation is given below. Additionally the extension of this technology is seen in the use of nano size zero valent iron (nZVI), which has been of interest recently due to the theoretical increase in remediation power due to the increase in SSA.

Zero Valent Iron (ZVI)

ZVI has been in use for a number of years as an alternative to the pump and treat method in groundwater remediation. It is readily available, cost effective and has been used in the treatment of aquatic systems contaminated with recalcitrant organic pollutants, primarily volatile organic carbons (Gillham and Ohannesin 1994; Matheson and Tratnyek 1994). Studies have shown that ZVI could remove over 90% of DDT [1,1,1-trichloro-2,2-bis(p-chlorophenyl)ethane] from contaminated aqueous systems (Boussahel et al. 2007; Sayles et al. 1997). In addition, ZVI also removes over 95% of DDD [dichlro-diphenyl-dichloro-ethane] and DDE [dichloro-diphenyl-dichloro-ethylene], the products of natural transformations of DDT (Sayles et al. 1997). When used in combination with ethylenediamine tetra-acetic acid, ZVI accelerates the decomposition of different organic solvents reaching removal efficiencies of 100% for 2-chlorophenol, 85% for phenol, 70% for o-cresol, 67% for aniline, and 28% for p-nitrophenol (Sanchez et al. 2007). In wastewater treatment, ZVI has been used to lower levels of certain toxic

contaminants such as hydrocarbon compounds, dyes, pesticides, and herbicides (Junyapoon 2005).

In addition to its use in the remediation of aqueous systems contaminated with organic pollutants, ZVI has also been used in remediation of some metal-contaminated waters (Blowes et al. 2000; Blowes et al. 1997; Cantrell et al. 1995; Powell et al. 1995). For instance, chromium (Cr) VI, can be reduced to Cr (III) through the reaction shown in equations 1 and 2, leading to the precipitation of Cr (III) oxyhydroxides, and therefore to its immobilization (Astrup et al. 2000; Blowes et al. 2000; Blowes et al. 1997; Bostick et al. 1990; Powell et al. 1995).

$$CrO_4^{2-} + Fe^0 + 8H^+ \rightarrow Fe^{3+} + Cr^{3+} + 4H_2O \quad (2\text{-}1)$$

$$(1\text{-}x)\ Fe^{3+} + (x)Cr^{3+} + 2H2O \rightarrow Fe_{(1-x)}CrOOH + 3H^+ \quad (2\text{-}2)$$

The efficiency of ZVI has been tested in experimental settings for the remediation of arsenic (As) contaminated waters, and for both As(V) and As(III), ZVI was able to lower initial high arsenic concentrations (mg/L range) to values below the current US-EPA action limit of 10 μg/L (Farrell et al. 2001; Lien and Wilkin 2005b; McRae et al. 1997). Besides the above two oxyanion-forming elements, the literature is quite abundant with research on the removal of several other metal cations from aqueous effluents using ZVI (e.g. (Bartzas et al. 2006; Blowes et al. 2000; Gu et al. 1998; Khudenko and Garciapastrana 1987). However, unlike the widespread use of ZVI, research focusing on the use of nano-ZVI (nZVI) particles in remediation of metal-contaminated systems is still in its early stages. Preliminary findings from studies dealing with As, Se, and Cr suggest that the efficiency of metal removal from aqueous

solutions could be significantly improved (Kanel et al. 2006; Li et al. 2006a; Mondal et al. 2004; Ponder et al. 2001; Ponder et al. 2000).

Despite the extensive use of ZVI in remediation studies, published research on the remediation of Hg-contaminated systems is still scarce. Wilkin and McNeil (2003) used ZVI to remove several metal cations, i.e. Fe, Al, Hg, As, Cd, Cu, Mn, Ni, and Zn, from synthetic acid mine solutions. In this study, initial Hg concentrations of about 3.1 mg/L were lowered to levels <0.07 mg/L. In a column study, Weisener et al. (2005) used a ZVI reaction medium to treat a contaminated groundwater with an initial total Hg concentration of about 40 μg/L , but this initial Hg level was decreased only to values much higher than the EPA's suggested 12 to 15 ng/L for discharged wastewater effluents.

Based on empirical knowledge, dissolved Hg can be removed from aqueous solutions containing ZVI through a combination of mechanisms that depend upon key factors such as Hg speciation, pH, redox conditions and competitive cations. Such mechanisms include but are not limited to (i) loss by volatilization following the reduction of ionic Hg to Hg^0, (ii) adsorption onto solid oxyhydroxides as the ZVI undergoes oxidation, and (iii) removal through formation and precipitation of the highly insoluble mercury sulfide complexes under anaerobic conditions.

Zero valent iron and volatilization of dissolved mercury through reduction to elemental mercury

When in contact with ZVI or nZVI, dissolved Hg^{2+} undergoes reduction to form Hg^0 as shown in Equation 3.

$$Hg^{2+}(aq) + Fe^0(s) \rightarrow Hg^0(g) + Fe^{2+} \quad (2\text{-}3)$$

In this case, formed Hg^0 will very quickly partition between the aqueous and gaseous phases due to its very low solubility in water, with reported K_H values ranging from 376 to 391 $\frac{L\,atm}{mol}$ at 20°C (Clever et al. 1985; Lin and Pehkonen 1998; Loux 2004; Sanemasa 1975; Schroeder et al. 1992). In addition to the volatilization through direct Hg^{n+} reduction by ZVI/nZVI, Hg^0 may also form when the produced Fe^{2+}(aq) interacts with ionic Hg as shown in equations 4 and 5 (Raposo et al. 2000; Zhang and Lindberg 2001).

$$Hg^{2+} + Fe^{2+} \rightarrow Hg^{+} + Fe^{3+} \quad (2\text{-}4)$$

$$Hg^{+} + Fe^{2+} \rightarrow Hg^{0}(g) + Fe^{3+} \quad (2\text{-}5)$$

Additionally, in natural aquatic systems, ionic Hg can be reduced to its elemental form by reacting with organic matter (Schluter 2000), sunlight (Zhang and Lindberg 2001) and through bacterial formation of Hg^0 (Gabriel and Williamson 2004; Leonhauser et al. 2006; Lin and Pehkonen 1999). One of the limitations of Hg^{n+} reduction to Hg^0 would be its availability for these different reactions. For instance, Hg^{2+} adsorption onto iron oxyhydroxides that form on the surface of corroded ZVI/nZVI would limit its availability and interactions in the above listed reactions.

Adsorption on iron oxyhydroxides

Iron particles can react with water under both aerobic and anaerobic conditions to form Fe^{2+} and Fe^{3+} as shown in equations 6 through 9 (Biernat and Robins 1972; Gu et al. 1999; Kenneke and McCutcheon 2003; Majewski 2006; Sayles et al. 1997).

under anaerobic conditions:

$$Fe^0 + 2H_2O \rightarrow Fe^{2+} + H_2 + 2OH^- \quad (2\text{-}6)$$

$$Fe^{2+} + H_2O \rightarrow Fe^{3+} + \frac{1}{2}H_2 + OH^- \quad (2\text{-}7)$$

under aerobic conditions:

$$2Fe^0 + O_2 + 2H_2O \rightarrow 2Fe^{2+} + 4OH^- \quad (2\text{-}8)$$

$$4Fe^{2+} + O_2 + 2H^+ \rightarrow 4Fe^{3+} + 2OH^- \quad (2\text{-}9)$$

Iron oxyhydroxide layers formed on the surface of ZVI/nZVI as corrosion products are made of one or more of the following amorphous minerals: lepidocrocite (γ-FeOOH), goethite (α-FeOOH), akaganeite (β-FeOOH), magnetite (Fe_3O_4), green rust (Fe(II)-Fe(III) hydroxyl salts), siderite ($FeCO_3$), depending on the system (Farrell et al. 2000; Gu et al. 1999; Huang and Zhang 2005; Huang et al. 2003; Phillips et al. 2000; Rangsivek and Jekel 2005; Ritter et al. 2003). Once formed these oxyhydroxides adsorb Hg^{2+} which becomes encapsulated into oxyhydroxide inner layers as observed by scanning electron microscopy (SEM) in a column study (Weisener et al. 2005).

Precipitation of dissolved mercury as sulfide complexes

The sulfate ion, SO_4^{2-}, is usually present in natural waters, and under favorable conditions (e.g. low pH), it can react with ZVI as shown in equation 10 (Weisener et al. 2005).

$$4Fe^0(s) + SO_4^{2-} + 10H^+ \rightarrow H_2S\,(g) + 4Fe^{2+} + 4H_2O \quad (2\text{-}10)$$

The produced sulfide can then react with ionic Hg to produce solid mercury sulfide (HgS) complexes (Hepler and Olofsson 1975; Hsu-Kim and Sedlak 2005; Paquette and Helz 1997; Weisener et al. 2005). Also the analysis of HgS precipitates found in such experiments have shown Hg and S in 1 to 0.85 ratio, suggesting HgS could form in low sulfide environments thus removing Hg from aqueous solutions (Weisener et al. 2005).

In addition to HgS, other Hg-sulfur complexes (e.g. $Hg(SH)_2^0$, $Hg(SH)_2^-$ and $Hg(SH)_2^{2-}$) may form, as predicted by thermodynamic models (Benoit et al. 2003; Miller et al. 2007).

Effect of pH, competitive ions, and mercury-binding ligands

Several cations can compete for the same adsorption sites on solid surfaces or in chemical reactions with binding ligands present in solution. A study investigating the role of both competitive cations and pH on Hg adsorption onto kaolinite, Sarkar et al. (2000) found that the addition of chloride would shift the pH at which 50% of Hg becomes adsorbed onto kaolinite from 3.4 to 7. Similarly, the pH at which the maximum amount of Hg adsorbed onto kaolinite shifted when nickel (Ni) was added to the mixture. However, no significant changes occurred when SO_4^{2-}, PO_4^{3-}, and Pb were added individually to the system. In contrast, Bartzas et al. (Bartzas et al. 2006) noticed an adverse effect related to the formation of sulfate green rust as an intermediate product of ZVI corrosion in sulfate treated systems.

In natural systems, there may be several different apparent redox levels. In these systems, the change in redox adjusts the tendency for key reactions to take place (Stumm and Morgan 1996). It is well known that natural systems cycle redox changes over time. Accordingly, the reaction mechanisms under which Hg is removed from aqueous systems by ZVI may change with varying redox levels, and some of the above discussed reaction mechanisms may occur simultaneously in natural systems.

Nano Zero Valent Iron (nZVI)

The use of nano materials (NM) has been increasing over the years. The higher efficiencies while using a smaller amount of material is one of the main reasons for

investigating the use of NM. The general characteristic of NM is the increase in surface area, which theoretically can increase reaction rates. The reason is that remediation is dependent on the surface interaction of the contaminant. A review by Narr et al. (2007) outlining the potential use of nanotechnology in wastewater/water treatment to use NM in pollution prevention, treatment and remediation. The use of NM can reduce the consumption of expensive chemicals and high energy consuming processes, like ultra violate light. New detection methods need to be created for these NM, and environmental models are essential. However, life cycle assessments and environmental impacts of these NM need to be investigated. In addition, human health impacts of NM are required prior to the release or usage into the environment.

Table 2-1. Site remediation using nano zero valent iron: List of recent projects (Li et al. 2006b)

Site	Location
Phoenix-Goodyear Airport (Unidynamics)	Phoenix, AZ
Defense Contractor Site	CA
Jacksonville dry cleaner sites, pilot tests using nZVI (several	FL
State Lead Site	ID
Groveland Wells Superfund Site	Groveland, MA
Aberdeen site	MD
Sierra Army Depot	NV
Pharmaceutical plant, Pilot test	Research Triangle park,
Industrial site	Edison, NJ
Picattiny Arsenal	Dover, NJ
Shieldalloy plant	NJ
Manufacturing Site	Passaic, NJ
Klockner Road Site	Hamilton Township, NJ
Manufacturing Plant	Trenton, NJ
Naval Air Engineering Station	Lakehurst, NJ
Confidential site, Pilot test	Winslow Township, NJ

Table 2-1. Continued.

Site	Location
Confidential site, Pilot test	Rochester, NY
Nease superfund site, Pilot test	OH
Former Electronics Manufacturing Plant	PA
Rock Hill, pharmaceutical plant, full scale using nZVI	SC
Memphis Defense depot	TN
Grand Plaza Dry Cleaning Site	Dallas, TX
Industrial plant, pilot test	Ontario, Canada
Public domain, Pilot test	Quebec, Canada
Solvent Manufacturing Plant, Pilot test	Czech Republic
Industrial Plant, Pilot test	Czech Republic
Industrial Plant, Pilot test	Germany
Industrial Plant, Pilot test	Italy
Brownfields, Pilot test	Slovakia

nZVI have been used in pilot scale and full scale facilities throughout the US and internationally, as shown in Table 2-1. Proposed usage of nZVI as a reactive media in permeable reactive barriers is shown in Figure 2-2. It illustrates how a contamination source leached into the groundwater, and nZVI particles injected directly into the contaminated plume. The contamination plume may be treated to remove organic (i.e. organic solvents, pesticides, and fertilizers) and inorganic contaminants (i.e. heavy metals). The fate, transport, and toxicity of nZVI have not been fully understood. In addition the reaction mechanism of these nano particles under specific conditions has not been investigated.

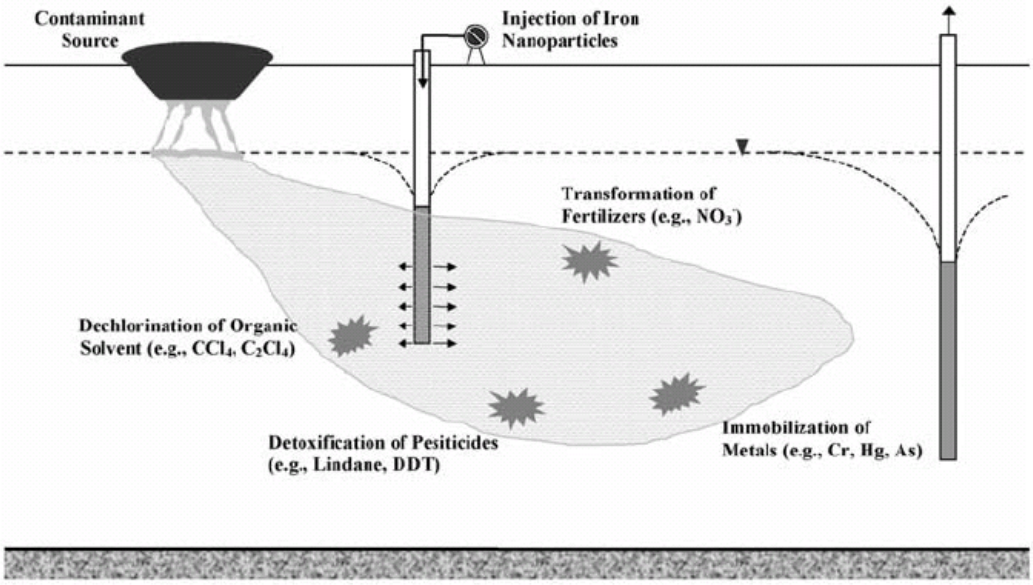

Figure 2-1. Schematic illustration of how nanoparticles could be used for in situ remediation of polluted ground waters (Zhang 2003).

nZVI and nitrate interaction

Synthesized nZVI with a diameter range of 1-100 nm and a BET (Brunauer Emmett and Teller) specific surface area of 31.4 m^2/g was used to remove 50, 100, 200, 400 mg/l of nitrate in deionized water with complete conversion to nitrogen gas in only 30 minutes (Choe et al. 2000). The effect of pH on nitrate removal was investigated with nZVI (particle size range of 50-80 nm) and a BET SSA of 37.83 m^2/g (Yang and Lee 2005). The isoelectric point was found to be at pH 7.3 for nZVI and at pH 5.4 the particles have the highest stability due to the large repulsive force acting on the particles. The removal rate of nitrate at low pH was highest. This is consistent with the results of having a more stable particle , which means less aggregation and optimal surface sites for remediation (Yang and Lee 2005). Zhang et al. (2006) also confirmed that at lower pH values nitrate reduction has a faster removal. The difference with the two works is that the latter used nZVI on supported graphite and the BET SSA for the

highest iron loading of 20% (by mass) was 6.18 m^2/g while the other did not use any support material. In all studies, as the iron content increased the amount of nitrate removed also increased (Choe et al. 2000; Yang and Lee 2005; Zhang et al. 2006). Biotic applications using nZVI to remediate nitrate showed that removal was highest when nZVI and biota was present (Oh et al. 2007).

nZVI and arsenic interaction

nZVI with a BET SSA of 24.4 m^2/g and a size distribution of 10 to 100 nm was used to treat arsenic from aqueous media. First order rate constants ranged from 0.07 to 1.3 min^{-1} for nZVI. These rate constants are 1000 times higher than reported rate constants when micron ZVI was used (Kanel et al. 2005). The isoelectric point of nZVI was determined to be at a pH of 7.8, which is similar to what Yang et al. (2005) found when removing nitrate. Outside the pH range of 4.5 - 10, arsenic adsorptions decreased (Kanel et al. 2005).

Similar particle characteristics of nZVI with a BET SSA of 33.5 m^2/g, and a size distribution of 50 to 100 nm was seen by Kanel et al. (2005) (Yuan and Lien 2006). The isoelectric point was determined to be at pH 4.4, which is significantly different from that obtained by Kanel et al. (2005) and Yang et al. (2005) (pH of 7.8 and 7.4 respectively). The difference might be due to the addition of $NaClO_4$ to the solution matrix while the others only used pure deionized water.

Kanel et al. (2006) gives an overview of nZVI versus ZVI on removing arsenic. The nZVI rates constants, as stated by Kanel et al. earlier in 2005, are about 1000 times greater than ZVI. However, the mass of arsenic removed for both ZVI and nZVI was similar (~100%). So using nZVI instead of ZVI suggests a faster rate but not an

increase in mass adsorbed. The usual time frame for remediation may take years with other adsorbents but nZVI shows promise as an adsorbent with less remediation time.

nZVI and chromium interaction

nZVI has also been used to treat chromium (Cr) contaminate in aqueous solutions. Ponder et al. (2001; 2000) used supported nZVI. In supported nZVI, the nZVI particles are dispersed in a fluid or gel to stabilize the nano particles. The support material may be a resin, silica gel or sand (Ponder et al. 2000). The BET SSA of the material used by Ponder et al. (2000) was 24.4 m^2/g. The rate constant for the resin supported material was highest, 1.18 h^{-1}, but for unsupported nZVI the rate constant was 1.16 h^{-1}. The supported material may not be needed (Ponder et al. 2000). The rate constants of granular ZVI were significantly less than that of the NM (Ponder et al. 2001; Ponder et al. 2000).

Niu et al. (2005) also used supported nZVI. Starch stabilized nVZI was used along with pure nZVI and ZVI powder for comparison purposes. Starch nZVI showed the highest Cr(VI) removal rate followed by pure nZVI, ZVI powder, and ZVI filling, respectively (Niu et al. 2005). Theoretically the surface area decreases in the same fashion. The initial pH affected the removal rate as well. As the pH decreased so did the rate of removal for Cr(VI) (Niu et al. 2005).

Xu et al. (2007) used a cellulose-based support for nZVI called sodium carboxy methyl cellulose (CMC). CMC without iron did not remove any of the chromium, which eliminates the effect of the support material. Column experiments showed that Cr(VI) was not found in the effluent even after six pore volumes but total chromium did appear in the first pore volume and decreased to zero after that (Xu and Zhao 2007).

CMC has not been the only support material for nZVI; carbon black has been used as well. Carbon black was used as the support material for nZVI to remove chromium. The BET SSA was found to be 130 m^2/g (Hoch et al. 2008), which is the highest seen in this review. However, carbon black by itself has a high BET SSA of 80 m^2/g (Hoch et al. 2008) as well. Additionally, when nZVI is synthesized, there are several starting solutions that can be used which results in different SSA. The four iron solutions and the surface area were ferric nitrate (130 m^2/g), ferric oxalate (64 m^2/g), ferric citrate (95 m^2/g) and ferrous acetate (38 m^2/g) (Hoch et al. 2008). The nZVI supported ferric nitrate removed Cr(VI) at a rate of 1.2 $h^{-1}m^{-2}$, which is similar to what has been seen previously (Hoch et al. 2008).

Synthesized nZVI with BET SSA of 24.4 m^2/g was used to investigate the reaction product of Cr(VI) (Manning et al. 2007). Li et al. (Li et al. 2008) found that the removal capacity for nZVI ranged from 180 to 50 mg Cr/g nZVI, while for macro ZVI the range was typically less than 4 mg Cr/g ZVI. The data from Li and Manning suggests that $Cr(OH)_3$ precipitates are the products formed when nZVI is used to remove chromium (Li et al. 2008; Manning et al. 2007).

CHAPTER 3
INVESTIGATION OF MERCURY AND IRON INTERACTIONS IN AQUEOUS SYSTEMS: IMPLICATIONS FOR WATER REMEDIATION

Introduction

Heavy metals are introduced to aquatic systems from both anthropogenic and natural sources, but unlike organic pollutants, metals released to the environment are not biodegradable and can undergo transformations that affect their potentials for bioaccumulation in food chains and toxicity to living organisms. Although much is now known on the biogeochemistry of several trace metals such as mercury (Hg), research on the development of cost-effective and environmental-friendly remediation techniques remains rather challenging. The now well-established effects of Hg on aquatic organisms and human health have led US regulatory agencies to contemplate stringent guidelines for Hg levels in waste gaseous and aqueous effluents**.** For instance, low Hg concentrations ranging from 12 to 15 ng/L are now being targeted for waste water effluents (Hanlon 2007)**.** Unfortunately, current methods for remediation of metal-contaminated environmental matrices often fail to meet the action limit levels imposed or targeted by federal and/or state regulatory agencies. In addition, the commercial use of available techniques remains limited due to several factors such as their prohibitive costs.

A wide variety of sorbents have been tested in studies focusing on the removal of pollutants from aqueous solutions, including zero valent iron particles (ZVI), which have been in use as an alternative to the pump and treat method for groundwater remediation. ZVI is both readily available and inexpensive. In fact, the current increasing trend in the use of zero-valent iron nanoparticles (referred to herein as nZVI) finds its origin in past intensive and still ongoing use of ZVI in the remediation of groundwater

contaminated with recalcitrant organic pollutants (Gillham and Ohannesin 1994; Matheson and Tratnyek 1994). The use of granular ZVI in permeable reactive barrier (PRBs) started in the 1990's;(Gillham and Ohannesin 1994; Gu et al. 1999; Reynolds et al. 1990), and has been found effective for the treatment of many organic pollutants such as volatile organic carbons in polluted ground waters (Gillham and Ohannesin 1994; Matheson and Tratnyek 1994). Besides organic pollutants, ZVI has also been used to treat metal-contaminated waters (Blowes et al. 2000; Blowes et al. 1997; Cantrell et al. 1995; Powell et al. 1995). In a laboratory study by Wilkin and McNeil (2003), the efficiency of ZVI to remove several trace metals, including Hg, from synthetic acid mine solutions resulted in significant decrease of Hg levels from initial concentrations of ~ 3100 μg/L to values <70 μg/L. Additionally, ZVI-packed columns have also been used as reaction media to treat a Hg-contaminated groundwater with an initial total-Hg (THg) concentration of about 40 μg/L, resulting in a THg concentration of 0.168 μg/L in the treated effluent (2005).

The use of nZVI in remediation can therefore be seen as an extension of the above ZVI technology. However, the use of nano-size particles could provide several advantages related to physicochemical characteristics specific to nanoparticles including the distinctive catalytic and chemical properties associated with the large surface-to-volume ratio characteristics of nano-size materials. The latter can lead to interesting and some time surprising surface and quantum size effects. nZVI is anticipated to be used as alternative or supplement to the conventional ZVI-PRB technology. For instance, injections of nZVI slurries targeting heavily contaminated

source areas or “hot spots” could add to the efficiency of traditional ZVI-PRBs that function as barriers to contain the dispersion of contaminants.

This study focuses on the potential of nZVI to remove Hg from waste water effluents. In fact, the interaction of metallic iron and Hg in aqueous solutions results in Hg removal from water through a combination of mechanisms that depend upon key factors such as Hg speciation, pH, oxidation-reduction potentials, the presence and types of binding ligands, as well as the presence of competitive cations. Such mechanisms include but are not necessarily limited to (i) loss by volatilization following the reduction of ionic Hg to Hg^0, (ii) adsorption onto solid oxyhydroxides as the ZVI surfaces undergo oxidation, and (iii) removal through formation and precipitation of highly insoluble Hg-sulfide species in sulfide rich anaerobic systems. Based on these Hg removal mechanisms, one could speculate that the efficiency of Hg removal by ZVI particles can be improved by increasing the surface area, and therefore, the reactivity of used particles. Accordingly, the currently emerging nanotechnology and the production of nZVI particles offer the opportunity to test the above hypothesis. In this study, ZVI and nZVI are used comparatively in laboratory experiments investigating their ability to (1) volatilize aqueous Hg and (2) act as sorbents for Hg dissolved in waters of different solution chemistries.

Materials and Methods

Iron Particle Characterization and Chemistry of Water Used in Laboratory Experiments

ZVI particles with a diameter size range of 1 to 2 mm were obtained from Alfa Aesar (PA, USA). The nZVI particles were purchased from Quantum Sphere, Inc (CA, USA), and had a particle size range of 15 to 25 nm as reported by the vendor. The N_2-

BET specific surface areas (SSA) of these particles were determined using a Quanto-Chrome NOVA 1200. The particle size distribution (PSD), zeta potential, and density of nZVI particles were determined using a Brookhaven Zeta Plus equipment and a Quanto-Chrome Ultra Pycnometer 1000.

Two types of waters were used in the batch experiments conducted in this study. The first type of water used was laboratory Nanopure® water, referred to herein as DI-water. The second water was a filtered (0.45 μm) wastewater effluent (WW) collected from a wastewater treatment facility located on the campus of the University of Florida. For the latter, major ions and dissolved organic carbon (DOC) were determined by ion chromatography (Dionex-IC320) and a Tekmar Dohrmann-Apollo-90000, respectively. The carbonaceous biological oxygen demand (CBOD) was obtained from the wastewater treatment plant's monitoring record.

Mercury solutions used in different experiments were prepared by spiking each of the above waters with aliquots volumes of a stock 1000 ppm solution of $Hg(NO_3)_2$ obtained from Fisher Scientific, USA.

Corrosion of Iron Particles and Temporal Changes in Specific Surface Areas: Effects of Water Chemistry

Experiments were conducted using Hg-free DI-water and WW to investigate temporal changes in iron particles' SSA as a function of solution chemistry. Briefly, for each of the iron particle type (i.e. ZVI and nZVI), treatments consisted of a total of 10 containers, each containing either 1g of nZVI or 5g of ZVI. Next, for each iron particle type, DI-water was added to five of the containers, while the other five were filled with WW to a final volume of 1.1 L. The containers were sealed and left at room temperature on a laboratory bench. At time 2, 4, 6, 8, and 10 days, selected individual containers

were removed and the oxidized Fe-particles harvested after discarding the liquid phase. The harvested particles were then dried and out gassed at 150^{o}C for 2 hours prior to analysis for SSA.

Volatilization of Dissolved Mercury by Iron Particles in Closed Batch Reactors

Batch experiments were conducted by mixing a pre-weighed mass of iron particles with a fixed volume of water containing a known amount of Hg. For these experiments, 50 mL serum vials pre-cleaned by soaking in 10% trace metal grade HNO_3 for 24 hours and rinsing with DI-water were used as batch reactors. Hg-spiked waters were equilibrated with known amount of iron particles. To account for the effect of temperature, both sample vials and vials containing elemental Hg used as standard for calibration purposes were maintained in a large bath at a fixed temperature. Serum bottles were incubated comparatively under light and dark conditions, with dark conditions achieved by fully wrapping each vial with aluminum foil. All treatments were prepared in triplicates. Over time, gas samples (100 μL) were withdrawn from the vial's headspace with a gas tight syringe, and injected into a stream of ultra high purity helium for the determination of Hg^0 content (Hg^0_{gas}), using cold vapor atomic fluorescence spectrometry (CV-AFS, Tekran-2500, Ontario, Canada). Levels of Hg^0 in the corresponding aqueous phase (Hg^0_{aq}) were calculated using Henry's Law. This approach allowed for the determination of the total amount of Hg^0 (Hg^0_T) produced in the reactor at any sampling time (i.e. $Hg^0_T = Hg^0_{aq} + Hg^0_{gas}$), and therefore the possibility to express the data as percent of initial Hg(II) in solution converted to Hg^0.

Effect of Dissolved Natural Organic Matter on Mercury Volatilization

Experiments were also conducted to investigate the effect of dissolved organic carbon (DOC) on the interaction of iron with dissolved Hg. For these experiments, water samples with different organic matter content and types were collected from the Suwannee River (SR) basin. The SR system contains three linked hydrologic units, each providing distinct hydrological characteristics and gradients in DOC and ionic strength (I). Briefly, in the upper watershed of the SR system, confinement of the Floridian aquifer provides surface drainage and sources of organic carbon from wetlands (e.g. the Okefenokee Swamp in southern Georgia). The boundary between the upper confined and middle unconfined watershed is a geomorphic feature called the Cody Scarp, below which ground water returns to the surface from many large springs, increasing ionic strength of surface waters. Finally, the river delta leads to the Gulf of Mexico and provides sites for collection of water samples with lower DOC and higher salinity. Ongoing studies in our laboratory (Gao et al. 2009) have shown that water samples collected from the headwaters and referred to herein as SR-1, the river mid-section (SR-2) and off the Suwannee River delta (SR-3) showed contrasting chemical compositions. Waters were filtered (0.45 μm) and analyzed by a Tekmar Dohrmann-Apollo-9000 for DOC, ion chromatography (Dionex DX-320) for major ions (e.g. Na^+, K^+, Mg^{2+}, Ca^{2+}, Cl^-, NO_3^-, and SO_4^{2-}), and phenolphthalein titration to pH 3.7 for total alkalinity. Table 3-1 and Figure 3-1 show trends of the major chemical parameters in these water samples. Only sample SR1 (dominated by allochtonous organic matter) and SR2 (site impacted by nutrients with a high production of autochtonous organic matter) were used in this study.

Batch experiments were conducted by mixing a pre-weighed mass of iron particles with a fixed volume of either SR1 or SR2 water samples containing a known amount of Hg.

Table 3-1. Chemical composition of water samples collected along the Suwannee River from headwaters to the river delta

Water Sample	pH	Alkalinity (mg/L as CaCO3)	Chloride (mg/L)	TOC (mg/L)
SR 1	4.70	6.0	6.2185	45.71
SR 2	7.15	88.0	6.9797	10.23
SR 3	7.56	132.0	13608.0	Not determined

For these experiments, 50 mL serum vials pre-cleaned by soaking in 10% trace metal grade HNO_3 for 24 hours and rinsing with DI-water were used as batch reactors. Hg-spiked waters, 25 mL, were equilibrated with known amount of iron particles, 0.5 g. The incubation procedure and analysis is the same as the one stated in the previous section.

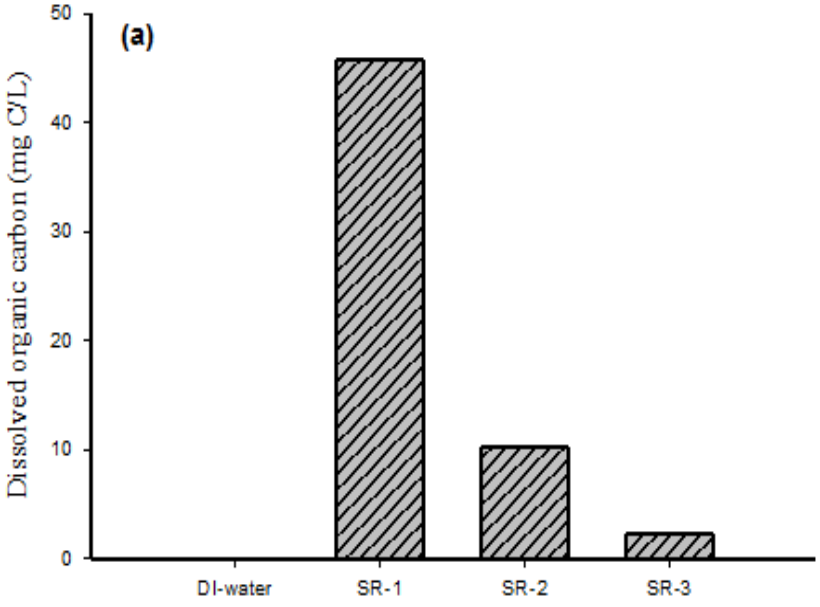

Figure 3-1: Trends of dissolved organic carbon (DOC) (adapted from Gao et al., 2009).

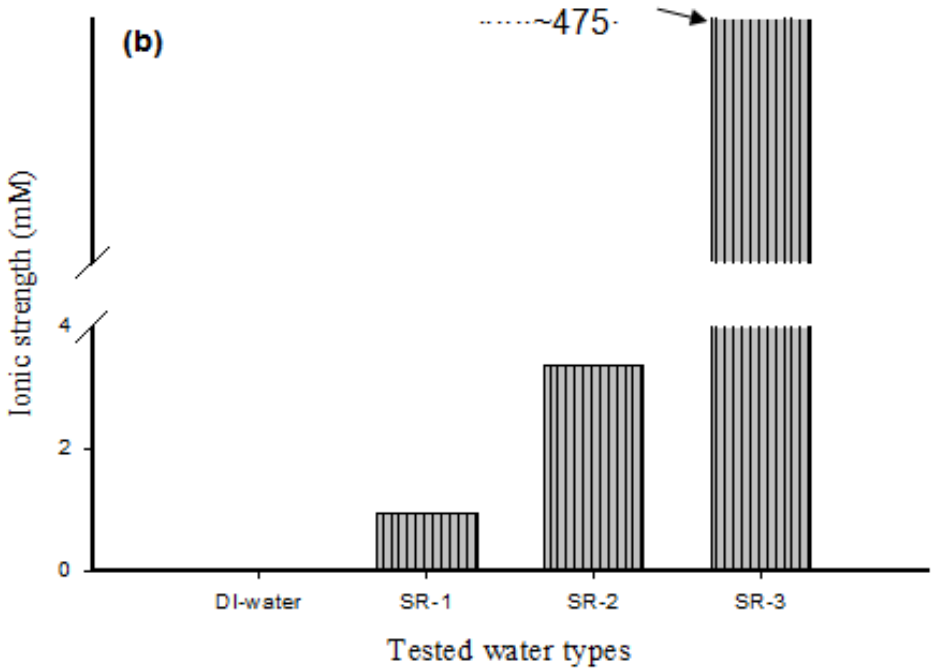

Figure 3-2. Trends of ionic strength (I) in waters of the Suwannee River (adapted from Gao et al., 2009)

Hg Sorption onto Zero Valent Iron and Nano Zero Valent Iron Particles

The maximum adsorption capacities of tested iron particles for Hg dissolved in DI-water or WW were determined by equilibration of prepared Hg solutions of known and increasing Hg concentrations (ranging from 100 to 500 mg/L) with a fixed amount of iron particles (i.e. 1.0 g for ZVI or 0.04 g for nZVI). All treatments were run in triplicates, and based on preliminary sorption kinetic results (*data not shown*), 1 mL aliquot of the aqueous phase was collected on the 10^{th} day of the equilibration process (plateau region of the adsorption curve) and analyzed for Hg remaining in solution. Hg was analyzed by the $SnCl_2$-reduction technique after sample oxidation by bromine monochloride and pre-reduction by hydroxylamine, followed by detection by cold vapor atomic fluorescence spectrometry (Tekran Model 2600). Details on used analytical procedures and QA/QC criteria (blanks and Hg standard solutions) have been

described in several of our earlier publications (Hovsepyan and Bonzongo 2009; Warner et al. 2005; Warner et al. 2004)

Following the water-particle mixing approach described above, the effect of pH on aqueous Hg removal by either ZVI or nZVI was also investigated. In this case, the pH of prepared mixtures was adjusted to 5, 7, or 8 using HCl or NaOH solutions. All treatments were run in triplicates, and the disappearance of Hg from solutions in batch reactors monitored over time through analysis of withdrawn aliquot samples by the $SnCl_2$-reduction technique and detection by CV-AFS.

Finally, the effect of initial Hg concentration on rates of Hg removal from aqueous phase by the two types of tested iron particles was investigated using Hg-solutions with a fixed pH of 7, while the range of Hg concentrations in used waters varied from 0.05 to 5 mg/L. For these experiments, the disappearance of Hg from aqueous solutions was monitored over time and analyzed as described above.

Statistical Analysis

To evaluate the significance of differences observed between treatments, a simple t-test for equal or unequal variance was used at a confidence level of 95%. Analysis was performed using the Microsoft Office Excel 2003 statistical data analysis tools.

Results and Discussion

Particle Characterization and Water Chemistry

The measured SSA of particles used in these experiments were 0.116 m^2/g and 30.5 m^2/g for ZVI and nZVI, respectively. The particle size distribution (PSD) of nZVI ranged from 345 to 558 nm with an average diameter of 492 nm when dispersed in DI-water and analyzed by dynamic light scattering technique (DLS). The PSD of nZVI dispersed in tested WW effluent ranged from 469 to 651 nm with an average value of

564 nm. Trends of zeta potential for nZVI particles suspended in DI-water and WW effluent as function of pH are shown in Figure 3-2. The point of zero charge (PZC) for particles suspended in DI-water occurs at a pH of ~4.15, a PZC value that is quite similar to that reported previously by Yuan et al.(2006). In WW effluent, the PZC dropped to a pH of ~2.1.

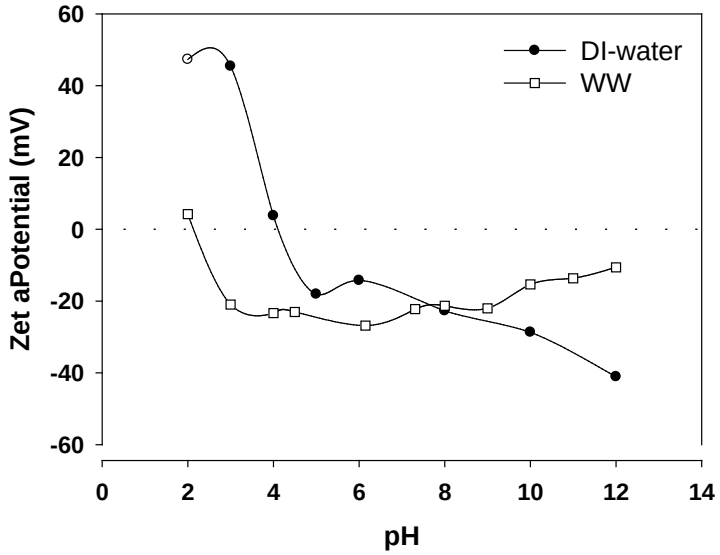

Figure 3-2. Effect of pH on zeta potential of nano-zero valent iron (nZVI) particles suspended in DI-water (●) and Wastewater Effluent (□). Plotted values are averages of 5 measurements and in all cases, error bars are very small and do overlap with symbols.

While DI-water used in our experiments can be considered as simple synthetic water, the WW effluent had complex solution chemistry (Table 3-2), including a background total-Hg concentration of 55 μg/L (or ppb) and a relatively high dissolved organic carbon content (8 mg C/L). Therefore, the difference in solution chemistry offered by these two waters allowed for the assessment of the effect of increasing water chemical complexity on interactions between Hg and metallic iron particles.

Table 3-2. Chemical composition of used wastewater effluent. Major ions were determined by ion chromatography. **DOC* = dissolved organic carbon; ***CBOD* **=** carbonaceous biological oxygen demand.

Analyzed parameters	Concentration (mg/L)
Cl^-	125.5
F^-	0.5830
$P\text{-}PO_4^{3-}$	7.079
$N\text{-}NO_3^-$	4.589
K^+	10.93
Mg^{2+}	33.62
Ca^{2+}	55.94
Na^+	60.23
SO_4^{2-}	201.5
DOC*	8.000
CBOD**	3.070
Total-Hg	0.0550

Kinetic Change of Specific Surface Area of Zero Valent Iron and Nano Zero Valent Iron in Deionized Water and Wastewater

To gain insight on the temporal effect metallic iron particles have on the two selected waters, measurements of SSA of particles exposed to Hg-free waters were conducted over time. The results are presented in Figure 3-3. From the raw materials (corresponding to the number 0 in Figure 3-3), it can be seen that exposure to water leads to increased SSA over time. However, there is a clear difference in the significance of values measured for ZVI (Fig. 3-3A) and nZVI (Fig. 3-3B). ZVI particles soaked in DI-water showed no significant change in SSA even after 10 days of exposure while contact with WW resulted in an order of magnitude increase from 0.116 m^2/g in raw particles to >2 m^2/g. A similar overall trend was obtained with nZVI, except that nZVI exposed to WW reached SSA in excess of 100 m^2/g from the initial 30.5 m^2/g.

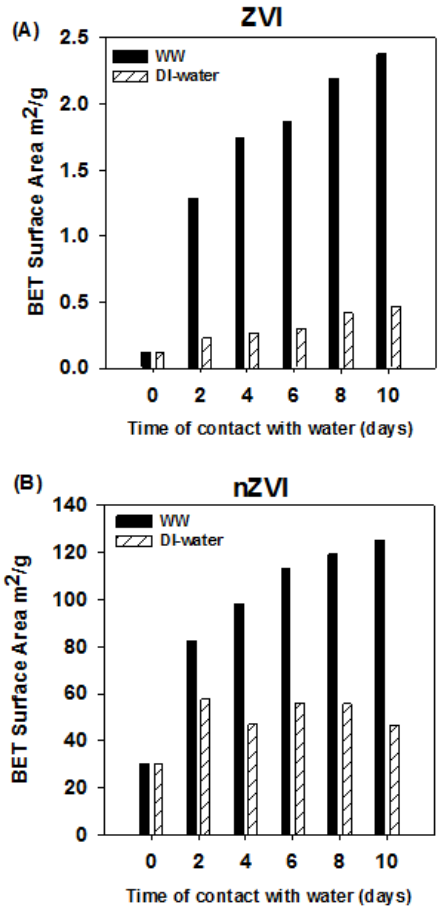

Figure 3-3. Effect of Water Matrix on Iron Surface Area.

The increase in SSA is likely due to the formation over time of oxyhydroxide coating layers on metallic iron particles, and the observed differences driven by solution chemistry. This is a well studied phenomenon, and depending on the chemistry of water, hydr(oxide) layers formed on the surface of ZVI and nZVI can include amorphous minerals such as lepidocrocite (γ-FeOOH), goethite (α-FeOOH), akaganeite (β-FeOOH), magnetite (Fe_3O_4), green rust (Fe^{II}-Fe^{III} hydroxyl salts), siderite ($FeCO_3$) (Farrell et al. 2000; Gu et al. 1999; Huang and Zhang 2005; Huang et al. 2003; Phillips et al. 2000; Rangsivek and Jekel 2005; Ritter et al. 2003). These oxyhydroxides would provide adsorption sites for metal cations such as $Hg(H_2O)_x^{n+}$, which would then become

encapsulated into the oxyhydroxides inner layers as observed by others using scanning electron microscopy (Weisener et al. 2005).

Mercury Volatilization by Metallic Iron Particles: Effect of Particle Size

In contact with metallic iron, dissolved ionic Hg can undergo reduction to form elemental mercury (Hg^0) as shown in equation 1.

$$Hg^{2+}_{(aq)} + Fe^0_{(s)} \rightarrow Hg^0_{(g)} + Fe^{2+} \quad (3\text{-}1)$$

In this case, formed Hg^0 would quickly partition between the aqueous and gaseous phases due to its very low solubility in water and reported K_H values ranging from 376 to 391 L.atm.mol^{-1} at 20^{0}C (Clever et al. 1985; Lin and Pehkonen 1998; Loux 2004; Sanemasa 1975; Schroeder et al. 1992). On the other hand, metallic iron particles can react with dissolved oxygen (DO) and water in corrosion reactions by which iron is oxidized as illustrated in equations 2 and 3.

$$2Fe^0_{(s)} + 4H^+_{(aq)} + O_{2(aq)} \rightarrow 2Fe^{2+}_{(aq)} + 2H_2O \quad (3\text{-}2)$$

$$Fe^0(s) + 2H_2O \rightarrow Fe^{2+}_{(aq)} + H_{2(g)} + 2OH^-_{(aq)} \quad (3\text{-}3)$$

In addition, Hg^0 may also be produced from the product of metallic iron oxidation (Fe^{2+}) as illustrated in the step-wise equations 4 and 5 (Raposo et al. 2000; Zhang and Lindberg 2001).

$$Hg^{2+} + Fe^{2+} \rightarrow Hg^+ + Fe^{3+} \quad (3\text{-}4)$$

$$Hg^+ + Fe^{2+} \rightarrow Hg^0_{(g)} + Fe^{3+} \quad (3\text{-}5)$$

Metallic iron particles can react with water under both aerobic (Eq. 6 and 7) and anaerobic (Eq. 8 and 9) conditions to form Fe^{2+} and Fe^{3+} as shown in the following equations (Biernat and Robins 1972; Gu et al. 1999; Kenneke and McCutcheon 2003; Majewski 2006; Sayles et al. 1997).

$$2Fe^0 + O_2 + 2H_2O \rightarrow 2Fe^{2+} + 4OH^- \quad (3\text{-}6)$$

$$4Fe^{2+} + O_2 + 2H^+ \rightarrow 4Fe^{3+} + 2OH^- \quad (3\text{-}7)$$

$$Fe^0 + 2H_2O \rightarrow Fe^{2+} + H_2 + 2OH^- \quad (3\text{-}8)$$

$$Fe^{2+} + H_2O \rightarrow Fe^{3+} + \frac{1}{2}H_2 + OH^- \quad (3\text{-}9)$$

These last four reactions bring about the possibility of oxyhydroxide coating layers on iron particles, and therefore, the presence of sorption sites for metal pollutants such as Hg as discussed earlier in relation with results presented in Figure 3-3.

Using closed batch reactors and Hg-containing DI-waters mixed with metallic iron particles, trends of volatilized Hg^0 were obtained from aliquot gas samples taken from the vials' headspace. The obtained results are presented in (Figure 3-4). In the presence of ZVI, Hg volatilization shows an increasing trend during the first 5 days of incubation, followed by a brief plateau, and then a progressive decrease over time to reach Hg levels below our analytical detection limit. In contrast, the interaction of dissolved Hg with nZVI resulted in instantaneous Hg reduction with peak volatilization in the first few minutes of contact, followed immediately by a sharp loss of Hg^0 from the gas phase.

As illustrated in Figure 3-5, the observed behavior of Hg throughout the above volatilization experiment is bracketed between dominant Hg-reduction and Hg-adsorption end-members. The observed peaks correspond to exposure periods during which rates of Hg reduction by metallic iron particles is significantly higher than that of metallic iron corrosion by both dissolved oxygen and water molecules.

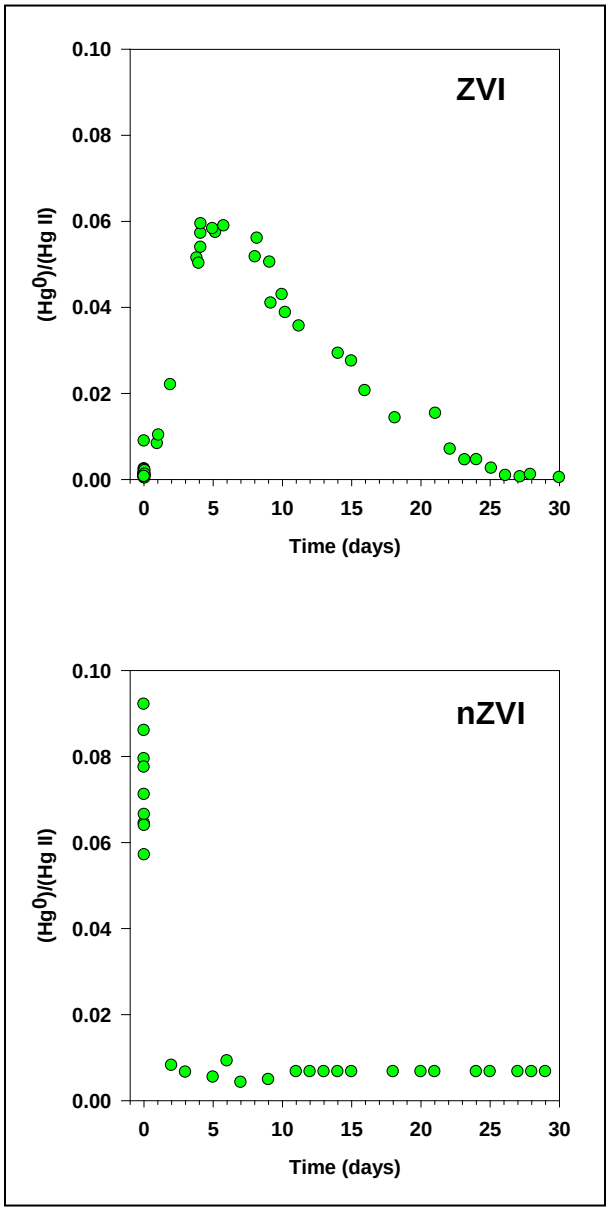

Figure 3-4. Temporal trends of Hg volatilization and sorption in a closed batch reactor containing 30 mL of DI-water with a concentration of 1.0 μg Hg/mL and 0.04 g of zero valent iron (ZVI) particles. For each sampling point, levels of Hg^0 in the aqueous phase were calculated using Henry's Law, and the total amount of produced Hg^0 determined as $Hg^0 = Hg^0_{aq} + Hg^0_{gas}$. Results are plotted as ratios of the above quantified Hg^0 to the initial total-Hg concentration (Y-axis) versus time.

However, as corrosion increases, the removal of Hg from solution through adsorption drives the depletion of $Hg^0_{(g)}$ from the reactor's headspace (Figure 3-5). This

is possible due to the metallic Hg reducing Fe^{3+} based on the serial arrangement of electrode potentials (i.e. electromotive series). However, results presented in Figure 3-4 show the difference in kinetic rates of these reactions when ZVI and nZVI are used. These results point to the importance of physicochemical characteristics specific to nZVI in impacting the rate of reactions between metallic iron and ionic Hg on one hand, and metallic iron and dissolved oxygen or water on the other.

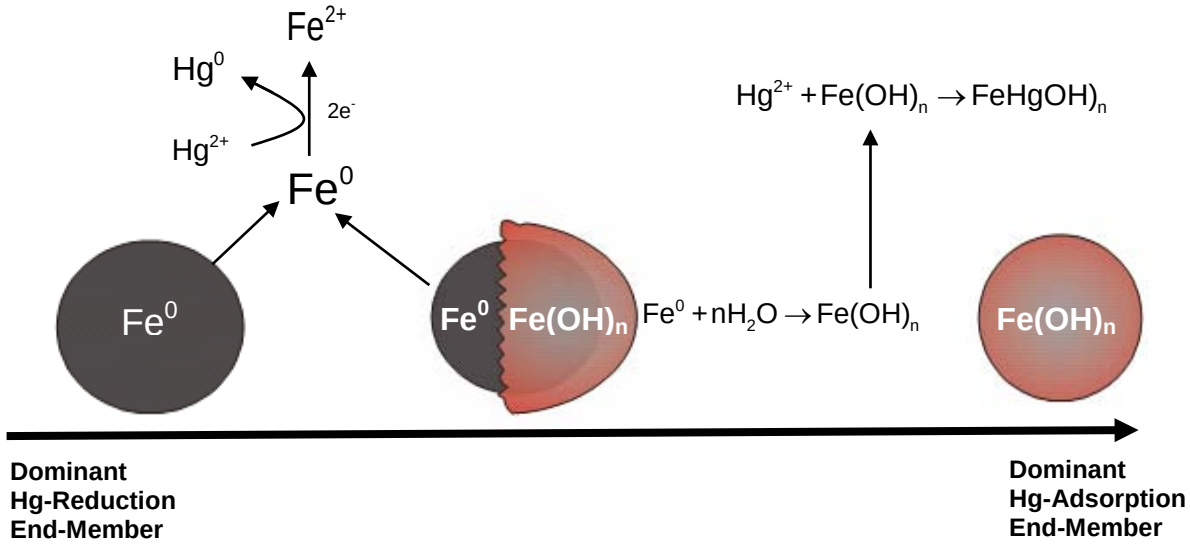

Figure 3-5. Simplified schematic representation of Hg interaction with metallic and corroded iron particles in aqueous solutions along a corrosion gradient. Hg-reduction dominates initially, and as iron corrosion reactions evolve, hydr(oxide) layers are formed on metallic iron surfaces and progressively, Hg adsorption becomes the dominant pathway for Hg removal from solution

Overall, Hg volatilization under used experimental conditions, and regardless of the type of metallic iron particles used, was rather minimal, representing <10% of total-Hg concentrations in the reactors.

When WW effluent instead of DI-water was used in experiments similar to the one discussed above, different volatilization patterns were obtained (Figure 3-6). Unlike the experiment with DI-water, here we tested the effects of pH change on Hg volatilization

by metallic iron particles under either light or dark conditions. First, volatilization was faster in the presence of nZVI, regardless of light/dark exposure conditions. Second, the volatilization step was followed by a plateau of Hg^0 concentration in WW-nZVI mixtures. On the other hand, ZVI-WW mixtures behaved differently, in that, at pH 5 very little Hg was reduced to Hg^0, and light conditions seemed to favor Hg-reduction and volatilization. In these reactors, obtained trends suggest that Hg volatilization can persist for a long time. At pH 7, WW containing ZVI showed a spike in Hg^0 concentration, but instead of a plateau as seen with nZVI, a slow but decreasing trend similar to that described in figure 3 is observed. Volatilization experiments at pH 8 gave Hg^0 levels and trends similar to those obtained with WW at pH 7 (data not shown). It is obvious that in this complex water matrix, Hg speciation and the presence of dissolved organic compounds play a role in the fate of Hg present in water. The use of Visual Minteq and parameters listed in Table 1 showed that for the used WW effluent, Hg would occur predominantly as $HgCl_2$ (70%) at pH 7, while the other species would be present at much lower proportions (e.g. 25% HgClOH, 3% $HgCl_3^-$, and 2% $Hg(OH)_2$). In contrast, Hg speciation in used DI-water at pH 7 was dominated by $Hg(OH)_2$ (99%). It appears that in addition to particles properties, Hg chemical speciation and the type of ligands present in solution would play a role in controlling the extent of Hg volatilization, probably through a combination of several mechanisms. This is because in natural aquatic systems, ionic Hg^{2+} can be reduced to its elemental form through abiotic reactions with organic matter (Schluter 2000), sunlight (Zhang and Lindberg 2001), and through microbial catalyzed formation of Hg^0 (Gabriel and Williamson 2004; Leonhauser

et al. 2006; Lin and Pehkonen 1999). Overall, the observed volatilization phenomenon impacted only a small fraction of dissolved Hg.

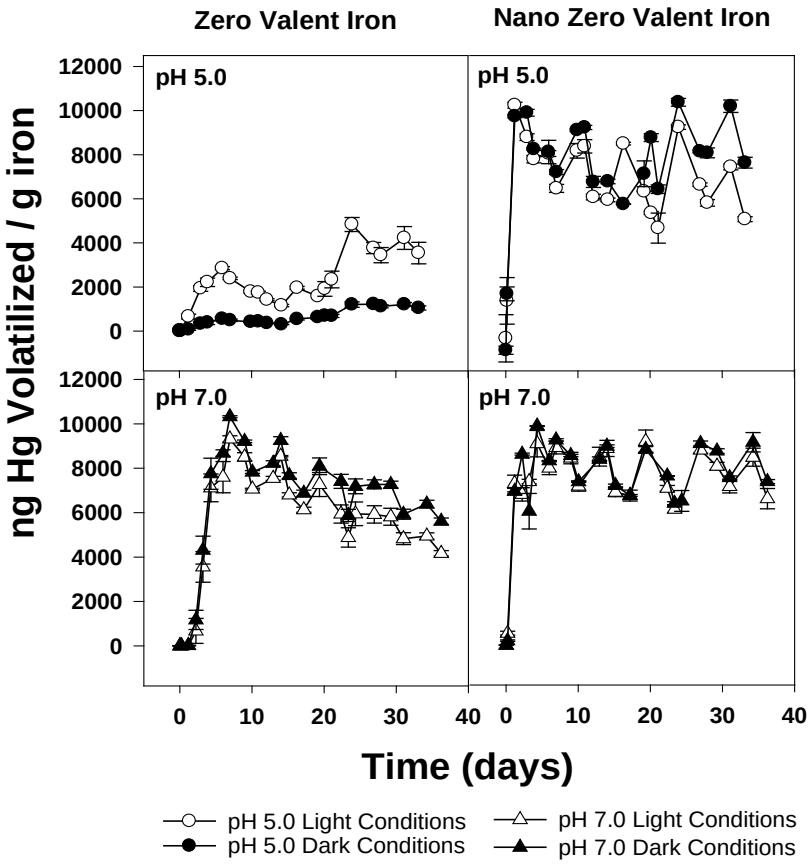

Figure 3-6. Temporal trends of Hg volatilization and sorption in closed batch reactors containing 25 mL of wastewater effluent with a concentration of 1 μg Hg/mL and 0.04 g of iron particles. For each sampling point, levels of Hg^0 in the aqueous phase were calculated using Henry's Law, and the total amount of produced Hg^0 determined as $Hg^0 = Hg^0_{aq} + Hg^0_{gas}$. Results are plotted as ratios of the above quantified Hg^0 to the mass of iron particles used

Effect of Dissolved Natural Organic Carbon on Volatilization of Aqueous Mercury

Results obtained from experiments investigating the effects of naturally occurring dissolved organic matter (DOC) on Hg-ZVI interactions are summarized in Figure 3-7. Control experiments (i.e. reactors with no ZVI addition) run in parallel with ZVI-spiked reactors show that the presence of iron inhibits Hg volatilization in DOC-rich waters

collected from the Suwannee River (site SR-1 with a DOC concentration of 45.71 mg C/L) (Figure 3-7).

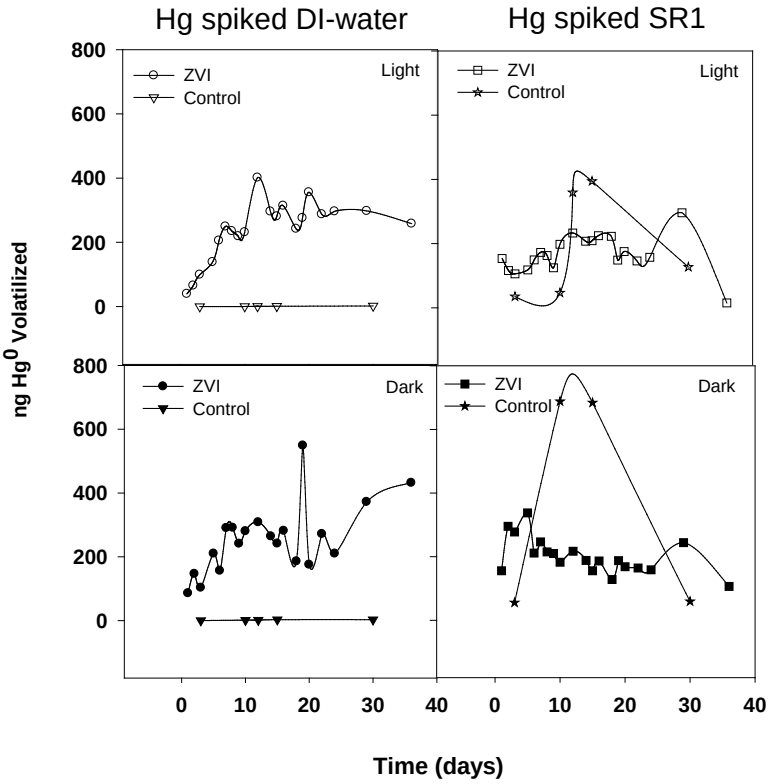

Figure 3-7. Effect of natural organic carbon (SR1) on Hg volatilization (300 μg/L)

The reduction and subsequent volatilization of Hg occurs when conditions are favorable to electron transfer to the Hg cation. Such electrons could come from several sources when dealing with natural water and its complex chemistry. For instance, in the presence of light, photocatalytic reactions can produce free radicals that can reduce Hg^{2+} to Hg^0 (Deng et al. 2009; Ravichandran 2004). However, Figure 3-7 shows however that Hg volatilization in these experiments could be quite independent of photo-catalyzed reactions, as the latter may not be the dominant pathway for induced Hg reduction. There are three different interactions that can occur, (i) DOC and Hg, (ii) DOC and iron, and (iii) Hg and iron.

Another type of electron donor is natural organic matter. It is known that Hg may be reduced directly by the humic and fulvic fractions of natural organic matter, see equation Equation 10 (Alberts et al. 1974; Ravichandran 2004; Skogerboe and Wilson 1981). Alberts et al. (1974) suggested that quinones (Figure 3-8) present in large organic molecules could act as electron donors for Hg reduction.

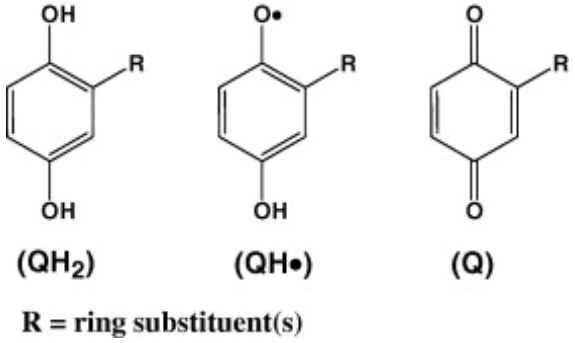

Figure 3-8. Quinones: hydroquinone (QH_2), fully oxidized quinone (Q), semiquinone radical ($QH^{\bullet}$) (Uchimiya and Stone 2009).

Uchimiya et al. (2009) proposed that electrons are transferred when hydroquinones (QH_2) is converted to Q, the fully oxidized quinone. The effect of DOC can be seen in Figure 3-7 when comparing the different iron treatments to the control samples. In the control samples, it is hypothesized that when the DOC is oxidized, Hg^{2+} in solution is reduced to Hg^0 and then subsequent volatilization. In addition, Hg can be adsorbed by DOC present in the natural water. Hg binds to the acid sites of DOC. These acid sites consist of carboxylic acids, phenols, ammonium ions, alcohols and thiols (Ravichandran 2004).

$$Hg^{2+} + 2DOC^{\bullet} \rightarrow Hg^0 + DOC \quad (3\text{-}10)$$

$$Hg^{2+} + nDOC^{n-} \rightarrow (DOC)_n Hg \quad (3\text{-}11)$$

This will decrease Hg availability to take part in other reactions. However, based on the results shown in Figure 3-7, Hg adsorption by DOC is not dominant because in control samples Hg volatilization is higher than in the presence of iron.

However, when ZVI is present, there may be other reactions occurring. For instance, ZVI may be favored more than Hg for reduction. Based on standard electrochemical potentials iron (E^0=-0.44V (Noubactep 2008) is thermodynamically preferred than Hg^{2+} (E^0=0.79V (Atkins 1994)). Additionally, DOC can be removed from solution by adsorption onto the ZVI surface thus decreasing irons reactivity (Hagare et al. 2001). It is apparent that iron introduction into SR waters inhibits the production of Hg^0. Hg and iron interaction can yield Hg volatilization and adsorption. ZVI bare surface can reduce Hg^{2+}. Overtime, iron oxyhydroxides can form and Hg can be removed from solution through adsorption onto these surfaces.

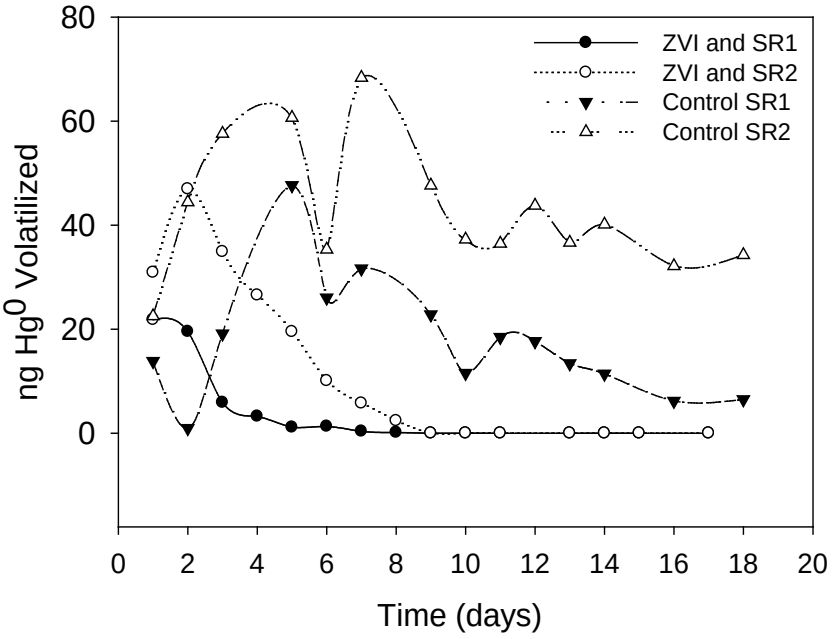

Figure 3-9. Effect of dissolved natural organic carbon on Hg reduction/volatilization

SR1 and SR2 water samples, which are characterized not only by different DOC concentrations (45.71 and 10.23 mg C/L, respectively), but probably by the type of

predominant organic compounds (with allochthonous organic carbon being dominant in SR1 while SR2 contains a significant authochtnonous fraction) were used comparatively. Figure 3-9 shows that as the organic carbon concentration is increased from sample SR2 to SR1, reactors without ZVI addition (controls) show an inverse trend in the amount of Hg volatilized. It is likely that the Hg/DOC ratios as well as the Hg-binding capacity of organic compounds present in these samples do control the reduction and subsequent volatilization of Hg. In contrast to these control samples, ZVI containing reactors exhibited much lower volatilization of Hg, but with SR2 (water with the smaller DOC concentration) leading to the highest Hg volatilization, comparatively. Therefore, Hg reduction/volatilization is limited in the presence of ZVI, but DOC concentration and probably the type of organic carbon compounds present play a role in determining the quantity of Hg volatilized.

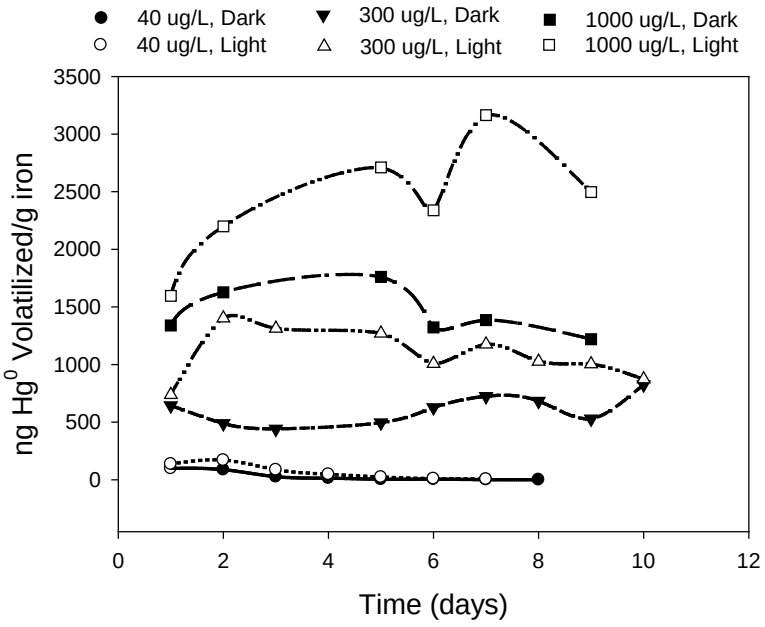

Figure 3-10. Effect of Hg concentration on its volatilization from SR1 waters

Figure 3-10 shows that when Hg concentration is increased from 40 to 1000 μg Hg/L the amount of Hg volatilized increases as well. This is due to increase in Hg for

reduction in the system whether it be by ZVI or DOC, as explained above. At the higher concentrations, light and dark conditions trends separate. This is caused by the presence of light in natural waters producing reactive oxygen species that may interact with Hg to form Hg^0 (Lalonde et al. 2004; Lin and Pehkonen 1999).

Mercury Removal from Solution by Zero Valent Iron and Nano Zero Valent Iron through Sorption

Hg loading capacity of both ZVI and nZVI at pH of 5.3 and 8.3 were measured using 100, 250, and 500 mg/L at a predetermined equilibration time of 10 days. Table 3-3 shows that nZVI has a higher Hg loading capacity than ZVI at different pH and concentrations. At pH 5.3 oxyhydroxide layers seemed to have formed at a faster rate thus removing approximately twice as much Hg from solution than at pH 8.3. However, when using the Langmuir adsorption model (R^2=0.99 for all treatments) the maximum adsorption capacity for ZVI and nZVI was determined to be 109 and 833 mg/g at pH 5.3, respectively. At pH 8.3 the maximum adsorption capacity of ZVI was higher, 120 mg/g, but lower for nZVI, 286 mg/g. Equation 3-12 shows the Langmuir model used where b is the adsorption maxima (mg/g), q is the amount adsorbed (mg/g) ,C_{eq} is the equilibrium solution chemistry (mg/L) and K_L is adsorption constant (intensity).

$$\frac{C_{eq}}{q} = \frac{C_{eq}}{b} + \frac{1}{bK_L} \qquad (3\text{-}12)$$

Based on preliminary studies on the effect of pH (5.0, 7.0 and 8.0) on sorption kinetics a pH of 7.0 was chosen for all adsorption studies. Figure 3-11 gives the results of Hg removal from solution by either ZVI or nZVI mixed with DI- water or WW with different initial Hg concentrations. The removal curves for both ZVI and nZVI in the

batch experiments showed similar removal trends when the initial Hg concentration varied.

Table 3-3. Hg loading capacity of ZVI and nZVI for Hg-spiked wastewater effluent at pH 5.3 and 8.3.

Initial Hg Concentration (mg Hg/L)	pH 5.3 mg Hg adsorbed/ g iron		pH 8.3 mg Hg adsorbed/ g iron	
	ZVI	nZVI	ZVI	nZVI
500	195.0	448.4	96.1	239.0
250	169.8	373.3	53.1	139.3
100	51.3	130.9	22.8	63.3

ZVI has been shown to remediate inorganic contaminants through co-precipitation or reductive precipitation (Blowes et al. 2000; Su and Puls 2001; Weisener et al. 2005). Weisener et al. (2005) showed that ZVI could interact with aqueous Hg present in groundwater to form Hg-sulfide complexes. These removals from aqueous solutions were found to take place on inner sphere complexes with the iron oxides (Fendorf et al. 1997; Lien and Wilkin 2005a; Su and Puls 2001). Despite the similarity in observed Hg removal trends, the removal rates determined by assuming pseudo-first order reactions produced rate constants of different orders of magnitude (Table 3-3).

Similar to the results reported by Sarathy et al. (2010), the rate constants are expressed as per mass (k_m) and as per specific surface area (k_s). Particles used were not suspended either by physical or chemical means therefore in these experiments the particles formed aggregates. The rate constants for ZVI are higher than that of its nanosize counterpart when rate constant values are expressed per surface area units. For example, Su et al (2001) expressed k values as per SSA because the iron particles were continuously suspended by a physical force. Additionally, as shown in Figure 3-2, the SSA changes over time when in contact with aqueous solutions, therefore

expressing the k values per mass will give a better and more accurate insight to the Hg and iron interaction. Su et al (2001) used powder and granular ZVI to remediate arsenic and found that there was no correlation between arsenic remediation and surface area. Therefore all the data shown is normalized based on mass.

As a matter of fact, other researchers have encountered similar issues when using nano particles to remediate chromium (VI) (Li et al. 2008), arsenic (Berger et al. 2006; Sharma et al. 2010), carbon tetrachloride (Nurmi et al. 2005), 1,2,3-trichloropropane (Sarathy et al. 2010), fluoride (Mohapatra et al. 2010) and other contaminants expressed loading capacity per mass basis. The kinetic rates for nZVI in Hg spiked WW and DI-water both are orders of magnitude higher than for ZVI when expressed as per mass basis. The rate constant for nZVI increased from 1.2505 to 2.6065 day^{-1}/g iron, when the initial concentration increased. However for ZVI the rate constants (k_m) at an initial concentration of 0.5 and 5 mg Hg/L for both DI-water and WW were not significantly different.

Table 3-4. Pseudo-first order adsorption rate constants for Hg on ZVI and *n*ZVI based on Hg-spiked deionized water and wastewater effluent (*k values are rate constants)

	Deionized water (DI)						Wastewater effluent (WW)					
Initial Hg Conc mg/L	ZVI $^*k_{DI}$			nZVI $^*k_{DI}$			ZVI $^*k_{WW}$			nZVI $^*k_{WW}$		
	r^2	day^{-1}/ g iron	day^{-1}/ SSA	r^2	day^{-1}/ g iron	day^{-1}/ SSA	r^2	day^{-1}/ g iron	day^{-1}/ SSA	r^2	day^{-1}/ g iron	day^{-1}/ SSA
0.05	0.94	0.081	3.5	0.95	1.5	0.010	0.95	0.044	1.9	0.78	1.3	0.008
0.5	0.99	0.065	2.8	0.87	0.83	0.005	0.97	0.081	3.5	0.95	2.0	0.013
5.0	0.94	0.060	2.6	0.92	2.5	0.016	0.99	0.075	3.2	0.97	2.6	0.017

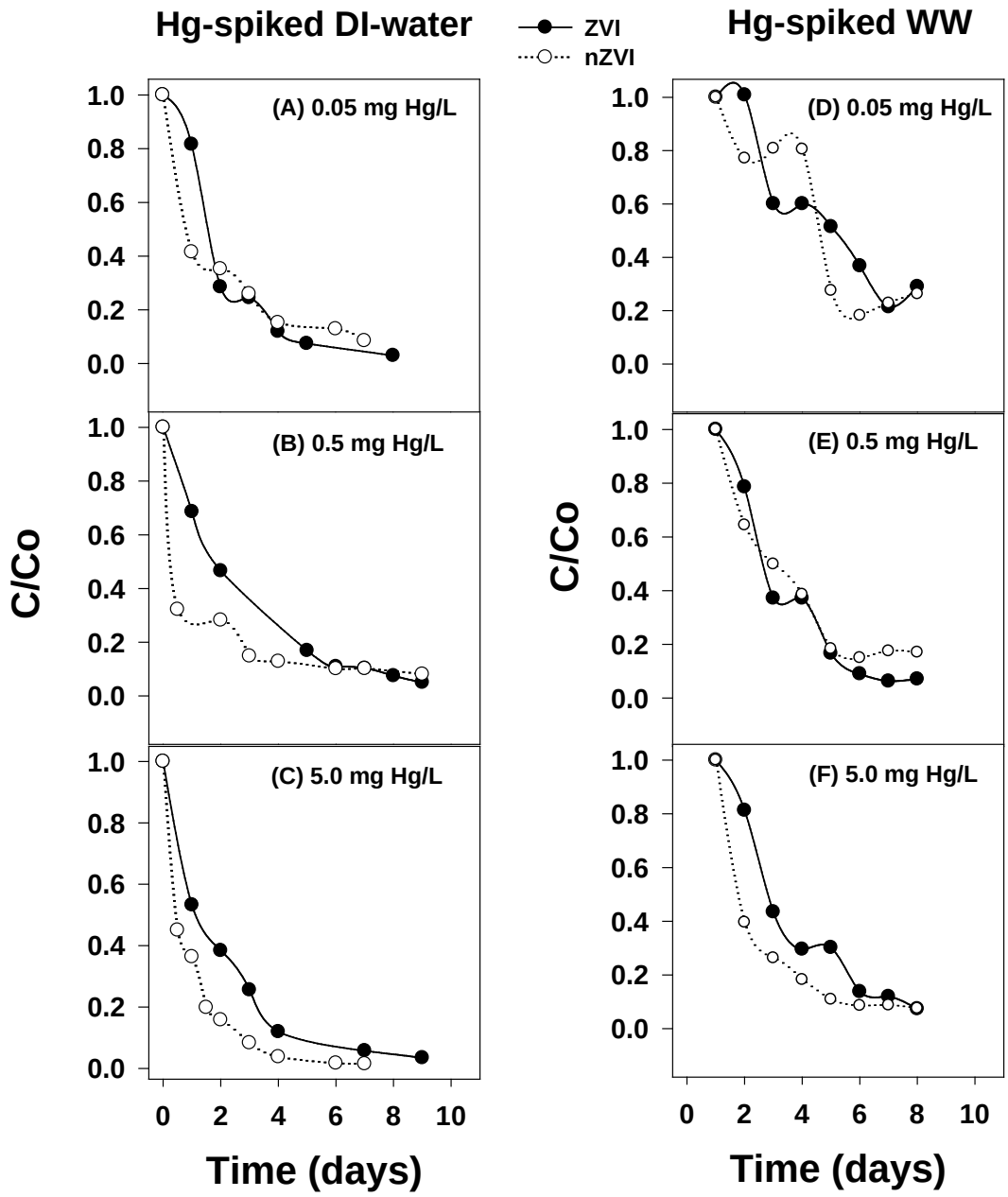

Figure 3-11. Effect of initial Hg concentration dissolved in either Deionized water (DI-water) or wastewater effluent (WW) on Hg adsorption by ZVI, (●), and *n*ZVI, (○) particles at pH 7. (A), (B), and (C) for Hg spiked DI-water. (D), (E), and (F) for Hg-spiked WW.

Conclusion

The interactions between iron and Hg exhibit two main mechanisms, volatilization and adsorption. In the batch studies, the volatilization rate for nZVI was faster than for

ZVI in DI-water. When WW effluents were used, the amount of Hg volatilized was the same for ZVI and nZVI. The total Hg volatilized was only 1%; therefore for both ZVI and nZVI volatilization is not dominant. All the volatilization experiments in this study were done in closed batch reactors, and further investigation is needed on Hg volatilization under open conditions. This would show if the flux of Hg volatilization is constant or if it is contingent on the Hg concentration in the system. In addition, the effect of different water chemistry might also be of interest. It is known that Hg can be volatilized by humic substances (Alberts et al. 1974; Ravichandran 2004).

The experimental and theoretical adsorption capacities show that nZVI has a higher adsorption capacity than ZVI. Further investigation using other natural waters with different chemistries might give more insight into how nZVI may be used to treat other effluents such as industrial or even drinking water. This would support the use of nZVI as a more efficient adsorbent than its granular counterpart, similar to the remediation of arsenic.

The kinetic studies show that when rate constants are express as per mass basis nZVI has a faster rate than ZVI. However the controversial issue is that these rate constants should be expressed as per surface area. This is because the hypothesis of using nano particles is to benefit from the much larger surface area. Although, when the rate constants are expressed as per surface area then ZVI exhibits a faster rate. Others in the literature as explained above have found similar trends. Su et al. (2009) showed that there is no correlation between iron surface area and remediation. Further investigation into explain this correlation is needed. Maybe the iron surface area does not play a role but the solution chemistry, which can be seen in Figure 3-2. The surface

area changes overtime when in contact with different water chemistries. Additionally the use of nZVI under dynamic conditions needs to be examined. If nZVI leaches into the environment via these remediation techniques, then knowledge of its fate and transport is needed.

CHAPTER 4
REMOVAL OF MERCURY FROM WASTEWATER EFFLUENT USING FLOW THROUGH COLUMNS PACKED WITH NANO ZERO VALENT IRON PARTICLES

Introduction

The development and use of engineered nanomaterials (NMs) are believed to offer great benefits to society through their exploitation within numerous industrial activities, and environmental, agricultural and medical research. With regard to the contaminated environmental systems, NMs have the potential to afford environmental benefits by enabling both the detection of pollutants and the remediation of contaminated environmental matrices. Of particular interest is the use of nano-zero valent iron particles (referred to herein as nZVI). Theoretical and practical evidence suggests that nZVI can be used to remediate sites contaminated with certain hazardous organic (e.g. PCBs) and inorganic (e.g. arsenic) chemicals, a process often termed "*nano-remediation*".

The current increasing trend in the use of nZVI finds its origin in past intensive and still ongoing use of bulk zero-valent iron (or ZVI), primarily as an alternative to the pump-and-treat technique for remediation of groundwater contaminated with recalcitrant organic pollutants (Gillham and Ohannesin 1994; Matheson and Tratnyek 1994). The use of granular ZVI in permeable reactive barrier (PRBs) for groundwater treatment started in early 1990s (Gavaskar 1999; Gillham and Ohannesin 1994; Gu et al. 1999; Reynolds et al. 1990), and since, over 100 such PRB structures have been constructed in the U.S. alone (Li et al., 2006). Although several studies have demonstrated that ZVI is effective for the treatment of many pollutants commonly found in polluted ground waters (e.g. perchloroethene, trichloroethene, carbon tetrachloride, energetic munitions such as TNT and RDX, legacy organohalogen pesticides such as lindane and DDT,

heavy metals, etc., important challenges that limit the practical application of granular ZVI-technology still exist. For example, a large amount (e.g., tons) of iron powder is usually needed even for a modest PRB structure. Costs associated with the PRB construction, especially for deep aquifers, remains too high for many potential users of the technology. Another important limitation is the relative lack of flexibility after a PRB is installed. Relocation or major modifications to the PRB infrastructure is often impractical. And besides ZVI, a number of sorbents including zeolite, hydroxyapatite have also been tested in PRB structures (Cundy et al. 2008; Moraci and Calabro 2010; Mulligan et al. 2001).

The nZVI technology is therefore seen as an extension of the above ZVI technology. It takes advantage of physicochemical characteristics specific to nano-size particles that result in distinctive mechanical, magnetic, electronic, catalytic, and chemical properties. The large surface-to-volume ratio characteristics of nano-size materials can lead to interesting and some time surprising surface and quantum size effects. Overall, as the size of the particles decreases, the proportion of surface and near surface atoms increases; and surface atoms would tend to have more unsatisfied or dangling bonds with concomitantly higher surface energy (Li et al. 2006a). Thus, the surface atoms would have a stronger tendency to interact, adsorb, and react with other atoms or molecules in order to achieve surface stabilization (Service 1998).

nZVI is anticipated to serve as either an alternative or supplement to the conventional ZVI-based PRB technology. For example, injections of nZVI could be used to address the heavily contaminated source area or other “hot spots” whereas the traditional ZVI-PRB would function as barrier to contain the dispersion of contaminants.

Because of their small size, nanoparticle slurries could be injected under pressure and/or even by gravity flow to the contaminated area and under certain conditions remain in suspension and flow with water for extended periods of time. Alternatively, nZVI can also be used in the treatment of wastewater effluent as investigated in this research.

Columns have been used in several past studies to determine the efficiency of sorbents such as ZVI in dynamic systems (Blowes et al. 1997; Gu et al. 1999; Matheson and Tratnyek 1994; Moraci and Calabro 2010). Example studies of the removal of pollutants from aqueous solutions using columns have used water contaminated with inorganic species such as hexavalent chromium (Cr^{+6}) (Astrup et al. 2000; Blowes et al. 1997; Puls et al. 1999), uranium (Morrison et al. 2001; Simon et al. 2003), arsenic (Koeber et al. 2005; Lien and Wilkin 2005b; Su and Puls 2003), nitrate (Till et al. 1998; Westerhoff and James 2003), and mercury (Hg) (Weisener et al. 2005). Column studies have also been used to determine the efficiency of sorbents on complex water matrices such as acid mine drainage (Wilkin and McNeil 2003).

In the only field pilot study of removal of Hg from groundwater using columns packed with ZVI, Weisener et al. (2005) were able to lower the concentration of treated waters from 40 μg/L to 4.0 μg/L (or 4000 ng/L). This drop of initial concentration to low ppb level is rather promising. The availability of highly sensitive analytical techniques (e.g. cold vapor atomic fluorescence spectroscopy or CV-AFS) detecting aqueous Hg in parts per trillion levels on one hand; and the potential for harm to aquatic biota by long term discharges of wastewater effluents containing Hg concentrations in the low ppb range has led the US EPA to target 12 to 15 ng/L as action limit concentrations for

discharged wastewater effluents (Hanlon 2007). Unfortunately, there is no remediation technique available, which removes aqueous Hg from wastewater effluents to such low levels.

The objective of this research is to use nZVI in column experiments to: (i) assess the potential of these NMs to remove Hg from aqueous effluents in flow-through columns; (ii) investigate the different parameters that affect the efficiency of Hg removal; and (iii) lay the groundwork for the development of remediation approach that meets the Hg concentration range targeted by the US-EPA.

Materials and Methods

Particle Characterization

For comparison purposes, the initial set of column experiments used both ZVI and nZVI. For these experiments, ZVI particles had a size ranging from1 to 2 mm and were obtained from Alfa Aesar (PA, USA). The nZVI particles were obtained from Quantum Sphere, Inc. (CA, USA), with vendor's reported particle size range of 15 to 25 nm. For these particles, the N2-BET specific surface areas (SSA) were determined using a Quanto-Chrome NOVA 1200 at the Particle Engineering Research Center, University of Florida. The measured SSA values were 0.116 m^2/g and 30.5 m^2/g for ZVI and nZVI, respectively.

Column Preparation and Setup

Polyvinyl chloride (PVC) columns were purchased from Alsco Industrial Co (Lithia Springs, GA). The columns were 20 cm long and had an inner diameter of 2.54 cm. Each column was fitted with PVC screw caps at both ends. The screw caps were perforated to hold a ¼" Teflon tubing which allowed controlled water pumping in and out of the columns. Before being capped, columns were packed with a "*reactive solid*

mixture" made of sand and iron particles. In fact, columns packed with 100% ZVI have been used by other researchers to remove Hg from ground water. Findings from these studies show that ZVI oxidation over time leads to the formation of thick oxyhydroxide layers and clogging of the columns (Cundy et al. 2008; Weisener et al. 2005). To avoid this outcome, a reactive mixture of sand and iron particles is used instead, and the mass of iron particles used to spike the sand was based on SSA equivalent. Accordingly, in these column studies, the reactive mixtures were made of sand containing either 0.03 g of nZVI or 8 g of ZVI dispersed in sand with a final total mass of 25 g. This reactive mixture was then sandwiched between support layers of 5 g of plain sand and glass wool, (see Figure 4-1). The inlets of the columns were connected to the Hg-containing influent container by pumps. High pressure pumps (LC 10AT Shimadzu) commonly used in High Performance Liquid Chromatography (HPLC) were used here to obtain an accurate control of flow rates. In addition, the use of such pumps allowed for a complete wetting of the columns and helped avoid the formation of voids filled with trapped air (Bartzas et al. 2006). The Teflon tubing on the outlet end was used to collect sample effluents over time.

Water Used in Column Studies and Experimental Protocol

The water used as influent in these column studies was a filtered (0.45 μm) wastewater effluent (WW) collected from the wastewater treatment facility located on the campus of the University of Florida. The background solution chemistry of used WW is presented in Table 4-1. Note a background total-Hg concentration of 55 μg/L and a dissolved organic carbon (DOC) content of ~8mg C/L was present in the WW.

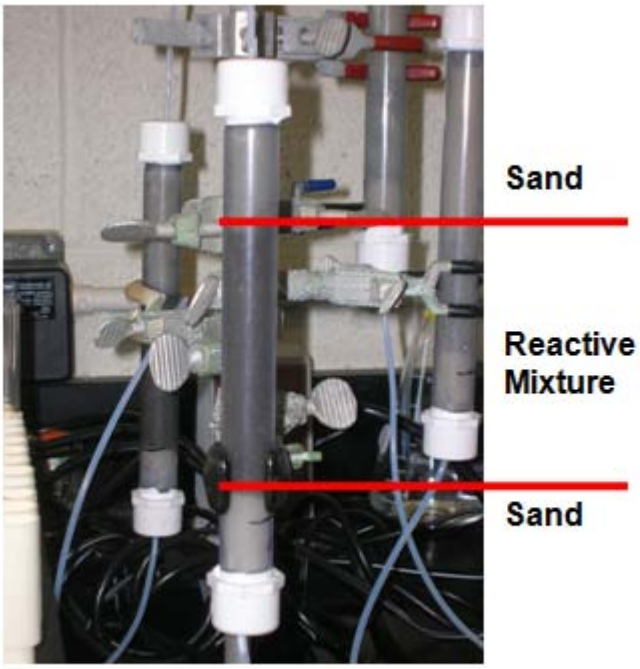

Figure 4-1. Picture of the experimental setup used in described column studies. The different layers are labeled, where the “reactive mixture” corresponds to the portion of the column containing a mixture of sand and iron particles in fixed ratios. 1:2.12 g/g for ZVI and 0.01:6.66 g/g for nZVI

The above background Hg level was increased intentionally prior to use in column experiments by spiking with aliquots of a $Hg(NO_3)_2$ solution (1000ppm standard solution obtained from Fisher Scientific, USA).

Table 4-1. Chemical composition of wastewater effluent used in column studies

Parameter	Concentration (mg/L)
Chlorine, Cl^-	125.5
Fluoride, F^-	0.583
Phosphate, PO_4^-	7.079
Nitrate, NO_3^-	4.589
Potassium, K^+	10.930
Magnesium, Mg^{2+}	33.620
Calcium, Ca^{2+}	55.940
Sodium, Na^+	60.230
Sulfate, SO_4^{2-}	201.5
Dissolved Organic Carbon	8.000
Carbonaceous Biological Oxygen Demand (CBOD)	3.070
Mercury Concentration	0.055

Prior to initiating the Hg removal experiments, columns packed with iron particles were first rinsed by pumping through de-ionized (DI) water for 24 hours at a flow of 50 μL/min. This first step was then followed by the introduction of a 0.1M sodium hydroxide (NaOH) solution. Columns were filled up with NaOH and left without flow for 120 hours contact, to help expedite the oxidation of metallic iron surfaces (Feng et al. 2007). This step was intended to favor the formation of oxyhydroxide layers that support the removal of Hg by adsorption and minimizes Hg losses from solution by volatilization. After rinsing with DI-water, Hg-containing influents were pumped up gradient through the packed columns to initiate the Hg removal from WW effluent experiments.

On temporal basis, effluent aliquots were collected at the outlet end of the column and analyzed for total Hg concentration. Hg was analyzed by the $SnCl_2$-reduction technique after sample oxidation by bromine monochloride (BrCl), pre-reduction by hydroxylamine and then detection by atomic fluorescence spectrometry (Tekran Model 2600). Details on used analytical procedures and QA/QC criteria (blanks and Hg standard solutions) have been described in several earlier publications by our research group (Hovsepyan and Bonzongo 2009; Warner et al. 2005; Warner et al. 2004)

Optimization of Mercury Removal in Columns Containing Nano Zero Valent Iron: Effects of Particle Mass, Flow Rate, and Water Chemical Composition

Additional experiments were conducted to assess the effects of selected key parameters on the ability of nZVI to remove Hg in flow-through columns. First, the effect of nZVI mass used to prepare the reactive media was investigated by running columns with nZVI content of 0.1% and 1.0% on a weight basis. Hg-containing effluents were pumped up gradient through the columns at a flow rate of 50 μL/min.

In a second set of experiments, by maintaining the nZVI content at 0.1%, the flow rate of 25 and 75 μL/min was used in addition to the 50 μL/min initial value and the effect of Hg removal assessed. Another set of experiments used hydrogen peroxide (H_2O_2) treated WW effluent at a final concentration of ~1% to help oxidize the dissolved organic compounds, and therefore, release Hg complexed by such organic ligands prior to introduction to the 0.1% nZVI columns.

Use of columns in series and study of the effects of competitive cations. In these experiments, two columns packed with 0.1% nZVI, and connected in series were used to (i) investigate the potential for increased Hg removal to ng/L level, and (ii) assess the impact of cation competition. The WW influent was pumped up gradient of column 1 and the effluent of column 1 was pumped up gradient of column 2. The effluent of column 2 was then sampled over time, and analyzed for total Hg as described earlier. A similar setup was used. However, to investigate the effects of Zn and Cd (Zn and Cd were added to used influents to produce final concentrations 100 μg/L or ppb for each) as competitive ions on Hg removal by nZVI.

Statistical Analysis

For all of the above experiments, duplicate columns were run, and whenever necessary, experiments were repeated. To evaluate the significance of differences observed between treatments, a simple t-test for equal or unequal variance was used at a confidence level of 95%. The analysis was performed using the Microsoft Office Excel 2003 statistical data analysis tools.

Results and Discussion

Effects of Iron Particle Size on Mercury Removal from Wastewater Effluent

Figure 4-2 gives the trends of Hg removal from the WW effluent in columns packed with nZVI and ZVI. The Hg effluent concentration (C) was normalized by the Hg influent concentration (C_o). The column breakthrough occurs when the effluent concentration matched the influent concentration and C/C_o equals 1. Once the column adsorption sites are saturated, the bound Hg has a tendency to be leached off. In Figure 4-2, C/C_o values greater than 1.0 occur when previously sorbed Hg leaches off the column. However, over time this level decreases back to the influent concentration.

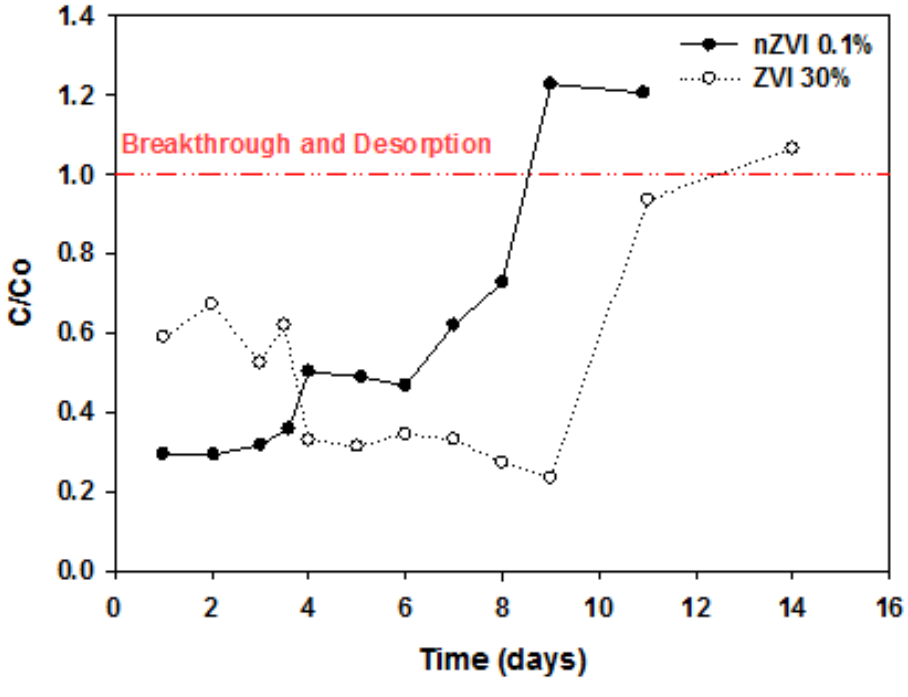

¶

Figure 4-2. Comparison of adsorption profiles of Hg onto ZVI and nZVI. The wastewater influent was spiked to produce a final total Hg concentration of 150 μg Hg/L. The weight percent of iron particles within the sand matrix was 0.1% and 30% for nZVI and ZVI, respectively and corresponding to a specific surface area of 0.92m^2. Column effluent fractions were taken over time, analyzed for total-Hg concentration and the result normalized to the influent Hg-concentration. C/C_0>1 indicates desorption of previously adsorbed Hg

The masses of iron particles used were selected to produce a similar exposed SSA of 0.92 m^2 by either ZVI or nZVI. The influent was pumped through these columns at a flow rate of 50 μL/min, and this value was determined based on preliminary laboratory tests (data not shown). The adsorption profile of nZVI can be divided into three different sections (Figure 4-2). The first section, day 1 through day 4, had a constant Hg concentration at around 40 μg/L. From day 4 to day 6, the removal efficiency decreased slightly with a second plateau formed at ~65 μg Hg/L. The last section is a linear increase in Hg concentration in the effluent leading to the break through at day 9. These trends suggest that the higher rate of nZVI oxidation results in an early Hg removal of Hg and an apparent progressive saturation that leads to a breakthrough passed 8 days after the start of the experiment. On the other hand, column packed with ZVI show a rather poor removal efficiency in the first 4 days, prior to exhibiting a removal efficiency similar to that obtained with nZVI in the first 4 days. Then a quick breakthrough at about 9 days is observed, as well. Assuming that adsorption onto Fe-oxyhydroxide is the main removal mechanism for both particle types; it appears that the rate at which these particles become coated with oxyhydroxide layers dictates their temporal efficiencies.

Blowes et al (1997) showed that when remediating Cr(VI), the particle size matters as they compared iron filings (0.5 -1.0 mm) to iron chips (1.0 – 5.0 mm). The fillings were more efficient. In this study, nZVI had a higher Hg loading when expressed per mass of sorbent basis (1791 and 7.821 μg Hg/g for nZVI and ZVI, respectively). However, when Hg loading was expressed per SSA, an opposite trend was obtained, with 58.71 and 67.24 μg Hg/m2 for nZVI and ZVI, respectively. From these column

studies, nZVI packed-columns decreased the levels of Hg present in the effluent from 150 μg Hg/L to ~30 μg Hg/L while ZVI lowered Hg levels down to only 60 μg Hg/L even though its Hg loading per SSA is higher than that of nZVI.

Effect of Nano Zero Valent Iron Mass on Mercury Removal

Figure 4-2 showed that nZVI has the potential of removing large amounts of Hg based on mass of adsorbent used. Therefore, increasing the mass of nZVI in the reactive mixture should theoretically increase the amount of Hg adsorbed. Figure 4-3 shows Hg removal profiles in columns packed with different masses of nZVI (0.1% or 0.025 g and 1.0% or 0.250 g). In Figure 4-3, C/C_o values greater than 1.0 occur when previously sorbed Hg leaches off the column as explained previously.

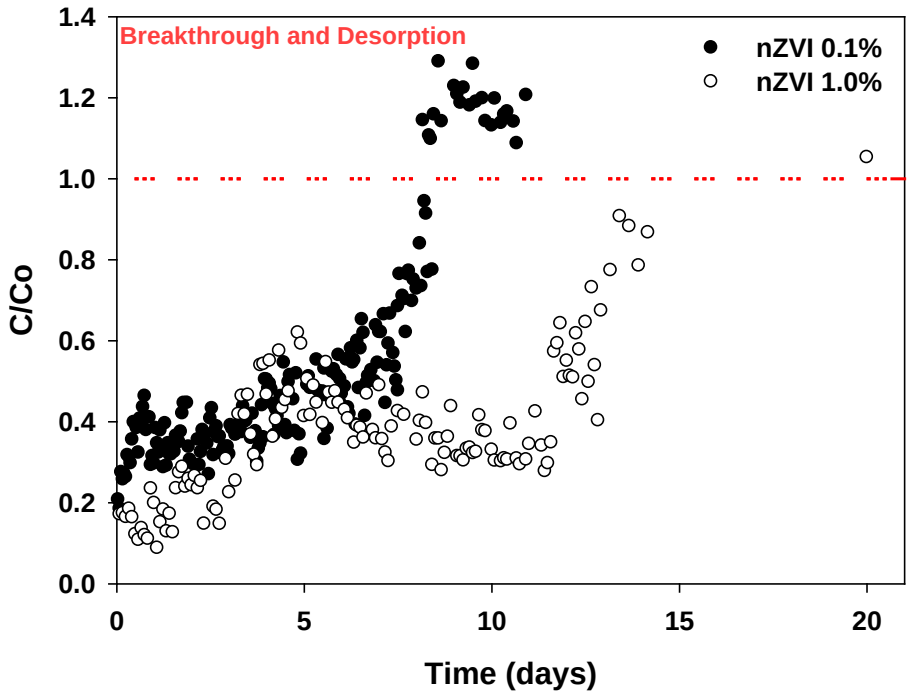

Figure 4-3. Trends of Hg removal from wastewater influent containing150 μg Hg/L in columns packed with nZVI at 0.1% and 1% per mass basis. The influent was pumped up gradient at 50 μL/min. Column effluent fractions were taken over time, analyzed for total-Hg concentration and the result normalized to the influent Hg-concentration. C/C_0>1 indicates desorption of previously adsorbed Hg

Increasing the mass of nZVI does increase the total amount of Hg adsorbed, and the breakthrough point is shifted from day 9 to day 14 (Figure 4-3). The total mass of Hg adsorbed was 44.77 and 84.03 μg Hg for columns with for 0.1% and 1.0% nZVI, respectively.

When expressed per SSA basis, the average amount of Hg removed by columns containing 1.0% nZVI was lower (11.02 μg Hg /m^2) than the Hg mass per SSA in the 0.1% nZVI column. Alowitz et al. (2002) obtained a similar trend with Cr(VI) adsorption studies, and where they showed a lack of correlation between metal removal and SSA (Alowitz and Scherer 2002). This observation suggests there are Hg fractions in solution not available for adsorption. One possibility is that Hg complexed to organic ligands could become unavailable for adsorption on Fe-oxyhydroxide layers, therefore, limiting the removal capacity of the iron particles. If true, the oxidation of dissolved organic matter present in the sample could help improve the removal efficiency, which is investigated in a latter section.

Effect of Flow Rate on Mercury Removal

Mercury adsorption was investigated under flow rate conditions of 25, 50 and 75 μL/min. The results are presented in Figure 4-4; C/C_o values greater than 1.0 occur when previously sorbed Hg leaches off the column.

As the flow rate is increased from 25 to 75 μL/min, the Hg loading increases and the lifetime of the column increases as well. However, when a flow rate of 500 μL/min was used (data not shown), no Hg removal occurred. This trend is opposite to some of the findings reported in the literature, in that decreasing flow rates increased removal efficiencies of ZVI for uranium (Morrison et al. 2001) and Hg (Weisener et al. 2005).

This discrepancy probably stems from a number of factors. First, the particle size used, and second, the amount of particles and column packing methods (100% ZVI versus reactive medium mixing sand and a small fraction of nZVI).

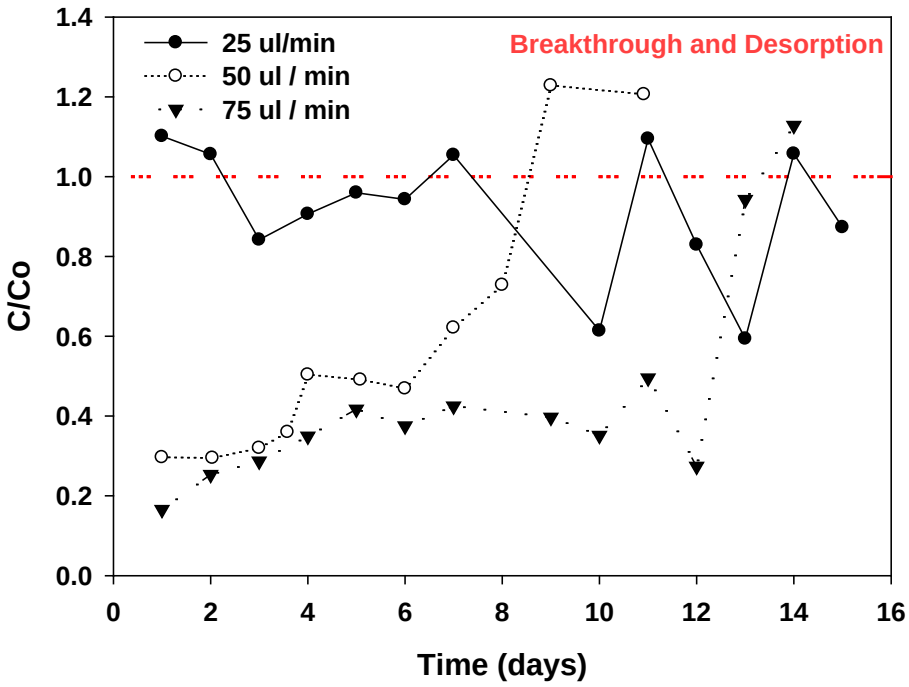

Figure 4-4. Effect of flow rates on adsorption profile of nZVI. Influents are Hg-spiked wastewater effluent (150 μg Hg/L). The weight percent of reactive media used was 0.1% nZVI. The influent was pumped up gradient at different flow rates (25, 50, 75 μl/min). Column effluent fractions were taken over time, analyzed for total-Hg concentration and the result normalized to the influent Hg-concentration. C/C_0>1 indicates desorption of previously adsorbed Hg

In fact, for the mixture of sand and nZVI used in this study, the excess sand might cause the so-called "*null pathways*" to form in the column due to differences in particle size between nZVI and sand (Wilkin et al. 2005a; Wilkin et al. 2005b). Figure 4-5, shows an idealized vertical cross section of a mixed reactive media. In this case, the white bigger circles represent sand particles and the smaller black circles represent nZVI particles. Two different pathways are shown in red. Solution in pathway 1 comes into

contact with more nZVI particles than in pathway 2, which can be qualified as “null pathway”. For adsorption to take place, the Hg needs to come into direct contact with the nZVI particles. It is possible that at very low flow rates through the column, null pathways are formed, and consequently, Hg is not adsorbed. However, as the flow rate is increased, Hg removal increases as well, which suggests a more uniform flow characteristics through the column and very little to no null pathway.

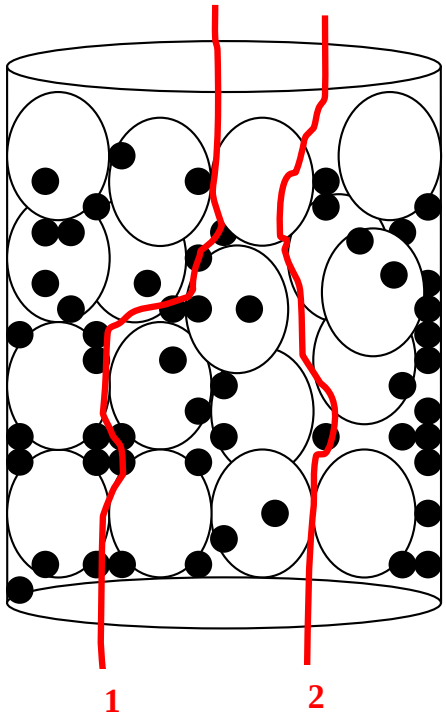

Figure 4-5. Cross sectional representation of the column’s reactive media

Hydrogen Peroxide Treatment of the Influent and Oxidation of Dissolved Organic Compounds to Improve Mercury Removal from Solution

The influent used in this study contained 8 mg /L of dissolved organic carbon (see Table 4-1). Accordingly, the high affinity of Hg for organic ligands may hinder the removal of Hg and limit the efficiency of these columns to levels much higher than the ng/L concentration range targeted by regulation agencies. This is likely one of the

reasons explaining the fact that Hg concentrations in the treated effluents never dropped down to low ng/L levels. Therefore, treating the influent with an oxidizing agent such as H_2O_2 (used at a final concentration of 1% (v/v) in this study) could help release Hg previously bound to dissolved organic matter (DOM).

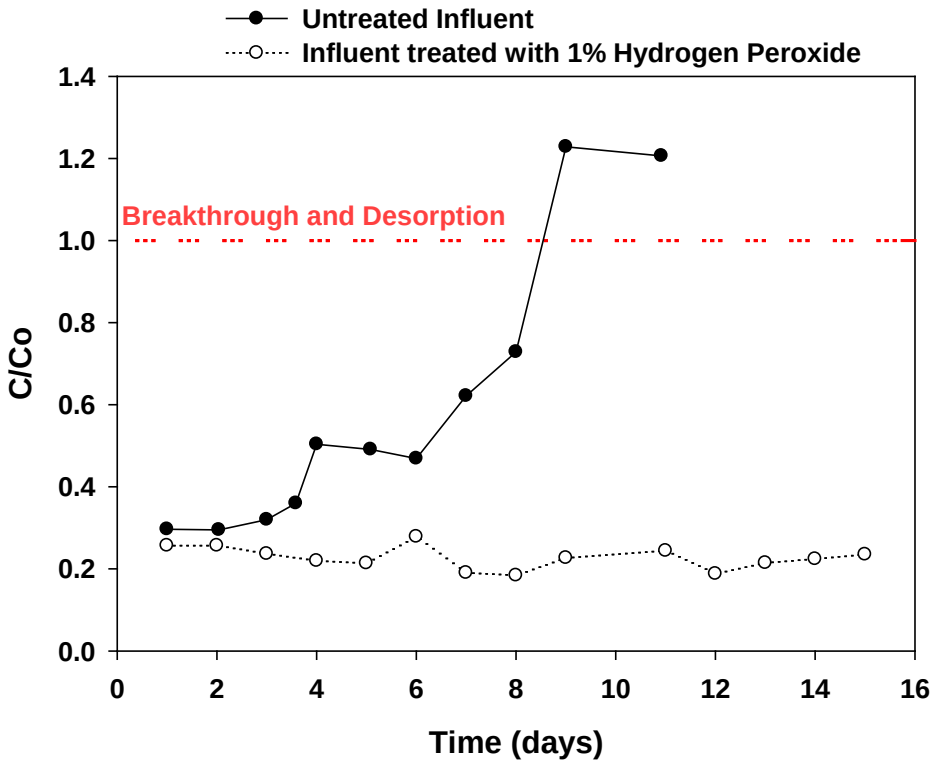

Figure 4-6. Effect of influent pretreatment on adsorption profile of *n*ZVI. Influent for column was Hg-spiked wastewater effluent (150 μg Hg/L). The influent was treated with 1% hydrogen peroxide to degrade any Hg bound to organic matter. The weight percent of reactive media used was 0.1% nZVI. The influent was pumped up gradient at 50 μl/min. Column effluent fractions were taken over time, analyzed for total-Hg concentration and the result normalized to the influent Hg-concentration. $C/C_0>1$ indicates desorption of previously adsorbed Hg

Using such an approach and running the influent through a nZVI packed column, the removal profile shown in Figure 4-6 was obtained. The H_2O_2-treated influent resulted in a steady concentration of 35 μg Hg/L in the effluent, and a significant delay of the breakthrough (>30 days) as compared to non-treated influent. However, this

treatment did not improve the column efficiency in terms of lowering Hg levels in the effluent to the12 to 15 ng/L levels. This could come from the inefficiency of the oxidizing agent at used concentration. In fact, the analysis of DOC in both untreated and treated influents showed only a slight drop from the initial 8 mg C/L to about 6 mg C/L in the untreated and treated influents, respectively (Figure 4-7).

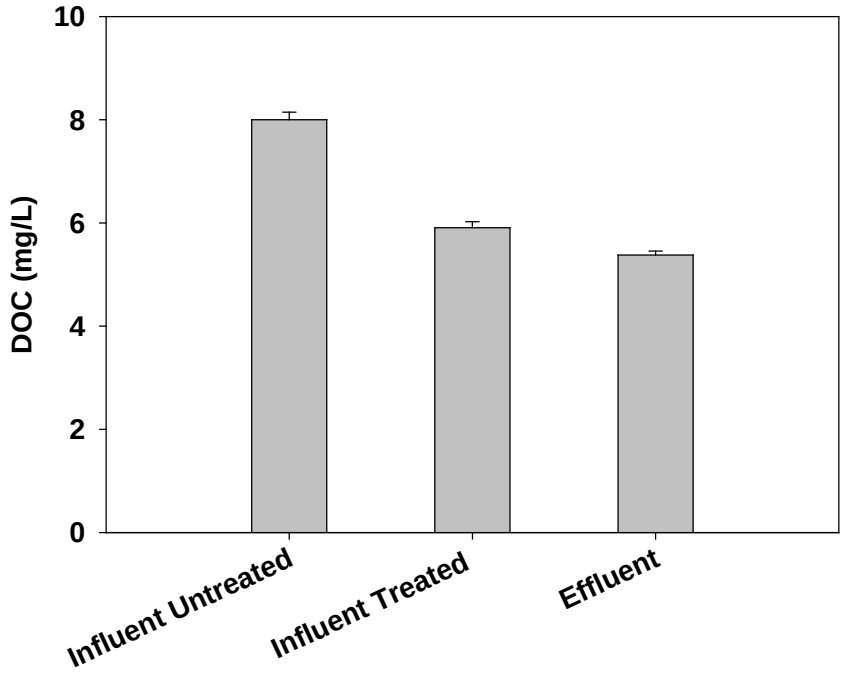

Figure 4-7. Effect of hydrogen peroxide (H_2O_2) treatment on dissolved organic matter present in wastewater used as influent in column studies.

This shows that the 1% H_2O_2 treatment used was not adequate to obtain a complete oxidation of DOM present in the effluent. A higher concentration of H_2O_2 or a much stronger oxidizing agent would have been more appropriate, and unfortunately, this was not accomplished in this study. One possibility for the poor DOM oxidation result could be the complex structure of organic matter present in used influent. A literature review published by Shon et al. (2006), and focusing on the type of organic matter present in biologically treated wastewater effluents identified a wide variety of

organic compounds (Figure 4-8). As shown in this figure, DOC present in such WW can contain recalcitrant compounds such as humic acids, which may strongly bind with metals while remaining hard to oxidize. The influent and effluent solutions used in this study were further characterized by fluorescence excitation-emission spectrometry. This technique scans the sample to produce an excitation-emission matrix (EEM).

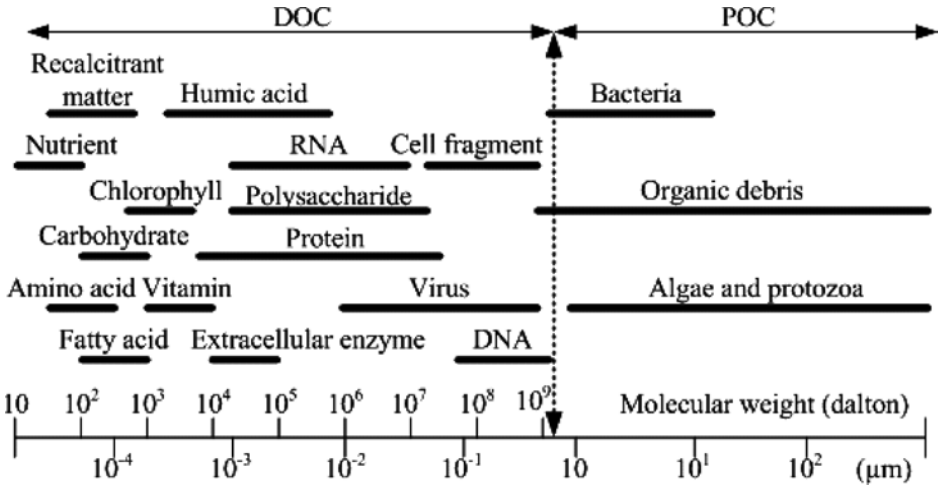

Figure 4-8. Organic constituents present in wastewater effluents (Shon et al. 2006).

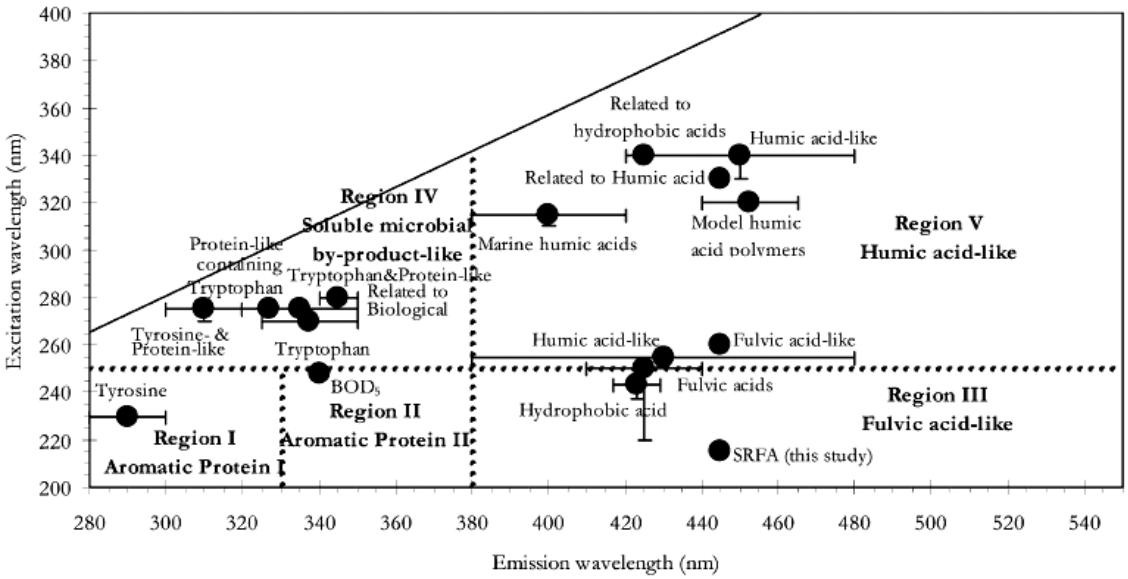

Figure 4-9. Excitation-emission peaks of dominant soluble organic matter compounds based on a literature review published by Chen et al. (2003).

The matrix consisted of emission wavelengths from 250 nm to 550 nm at 2 nm intervals and excitation wavelengths from 220 nm to 400 nm at 5 nm intervals with a scan speed of 1500 nm/min. In general, data obtained from EEM studies are graphed in three dimension plots – and where the y-axis represents the excitation wavelength, the x- axis represents emission wavelength, and the z-axis represents the intensity of the peak at that specific excitation and emission point. Using this technique, Chen et al. (2003) mapped different types of organic matter into different spectral regions (Figure 4-9). This graph is subdivided into five regions based on the most dominant organic fractions as follows:

- Regions I and II: aromatic proteins, boundaries are at shorter excitation wavelength <250 nm and shorter emission wavelength <350 nm
- Region III: fulvic acid like organics, boundaries are at shorter excitation wavelength <250 nm and longer emission wavelength >350 nm
- Region IV: soluble microbial by product, boundaries are at intermediate excitation wavelength 250-280 nm and shorter emission wavelength <380 nm
- Region V: humic acid like organics, boundaries are at longer excitation wavelength >280 nm and longer emission wavelength >380 nm

This map can be used as a guide to distinguish the type of organic carbon present in the sample by matching peaks in the different regions shown above. Figure 4-10 gives the EEM of the influent without treatment (A), H_2O_2-treated influent (B), and that of the column effluent from treated influent (C). From these figures, two main observations can be made. First, peaks corresponding to 2 to 3 major organic compound types are present with the same intensity in both the treated and untreated water influents. Second, compounds giving the dominant peaks can be roughly assigned to regions I, III, and IV (e.g. aromatic proteins, fulvic acids, and soluble microbial by-products)IV.

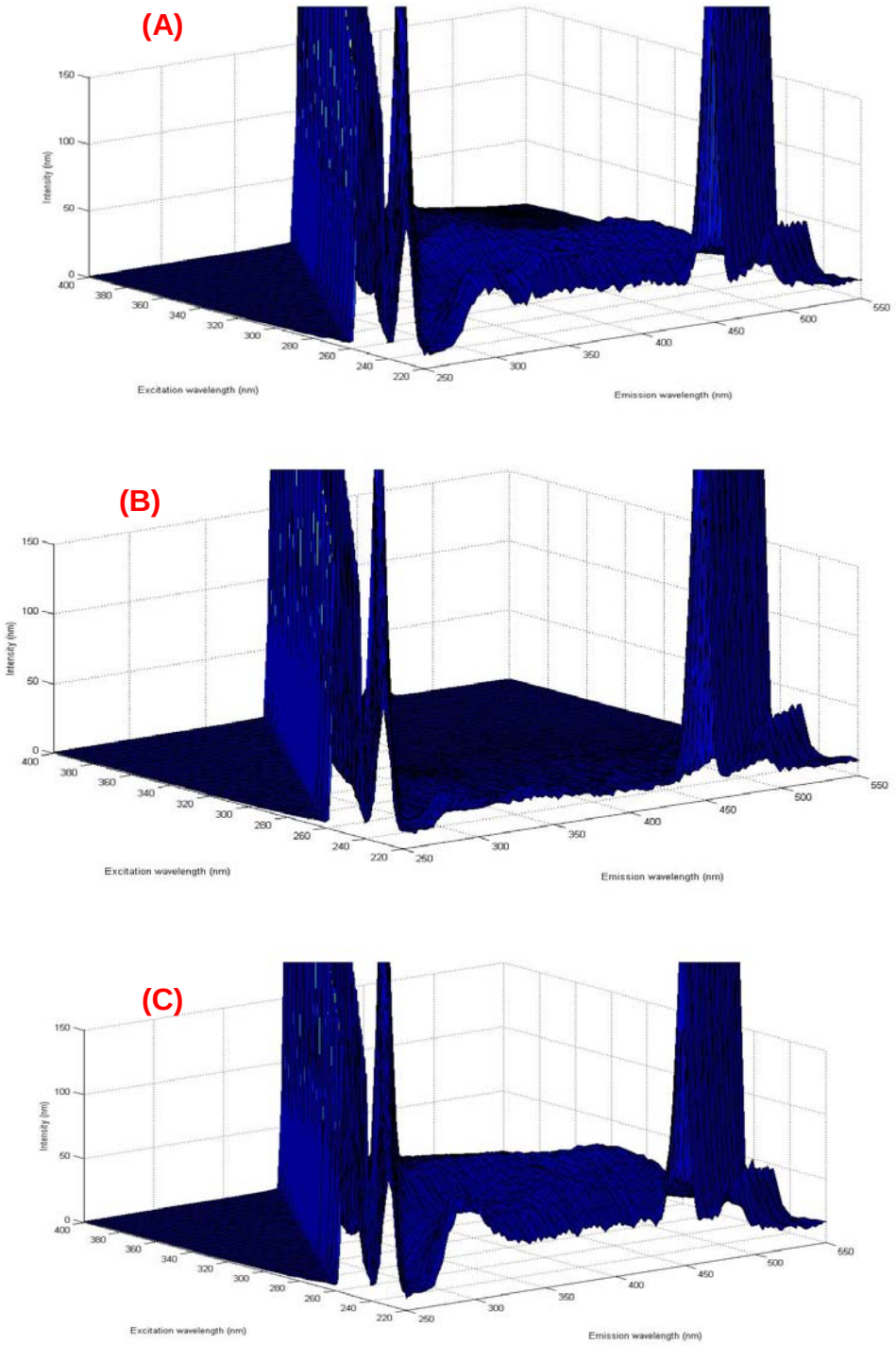

Figure 4-10. Excitation emission spectra to determine dominant organic species present. (A) column influent untreated, (B) column influent treated with 1% hydrogen peroxide, and (C) column effluent. The x axis is the emission wavelength (nm), the y-axis is the excitation wavelength (nm) and the z axis is the peak intensity.

The used H_2O_2 treatment was n therefore not strong enough to break down these organic compounds. As observed in Figure 4-10, the influent did have some minor peaks in region II, III, IV, and V which were reduced after the H_2O_2 treatment. However, the extent of the dominant peaks remained the same. This is a likely explanation as to why Hg removal efficiency did not increase after H_2O_2 treatment. However, the observed delayed breakthrough (Figure 4-6) on the other hand suggests that H_2O_2 treatment some beneficial effects including a contribution to the oxidation of iron particle surfaces, and therefore the increase in Hg adsorption capacity. Unfortunately, Hg bound to complex DOM compounds remained in solution and were able to pass through the column unretained.

The potential of H_2O_2 to decrease total-Hg levels of the influent by volatilization prior to pumping through the column was also investigated. This is because H_2O_2 has been linked to the volatilization of Hg in natural waters (Amyot et al. 1997; Amyot et al. 1994; Schroeder et al. 1992). Experiments to verify this possibility were conducted over a 20-day time period. 25 mL of WW was treated with 1% H_2O_2 was added to 50 mL headspace vials. The vials were capped and allowed to incubate for 20 days, after which 100 μL headspace gas samples were analyzed for Hg^0. Levels of Hg^0 in the corresponding aqueous phase (Hg^0_{aq}) were calculated using Henry's Law. This approach allowed for the determination of the total amount of Hg^0 (Hg^0_T) produced in the reactor (i.e. $Hg^0_T = Hg^0_{aq} + Hg^0_{gas}$). Figure 4-11, shows the extent of Hg volatilization from WW samples untreated and treated with H_2O_2..

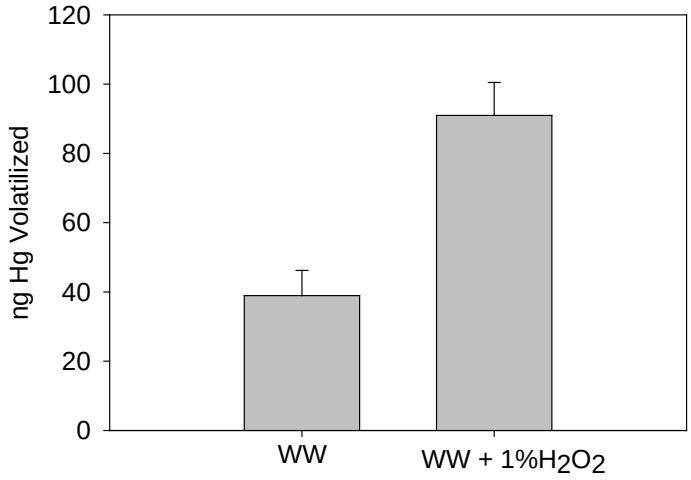

Figure 4-11. Volatilization of Hg in wastewater effluent (WW) and WW treated with 1% hydrogen peroxide (H_2O_2) with an incubation time of 20 days in closed headspace vials. Levels of Hg^0 in the corresponding aqueous phase (Hg^0_{aq}) were calculated using Henry's Law. This approach allowed for the determination of the total amount of Hg^0 (Hg^0_T) produced in the reactor at any sampling time (i.e. $Hg^0_T = Hg^0_{aq} + Hg^0_{gas}$). Y-axis represents the mass of total Hg^0 produced in ng.

WW samples treated with 1% H_2O_2 volatilized more Hg, 91 ng Hg^0, than untreated WW samples, 39 ng Hg^0, over the 20 day incubation period. This was about 2.42% and 1%, of the total Hg in the system, which was 3750 ng Hg, for treated and untreated samples, respectively. These results suggest that H_2O_2 induced Hg loss by volatilization could be considered negligible within the time frame used for column studies described herein.

Mercury Removal Using Column in Series and Effect of Zinc and Cadmium as Competitive Cations

The above tested changes in nZVI mass, influent flow rates, and influent oxidation with H_2O_2 have decreased the effluent concentration of Hg, but not down to the acceptable low ng/L levels mentioned earlier. To verify the fact that this Hg removal limitation was likely due to Hg speciation, two columns joined in series were used to

expose Hg exiting the first column to fresh nZVI surfaces and potentially decrease the concentration of Hg at the outlet of the second column. Figure 4-12 shows data comparing Hg trends in effluents from a single column versus two columns used in series with all operating parameters being identical. In Figure 4-12 C/C_o values >1.0 occur when previously sorbed Hg leaches off the column.

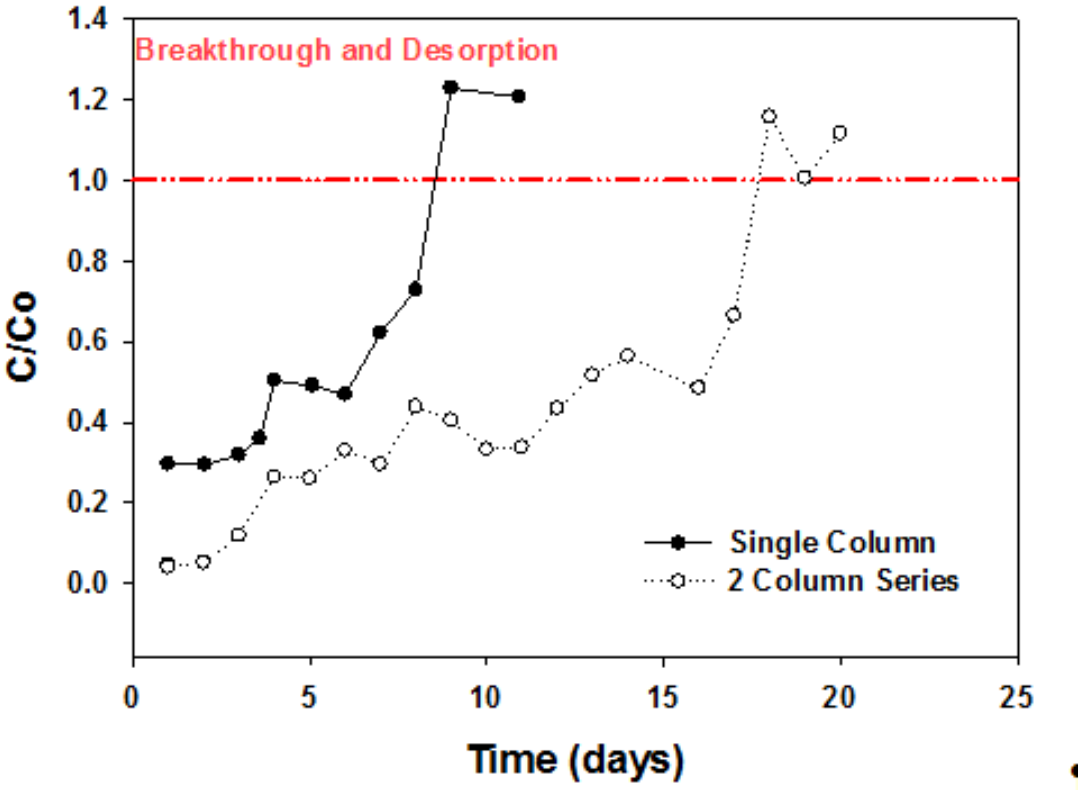

Figure 4-12. Mercury removal from wastewater (WW) effluent in a single column and two columns used in series. Used influent solution was spiked with Hg to a final concentration of 150 μg Hg/L. The weight percent of reactive media used was 0.1% nZVI. The influent was pumped up gradient at 50 μL/min. Column effluent fractions were taken over time, analyzed for total-Hg concentration and the results normalized to the influent Hg-concentration. C/C_0>1 indicates desorption of previously adsorbed Hg

The first 4 days of the column in series brought Hg concentrations down to 10 μg Hg/L. However this range increases over time and plateau around 45 μg/L from day 4 to

day 9. The residual Hg not being adsorbed may be due to the unavailability of Hg and lack of interaction with oxidized iron particle surfaces. Additionally, based on EEMs data presented in Figure 4-10, Hg is likely bound to aromatic proteins, fulvic acids, and soluble microbial byproducts.

Since columns used in series seemed to slightly improve Hg removal from solution, this setup was used to test if the presence of competitive cations in influent water would compete with Hg for adsorption sites. For that purpose, cadmium (Cd) and zinc (Zn) were chosen. Cd, Hg, and Zn belong to Group IIB in the periodic table of the elements and have a number of similar geochemical behavior, such as their strong affinity for sulfur containing compounds and their classification on the Goldschmidt's scale (Krauskopf and Bird 1995). In addition, they exhibit similar ionic radius and electronegativities (Table 4-2) (Jing et al. 2007; Krauskopf and Bird 1995).

Table 4-2. Ionic radii and electronegativities (Krauskopf and Bird 1995).

Element	Ionic radius(Å)	Electronegativity
Hg	1.02	1.9
Cd	0.95	1.7
Zn	0.74	1.7

Figure 4-13 shows how the addition of Cd and Zn affects the adsorption of Hg and C/C_o values greater than 1.0 occur when previously sorbed Hg leaches off the column.

These cations, at the concentrations tested, did not have a significant effect on the Hg adsorption onto nZVI. The slightly higher electronegativity of Hg as compared to Cd and Zn leads to a greater affinity of ionic Hg for negatively charged oxygen from iron oxyhydroxide layers.

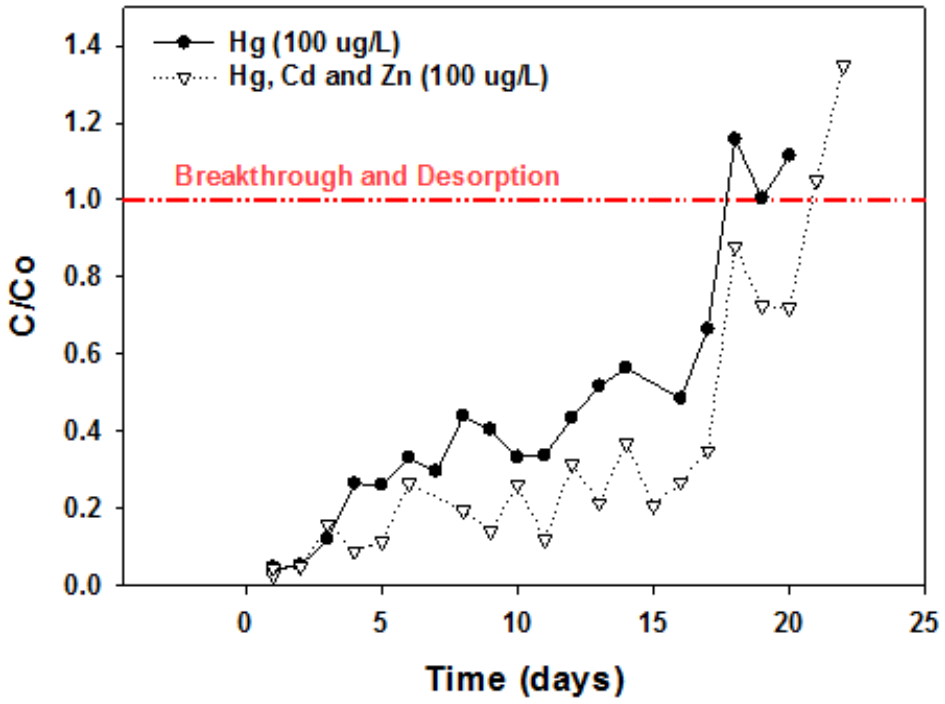

Figure 4-13. Effect of cadmium (Cd) and zinc (Zn), on the removal of Hg from a wastewater used as influent in a study using two 0.1%-nZVI packed columns in series. Used influent solution was spiked with Hg to a final concentration of 150 μg Hg/L. The weight percent of reactive media used was 0.1% *n*ZVI. The influent was pumped up gradient at 50 μL/min. Column effluent fractions were taken over time, analyzed for total-Hg concentration and the result normalized to the influent Hg-concentration. $C/C_0>1$ indicates desorption of previously adsorbed Hg

Scanning Electron Microscopy Characterization of the Reactive Media

Scanning electron microscopy (SEM) was used to analyze the nZVI particles before and after Hg removal experiments. The purpose of this effort was to indentify the presence of Hg on the surface of nZVI particles used in the make up of the reactive media. SEM images of raw nZVI (Figure 4-14) show that the raw nZVI particles are dominantly aggregated. The coupling of SEM to energy dispersive spectroscopy (EDS) analysis of the sample showed oxygen peaks (see red box), suggesting the presence of oxides on nZVI surfaces before they were treated with NaOH and used in Hg-removal laboratory experiments. This could have contributed to the extent of Hg retention by

nZVI containing columns in the first few days of the Hg removal experiments (see Figure 4-2).

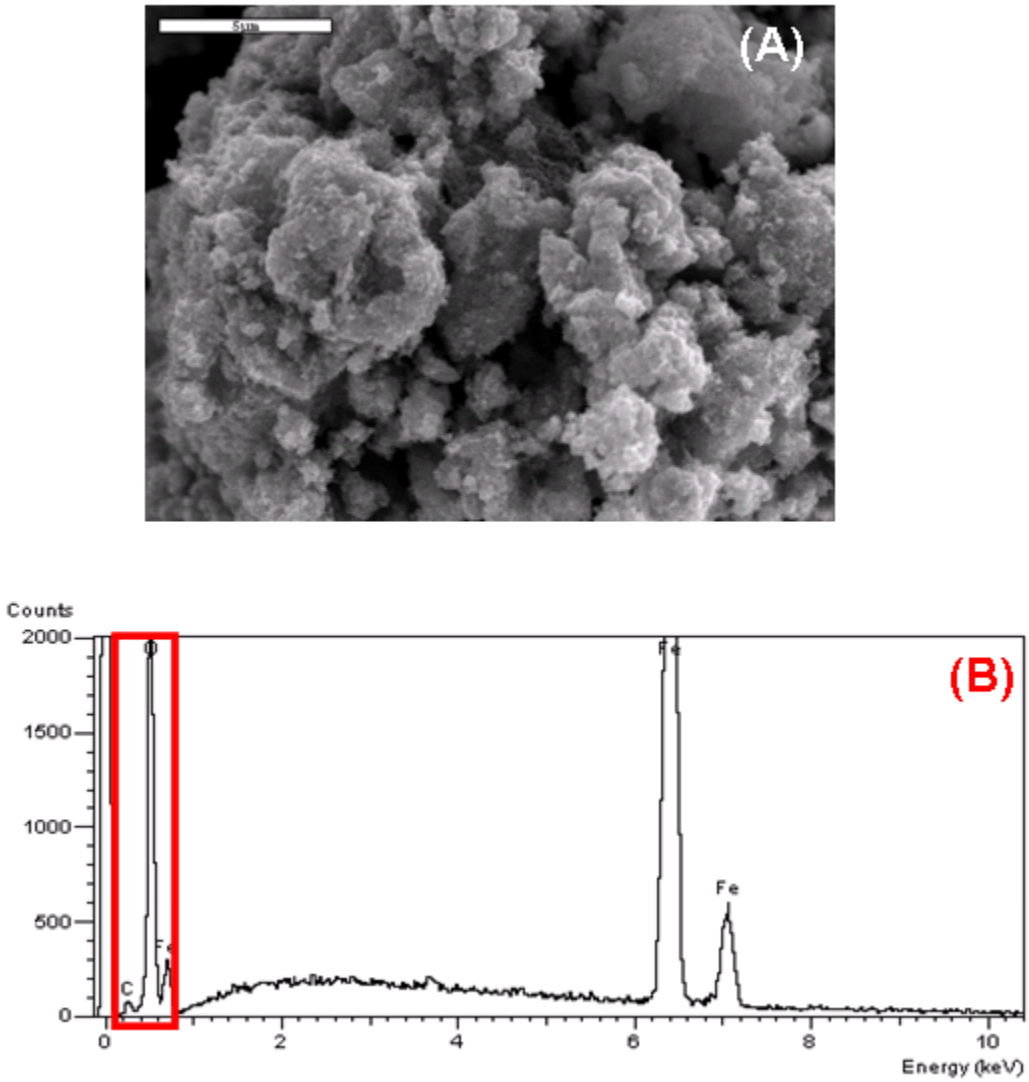

Figure 4-14. (A) SEM image of pure nZVI at 600x. (B) EDS spectrum of pure nZVI. The presence of a large oxygen peak is highlighted by red box.

At the end of these Hg removal experiments, a fraction of the reactive media (i.e. mixture of sand and nZVI) was sampled, freeze-dried and then analyzed by SEM-EDS. Figure 4-15 shows the corresponding SEM images of materials obtained from the first column (column 1). Figure 4-15A shows a sand particle with iron oxides on the surface.

Similarly, analysis of column 2 shows iron oxides on the surface (Figure 4-15B). Figure 4-16C shows a higher resolution of the framed red box where the iron oxides are formed on the surface of the sand particles. Overall, since the dominant sand matrix was made of much larger particles than those of nZVI, even when aggregated, Fe is therefore detected onto those sand particles, which are acting as support materials.

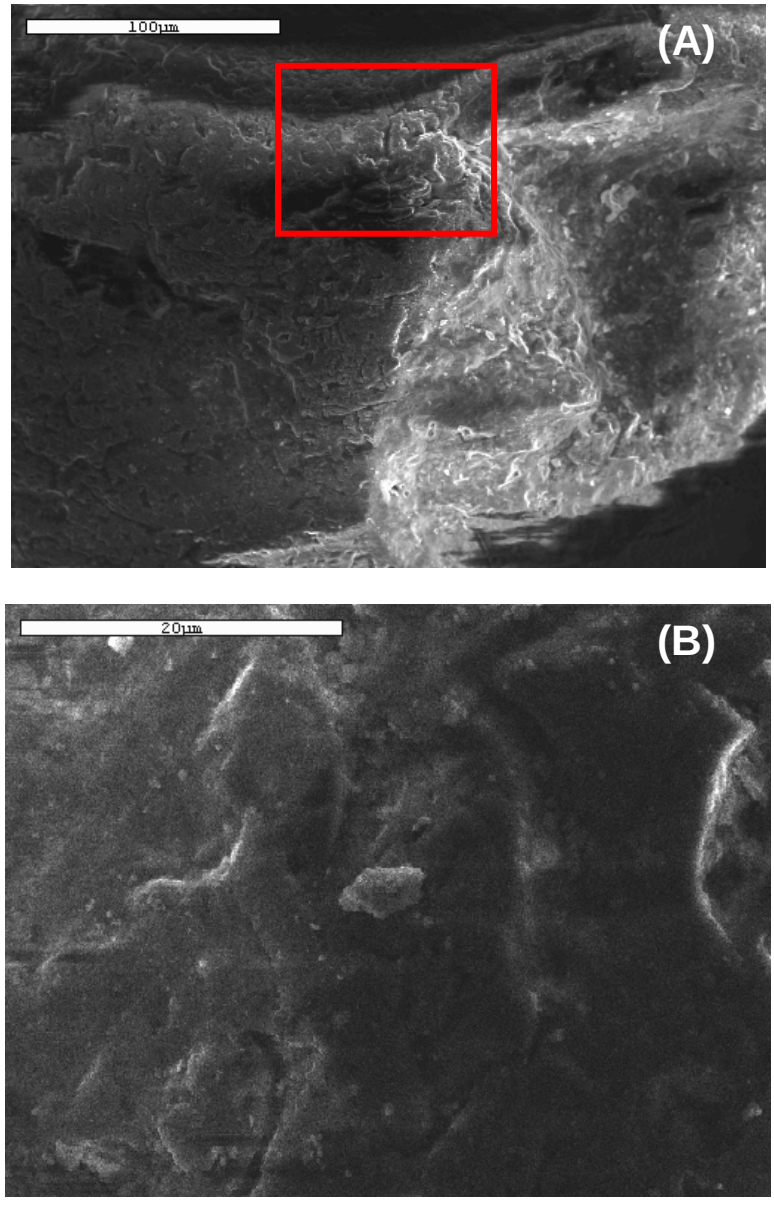

Figure 4-15. SEM image of the column's reactive media in series. (A) column 1 resolution of 400x, (B) column 2 resolution of 2500x

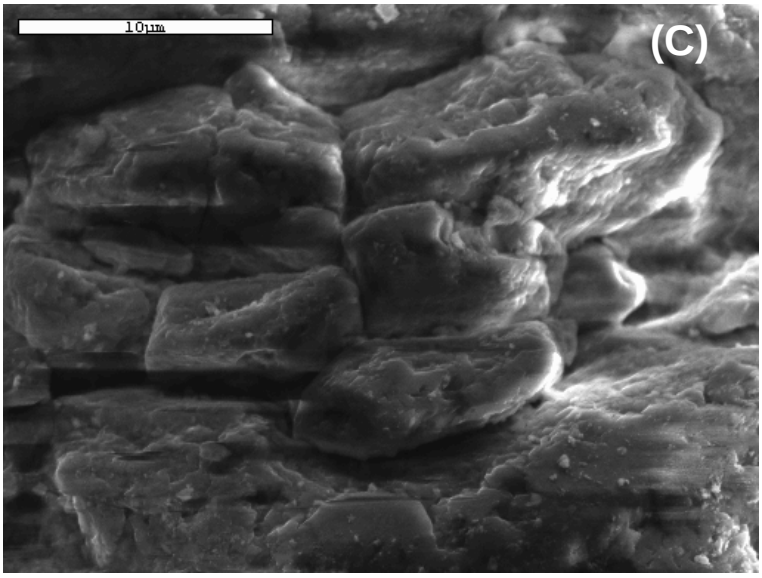

Figure 4-16. SEM image of the column's reactive media in series (C) red box zoomed in of Figure A at a resolution of 4000x.

EDS was done on the same particles and the results are shown in Figure 4-17. The spectrum shows high peaks of silica and oxygen, and peaks for iron and aluminum. The silica as expected comes from the sand particles. The aluminum and chlorine may be from the WW, as these substances are present in WW treatment. The iron intensity is very small and comes from the nZVI. This technique was used to show that Hg is adsorbed on the surface. Due to sensitivity in the technique, Hg was not detected with 100% confidence. It is speculated that the peak highlighted in the red box in Figure 4-17A, comes from Hg. The high intensity of silica and oxygen can produce peaks for a silica-oxygen compound and when the energies are summed the peak should be seen at 2.26 keV. Similarly, the Hg peak should be seen at 2.20 keV. Therefore based on just this EDS spectrum, it is unclear if the peak is from Hg or from silica-oxygen. However, the SEM/EDS sample of column 2 in the series, Figure 4-17B, did not show a peak in this region. Column 2 should have less Hg than column 1.Thus, it can be said that the peak from column 1 comes from the Hg on the surface. To summarize column 1

adsorbed available Hg (peak in Figure 4-17A), while column 2 did not adsorb any Hg (no peak). This confirms that Hg bound organic compounds are unavailable for adsorption; consequently column 2 did remove any Hg.

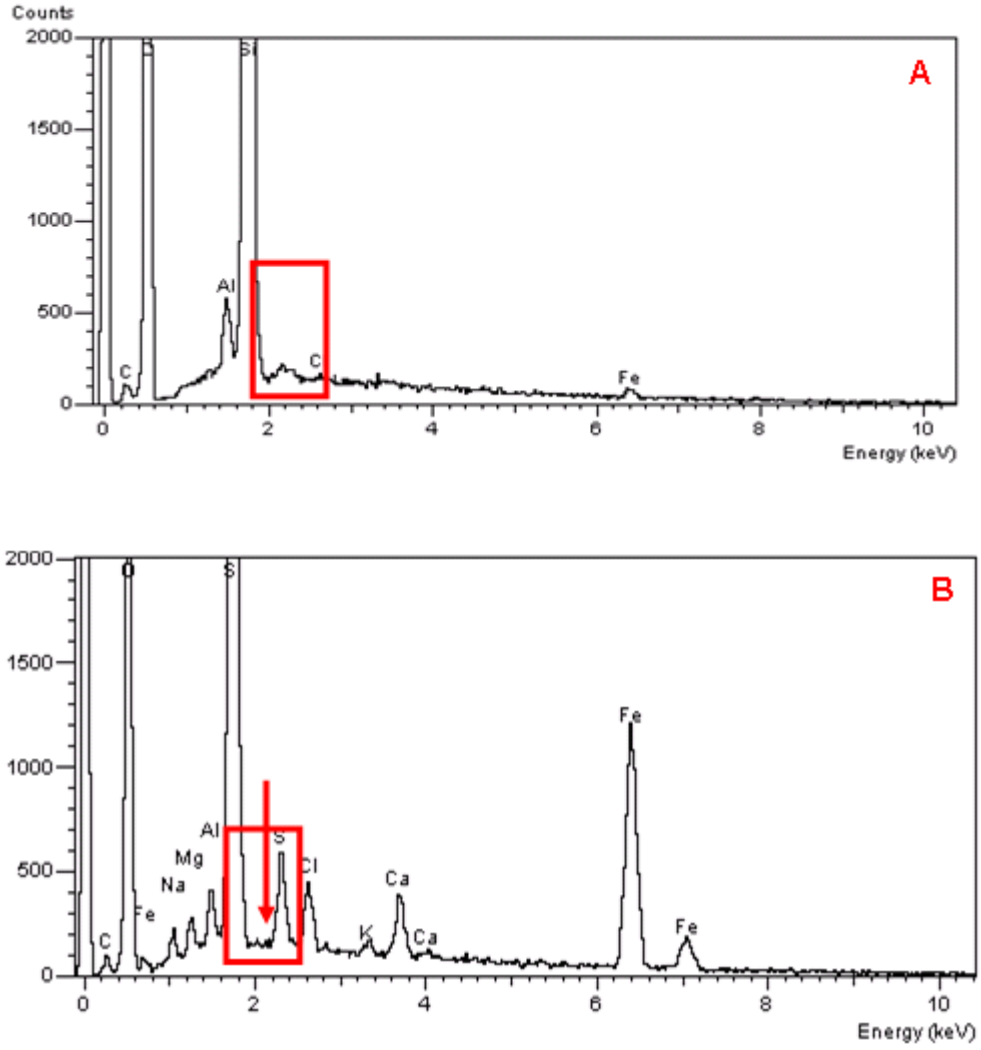

Figure 4-17. Energy dispersive spectra analysis of column 1 (A) and column 2 (B) in the column series

Conclusion

This study investigated the possibility of using the different interactions between zero-valent iron particles and dissolved Hg towards the development of a technology for Hg removal from contaminated wastewater effluents. Results obtained from column

studies show that nZVI has the potential to adsorb Hg from aqueous solutions, but several factors may play a significant role in reaching an ideal efficiency in terms of Hg removal. Such factors include influent characteristics, the speciation of Hg in the solution to be treated, the flow rate used to pump the Hg-contaminated water through the column, the mass and probably the degree of aggregation of nano-sized particles, the pH of solution, and specific characteristics of the columns (length, width, single column, more than 1 column used in series). The effect of particle size seems to be in favor of nZVI as compared to ZVI, mostly in terms of rates of particle oxidation and early Hg removal by adsorption. Based on experimental conditions used in this study, over time, nZVI not only becomes saturated, but also releases previously adsorbed Hg. With regard to the pumping flow rate, an increase from 25 to 75 μL/min improved the removal efficiency and delayed the breakthrough time. However, when the flow rate was increased to values as high as 500 μL/min, no Hg adsorption occurred. This can be a serious limitation with regard to large scale application. Ideally, further studies should focus on the identification of ideal conditions for higher Hg removal efficiencies under conditions that can be easily scaled up for industrial application. Overall, the use of nZVI to remove Hg from aqueous effluents could be considered promising, but more studies are to obtain operating conditions that will decrease effluent Hg concentrations to the ideal ng/L range. Only then, effort should be invested in the evaluation of the potential for the regeneration of nZVI and its re-use.

CHAPTER 5
IRON-MERCURY INTERACTIONS: EFFECTS ON MERCURY BIOAVAILABILITY AND METHYLMERCURY PRODUCTION IN FRESHWATER SEDIMENTS

Introduction

The speciation and concentration of mercury (Hg) available to methylating bacteria are key variables for the rate of methylmercury (MeHg) production in sediments. The chemical speciation of Hg in aquatic systems is strongly influenced by several parameters including the redox potential and pH conditions, as well as the concentrations of inorganic and organic complexing agents. Both Hg^{2+} and $MeHg^{+}$ cations have a high tendency to form thermodynamically stable complexes, in particular with soft ligands such as reduced sulfur species (Ullrich et al. 2001). In the absence of reduced sulfur ligands, the speciation of inorganic Hg in freshwaters seems to be dominated by three uncharged complexes: $Hg(OH)_2$, HgOHCl, and $HgCl_2$. With regard to organomercury species, thermodynamic calculations predict that CH_3HgOH would be the most stable species in most freshwater environments, whereas CH_3HgCl would dominate in seawater (Craig 1986; Stumm and Morgan 1996).

The mobility and bio-availability of Hg species in aquatic and soil environments are affected by physicochemical processes such as complexation, precipitation, dissolution, and adsorption. In Hg-impacted watersheds, organic matter is usually a very good predictor of Hg^{2+} in surface waters, as dissolved organic matter (DOM) increases the solubility of Hg, mostly through coordination to thiol groups associated with complex organic ligands such as humic and fulvic substances.

An extensive review of factors controlling Hg methylation including redox conditions was published by Ulrich et al., (2001). Understanding the distribution of redox processes is essential for predicting the fate of certain environmental contaminants.

With regard to Hg, the dissolution of certain oxide minerals, primarily Mn and Fe oxyhydroxides in reducing environments releases Hg and other metals adsorbed onto them, thereby increasing Hg bioavailability to methylating microorganisms. This is due to their large surface area and high capacity to adsorb and co-precipitate Hg, and to re-release it as redox conditions shift from oxic to anoxic (Fagerstr.T and Jernelov 1972). Many workers have found the distribution and concentration of dissolved and particulate Hg species to be influenced, among other factors, by the redox cycling of Fe, and less frequently Mn (e.g. (Bloom et al. 1999; Bonzongo et al. 1996; Gagnon et al. 1997; Gobeil and Cossa 1993; Hurley et al. 1991; Mason and Sullivan 1999; Quemerais et al. 1998; Regnell et al. 1997). Bloom et al. (1999) reported, for example, that the mobility of MeHg in estuarine surface sediments was linked to the Fe redox cycle, while the mobility of Hg^{2+} was controlled by the formation of soluble polysulfide or organic complexes. The formation and dissolution of Fe and Mn oxides is strongly controlled by the redox state and oxygen content of waters and sediments. In anoxic conditions, oxyhydroxides dissolve and release any associated Hg (Cossa and Gobeil 2000; Gagnon et al. 1997; Gobeil and Cossa 1993), which is thought to be one reason for the frequently observed Hg and MeHg enrichment in seasonally anoxic waters (Cossa et al. 1994; Hurley et al. 1991; Watras et al. 1995). Seasonal and diurnal trends in MeHg concentrations in sediment pore waters may also be linked with redox effects (Covelli et al. 1999; Gill et al. 1999). Oxyhydroxides can also form labile complexes with organic matter and clay minerals and this has the potential to increase their metal scavenging capacity (Meili 1997).

The production of MeHg in sediments is controlled primarily by the availability of the different mineral and organic Hg-fractions. The use of KOH as an extractant in the chemical Hg fractionation process is based on its ability to solubilized organic matter bound-metals. Similarly aqua regia is used to solubilize the Hg that is tightly bound to sulfide minerals. The relationship between potential rates of MeHg production and certain sediment Hg-fractions (KOH and aqua regia extracted) can be used as proxy for Hg availability to methylating agents. For instance, as organic matter undergoes degradation in sediments, it releases previously bound-Hg, making it available to microorganisms. Another important aspect of Hg bioavailability is its affinity with soft ligands, mostly reduced sulfur species. Reduction of sulfate and precipitation of Hg sulfides can limit bioavailability. However, under specific laboratory conditions, it has been hypothesized that neutrally charged aqueous Hg-sulfide species could become methylated by SRB (Benoit et al. 2001; Benoit et al. 1999). This latter observation is based on simply on geochemical equilibrium predictions and not the chemical analysis of different Hg species.

In aquatic environments, zero-valent iron particles can react with water under both aerobic and anaerobic conditions to produce the oxidized Fe^{2+} and Fe^{3+} species (Biernat and Robins 1972; Gu et al. 1999; Kenneke and McCutcheon 2003; Majewski 2006; Sayles et al. 1997). These conditions would favor the formation of relatively stable iron oxyhydroxide amorphous minerals such as γ-FeOOH, α-FeOOH, β-FeOOH, Fe_3O_4, and $FeCO_3$, (Farrell et al. 2000; Gu et al. 1999; Huang and Zhang 2005; Huang et al. 2003; Phillips et al. 2000; Rangsivek and Jekel 2005; Ritter et al. 2003). While the formation of such oxyhydroxides Fe minerals would likely increase the adsorption of

dissolved Hg^{2+}, the release of dissolved Fe^{2+} ions under predominant anoxic conditions could increase the availability of Hg through the removal of dissolved sulfide through formation of pyrite (FeS) minerals and reduction of Hg precipitation as HgS minerals. The balance between these different processes would be dictated by key environmental parameters such as pH, type and quantity of dissolved organic matter, and redox conditions.

In this study, the Hg-methylation potential of anoxic sediments in the presence of zero-valent iron particles was investigated with the goal to determine if Hg naturally occurring or added to sediments could be made available to methylating microorganisms. Sulfate has also been identified as the primary parameter controlling the methylation of Hg in aquatic systems (Ulrich et al., 2001). Therefore, experiments were designed to take into account the potential effects of sulfate concentrations.

Materials and Methods

Sediment and Water Samples Used in Hg Methylation Studies

Sediment and water samples were collected from the East Fork Poplar Creek watershed (latitude 35.990683 and longitude -84.317183) near Oak Ridge Tennessee, USA. Figure 5-1 shows the geographical location of the sampling site, labeled by a star. This site has been on US EPA Superfund list since 1989 and is known to be heavily contaminated with Hg (Dong et al. 2009; Miller et al. 2009).

Water samples were collected in large acid pre-cleaned high density polyethylene (HDPE) containers using ultraclean sampling techniques for trace metal sample collection. Sediment samples were collected after removing the surface layer of decomposing litter and scooping of exposed sediments.

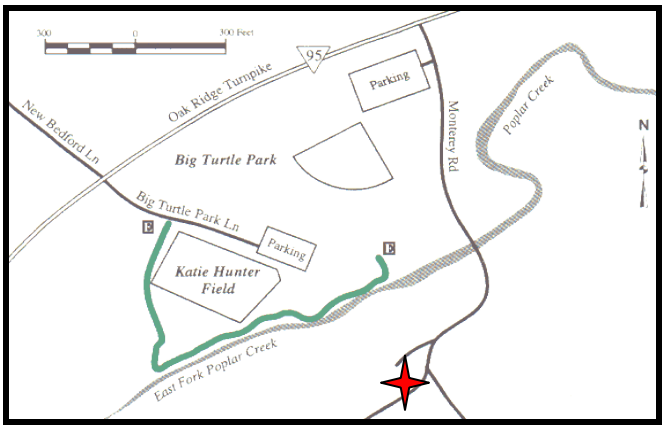

Figure 5-1. Map of East Fork Poplar Creek in Big Turtle Park Greenway in Oakridge,TN. Sediment and water samples were collected from a noted by a star on the map (latitude 35.990683 and longitude -84.317183 in decimal degrees).

Sediment samples were placed into clean plastic bags. Both water and sediment samples were kept in large coolers packed with ice, and the load transported back to our laboratory at the University of Florida. Once back to the laboratory, the sediment was sieved through a 2.0 mm mesh to remove large plant and rock debris while the water was filtered through a 0.45 μm filter. Both types of samples were then stored refrigerated at 4^{o}C pending use in different laboratory analyses. Ion chromatography (IC), inductively coupled plasma atomic emission spectroscopy (ICP-AES), and loss on ignition techniques were used to determine the concentrations of major ions, metals other than Hg, and the organic content of sediment samples. Although important the analysis of the data, the physical characteristics of used sediments (size fraction and mineralogy) were not determined due to limited access to analytical equipment.

Determination of Total- and Methyl-mercury

Sediments samples placed in Teflon tubes were first digested by aqua regia (HCl and NO_3 in a 3:1 ratio volume/volume) at sub-boiling temperature for about 12 hours (overnight digestion). Cold acid digestion was used for aqueous samples using bromine monochloride. In both cases, digested samples were analyzed by the $SnCl_2$-reduction

technique, followed by detection with cold vapor atomic fluorescence spectrometry (CV-AFS, Tekran Model 2600). Details on used analytical procedures and QA/QC criteria (blanks and Hg standard solutions) have been described in several of our earlier publications (Hovsepyan and Bonzongo 2009; Warner et al. 2005; Warner et al. 2004).

MeHg present in sediment samples was determined using methods published in the literature (Bloom 1989). Sediment samples (~1g) were first digested with 10 mL of 25% KOH in methanol at 70^{o}C for 12 hours. This step is used for the solubilization of organic compounds present in sediment including MeHg. Next, the obtained extract is diluted to a known volume (25 mL) of which an aliquot was used for MeHg determination. Prior to analysis, the pH of the aliquot sample was buffered to 4.5 using an acetic acid buffer. The sample was then treated 100μL, of sodium tetraethylborate to convert Hg compounds present in the samples to highly volatile species as shown in equations 5-1 and 5-2 Through these reactions, ionic Hg present in the sample becomes converted to di-ethyl-mercury (Eq. 5-1) while MeHg cation becomes ethylated to form methyl-ethyl-Hg (Eq. 5-2).

$$2NaB(C_2H_5)_4 + Hg^{2+} \rightarrow 2B(C_2H_5)_3 + Hg(C_2H_5)_2 + 2Na^{+} \quad (5\text{-}1)$$

$$NaB(C_2H_5)_4 + CH_3Hg^{+} \rightarrow B(C_2H_5)_3 + CH_3HgC_2H_5 + Na^{+} \quad (5\text{-}2)$$

This approach allows for increased volatilization of these organo-mercuric compounds. Sampling of the headspace after equilibration and species separation by gas chromatography and pyrolysis allowed for the detection of atomic Hg by CV-AFS.

Speciation of Solid Phase Mercury in Collected Sediment Samples

The selective Hg-extraction method specific for biogeochemically relevant Hg fractions in solid materials developed by Bloom et al., (2003) was used in this study.

The method identifies five different Hg fractions based on the type of chemical extractant used during a sequential procedure. The different chemical solutions used as extractants as well as the corresponding Hg-fractions and time of extraction are shown in Table 5-1.

Table 5-1. Selective extraction fractions of mercury. Adapted from Bloom et al., 2003

Targeted Geochemical Fractions	Extractant Solutions (V=30 mL)	Extraction Time (Hours)
F1: Easily exchangeable Hg	DI-water	2
F2: 'Humic stomach acid' soluble	0.1MCH_3COOH and 0.01MHCl	4
F3: Organo chelated	1M KOH	6
F4: Elemental Hg	12M HNO_3	8
F5: Mercuric sulfide	Aqua Regia (10:3 ratio of HCl:HNO_3)	12

At the end of each shaking step, except for step number 5, sediment samples were centrifuged for 30 min at 3000 rpm and the supernatant removed and placed in acid pre-cleaned Teflon containers. Next, the solid pellet was rinsed with digestion solution, centrifuged, and the collected supernatants combined. The latter was then filtered through a 0.45 μm filter and treated with bromine monochloride, a strong oxidizing solution, to help maintain the extracted Hg into solution pending analysis.

Investigation of the Effect of Changing Sulfate Concentrations on the Biotransformation of Mercury in Sediment Slurries Containing Fixed Iron Masses

In this series of laboratory experiments, microcosm studies were conducted to investigate the interaction of iron and Hg already present in sediments (i.e. no Hg spikes) on the bioavailability and biotransformation of sediment Hg. Serum vials (50mL) pre-cleaned by soaking in 10% trace metal grade HNO_3 for 24 hours and thoroughly rinsed with Nanopure water were used as reactors for batch incubation studies. Sediment slurries were prepared by adding 10 mL of site water to 1 g of sediment,

following a procedure widely reported in the literature on methyl-Hg production studies (Slowey and Brown 2007; Ullrich et al. 2001). The above mixture was first allowed to equilibrate for 24 hours and a pre-weighed and fixed mass of ZVI (0.2g) or nZVI (0.01) was added to the sediment slurries. Next, sulfate was added in increasing concentrations (200, 500, 1000 μM) to produce three different Fe/sulfate ratios. Sulfate is used by sulfate reducing bacteria (SRB) as terminal electron acceptor during anaerobic respiration, and MeHg production in anoxic environments has been found linked primarily to the activity of SRB (Ulrich et al., 2001). Experimental parameters used in this study are summarized in Table 5-2.

Slurries were next de-aerated by bubbling with ultrapure nitrogen, the vials hermetically sealed, and the mixture left to incubate for 25 days. Note that no Hg was added to these vials as these experiments focused on the biotransformation of Hg already present in sediment as a function of changing Fe/SO4 ratios. At the end of the incubation period, 2 mL of slurries were withdrawn and processed for the analysis of both MeHg and total-Hg concentrations.

Table 5-2. Experimental Design for Hg Methylation in Sediment slurries containing Fixed Iron Amounts and Changing Sulfate Concentrations

	Sediment (g)	Site Water (mL)	Sulfate Conc. Added (μM)	Iron Added (g)
Control 1	1.0	10	0.0	None
Control 2: ZVI	1.0	10	0.0	0.20
Control 2: nZVI	1.0	10	0.0	0.01
Control 3	1.0	10	500	None
Treatment 1: ZVI	1.0	10	200	0.20
Treatment 1: nZVI	1.0	10	200	0.01
Treatment 2: ZVI	1.0	10	500	0.20
Treatment 2: nZVI	1.0	10	500	0.01
Treatment 3: ZVI	1.0	10	1000	0.20
Treatment 3: nZVI	1.0	10	1000	0.01
Treatment 4: ZVI	1.0	10	500	2.60

Investigation of the Effect of Changing Iron Masses on the Biotransformation of Mercury in Sediment Slurries Containing Sulfate Concentrations

Using a procedure similar to the one described above, batch experiments were conducted, and this time, the mass of iron added to the sediment slurries varied while the concentration of sulfate was maintained constant. The experimental conditions are summarized in Table 5-3.

Table 5-3. Experimental Design for Studies on Hg Methylation in Sediment Slurries with Fixed Sulfate Concentrations and Changing Iron Masses

	Sulfate Conc. Added (μM)	Mass of Iron (g)
Iron 1: ZVI	1000	0.500
Iron 1: nZVI	1000	0.020
Iron 2: ZVI	1000	0.100
Iron 2: nZVI	1000	0.005

Effect of Iron on the Biotransformation of Newly Added Hg into Sediments

In contrast to the above experiments focusing on *in-situ* Hg, this second set of incubations assessed the effect of iron-mercury interactions on the availability of Hg newly added to sediments using microbial Hg-methylation as surrogate for bioavailability. The experimental approach was similar to the one described above, except that in this specific case, sediment slurries were spiked with Hg (using a 1000mg/Lstock solution of $Hg(NO_3)_2$ from Fisher Scientific, USA) to produce a final slurry concentration of 1.0 mg/L. Experimental parameters are presented in Table 5-4.

Table 5-4. Experimental Design for Hg Methylation Studies in Sediment Slurries Spiked with $Hg(NO_3)_2$ in Addition to Iron and Sulfate

	Sediment (g)	Site Water (mL)	Sulfate Conc. Added (μM)	Hg Conc. Added (mg/L)	Iron Added (g)
Control 1	1.0	10	0	1.0	none
Control 2	1.0	10	200	1.0	none
Control 3	1.0	10	1000	1.0	none
Treatment 5: ZVI	1.0	10	200	1.0	0.20

Table 5-4. Continued.

	Sediment (g)	Site Water (mL)	Sulfate Conc. Added (μM)	Hg Conc. Added (mg/L)	Iron Added (g)
Treatment 5: nZVI	1.0	10	200	1.0	0.01
Treatment 6: ZVI	1.0	10	1000	1.0	0.20
Treatment 6: nZVI	1.0	10	1000	1.0	0.01

Statistical Analysis

To evaluate the significance of differences observed between treatments, a simple t-test for equal or unequal variance was used at a confidence level of 95%. The calculations were performed using Microsoft Office Excel 2003 statistical data analysis tools, see Appendix A.

Results

The site water used in these laboratory experiments had a pH of 7.02 and a total-Hg concentration of 140 μg Hg/L (or ppb), a rather high dissolved Hg concentration indicative of the contamination level of the creek under study. This water contained an average DOC concentration of 7.2 mg C/L and a major ion composition listed in Table 5-6. Used sediments had a pH of 7.46, and a total-Hg concentration of 11 mg Hg/kg (or ppm). The sediment's organic content was about 8% as assessed by loss on ignition. Metal and major ion data for both water and sediment used are presented in Tables 5-5 and 5-6.

Based on these data, the concentration of sulfate naturally present in used sediment slurries was approximately 0.18 μM, based on the mixture of 1 g of sediment and 10 mL of site water.

Table 5-5. Average metal concentrations found in sediment and site water determined by ICP-AES.

Metals	Sediment (mg/g)	Site Water (mg/L)
Aluminum (Al)	3.026	0.117
Arsenic (As)	0.002	0.003
Calcium (Ca)	0.698	29.341
Cobalt (Co)	0.004	0.003
Iron (Fe)	6.562	0.194
Potassium (K)	0.235	2.702
Magnesium (Mg)	0.515	8.059
Manganese (Mn)	0.440	0.004
Sodium (Na)	<0.033	2.093

Table 5-6. Average major ions found in sediment (water soluble fraction) and used natural water, analyzed by ion chromatography (ND = not determined).

Ions	Sediment (*water soluble fraction*) (mg/g)	Site water (mg/L)
Chloride, Cl^-	0.11	3.93
Sulfate, SO_4^{2-}	0.07	9.85
Nitrate, NO_3^-	0.05	2.13
Sodium, Na^+	ND	2.94
Potassium, K^+	ND	1.34
Calcium, Ca^{2+}	ND	22.84

Accordingly, sulfate concentrations used to spike the sediment slurries resulted in a significant increase (200, 500, and 1000 μM), and this choice was based on reports from the literature on sulfate concentrations that stimulate Hg methylation in sediments of different aquatic systems (Chen et al. 1997; Gilmour and Henry 1991; Harmon et al. 2004; Harmon et al. 2007; Mehrotra and Sedlak 2005). Figure 5-2 shows the results of the effect of varying sulfate concentrations in sediment slurries with fixed amounts of iron particles. No significant differences were observed between values obtained from control samples and sulfate-treated slurries at the 95% confidence level. Additionally, there was no significant difference between the samples containing ZVI and nZVI.

The measured specific surface area (SSA) was 0.116 m^2/g and 30.5 m^2/g for ZVI and nZVI, respectively. Based on the total mass of either ZVI or nZVI used in these experiments, an estimated SSA 0.0232 m^2 and 0.305 m^2 could be calculated for the two types of iron particles respectively. There was no significant difference between the MeHg produced when equal surface area was used for ZVI and nZVI.

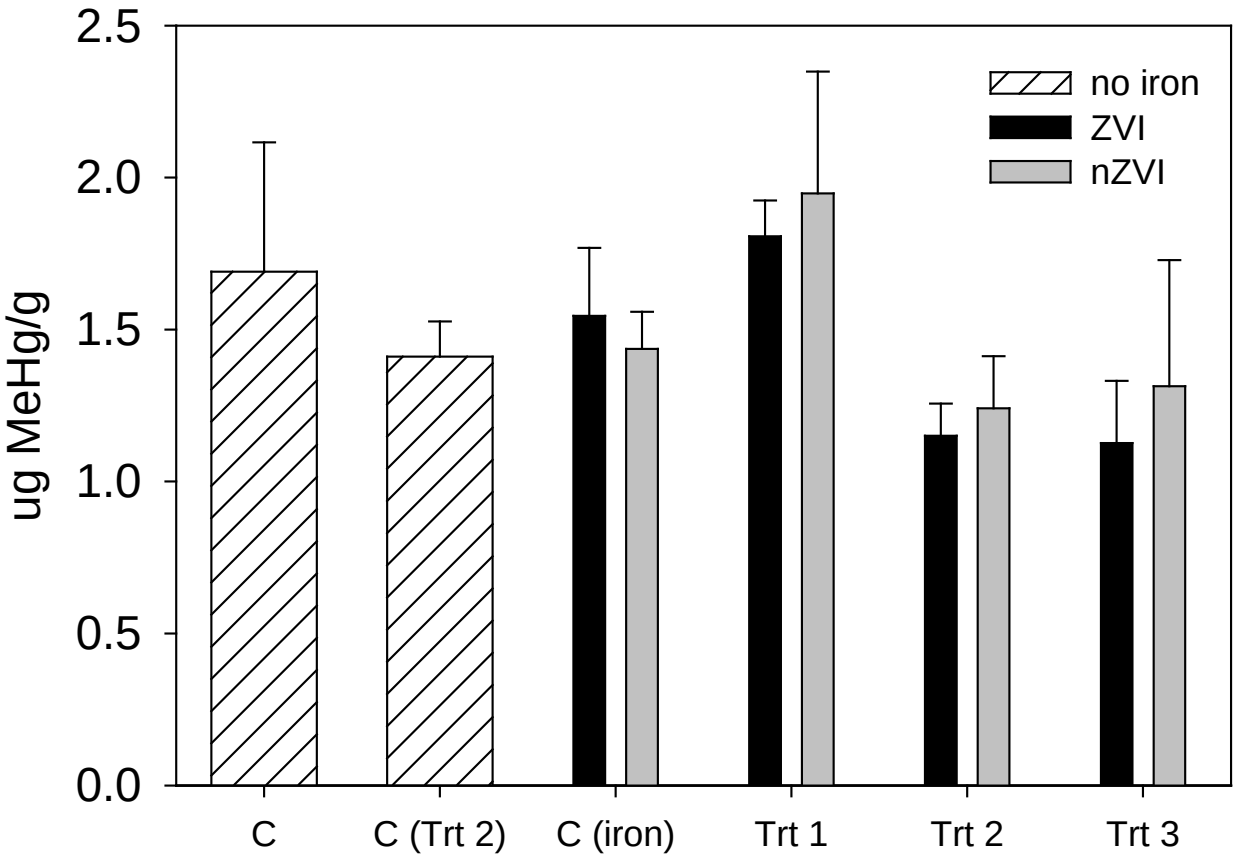

Figure 5-2 Methyl mercury produced in Hg contaminated sediments with sulfate addition after 25 days of incubation. Control: sediments only, C(Trt 2): sediments + 500 μM sulfate, C(iron): sediments + iron only, Trt 1: sediments + 200 μM sulfate added + iron, Trt2: sediments + 500 μM sulfate added + iron, Trt 3: sediments + 1000 μM sulfate added + iron

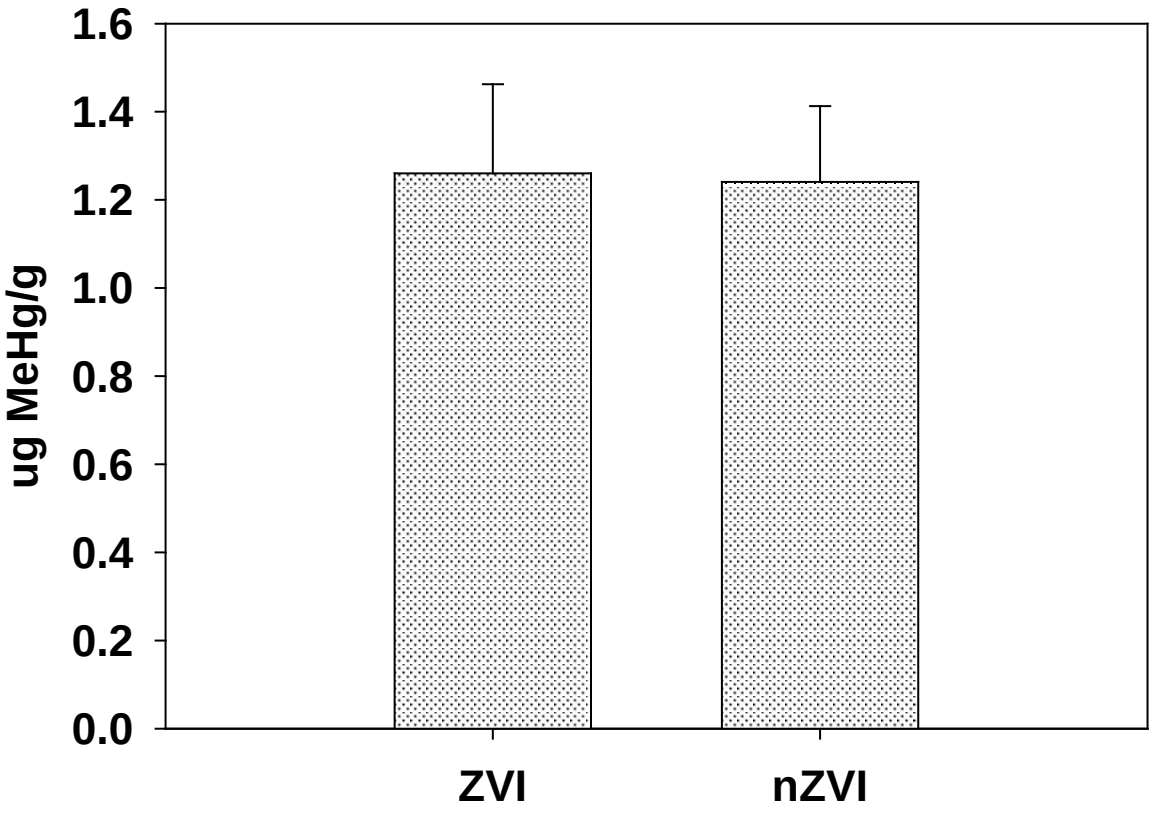

Figure 5-3. Effect of particle size with a sulfate concentration of 500 μM treatment added to sediments. The mass of ZVI used matched the surface area of the mass of nZVI used.

Varying the mass of iron particles in sediment slurries with sulfate concentration fixed at 1000 μM (or 1mM) gave the results presented in Figure 5-4. For ZVI, as the iron particle mass decreased the amount of MeHg produced decreased as well. In the presence of nZVI,a bell shaped trend was observed, in that slurries spiked with the intermediate tested mass on nZVI (0.01g) exhibited the highest MeHg production. The highest mass of iron particles, (0.2 g), had a significantly lower MeHg production than both slurries with 0.01 g and 0.005 g.

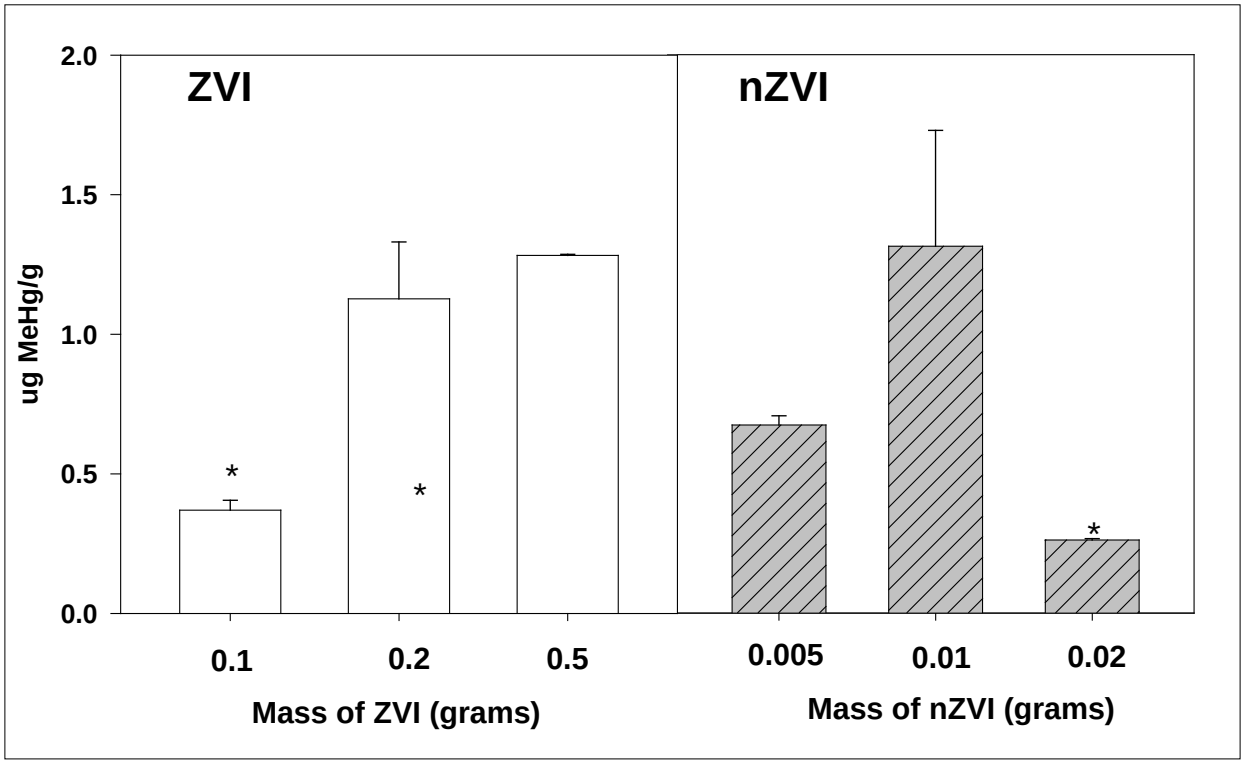

Figure 5-4. Effect of different iron masses on MeHg production in sediment slurries containing 1 mM of sulfate. (*) represents significant differences at 95% confidence level

The results obtained from the above experiments show no to very little impact of iron particles on the transformation of Hg in sediments. One reason could be the limited bioavailability of Hg naturally occurring in used sediments. The speciation of solid phase Hg in used sediments based on the sequential extraction technique described in the method section showed that Hg in used sediments is present predominantly in the non available form, including up to 68% of total-Hg found in the organic-bound fraction and another 14 to 15% found in fractions which are not readily bio-available (Bloom et al., 2003).

It was therefore assumed that spiking the sediments with a known amount of Hg would increase the amount of its bio-available fraction and therefore MeHg production. Under such conditions, a better assessment of the potential iron-mercury interactions on

MeHg production in sediments could be made. Therefore, experiments similar to treatments 1 (200 μM sulfate added) and 3 (1000 μM sulfate added) shown in Figure 5-2 were used, except that in this case, sediment slurries were supplemented with Hg salt to a final concentration of 1 mg Hg/L. The obtained results are shown in Figure 5-5 in comparison with control non-spiked slurries.

In ZVI-containing slurries, no significant difference in levels of MeHg produced was observed between the Hg-spiked and non-spike Hg sediments. However, in nZVI-treated slurries, a significant difference in the amount of MeHg produced was observed for slurries containing 1 mM of sulfate.

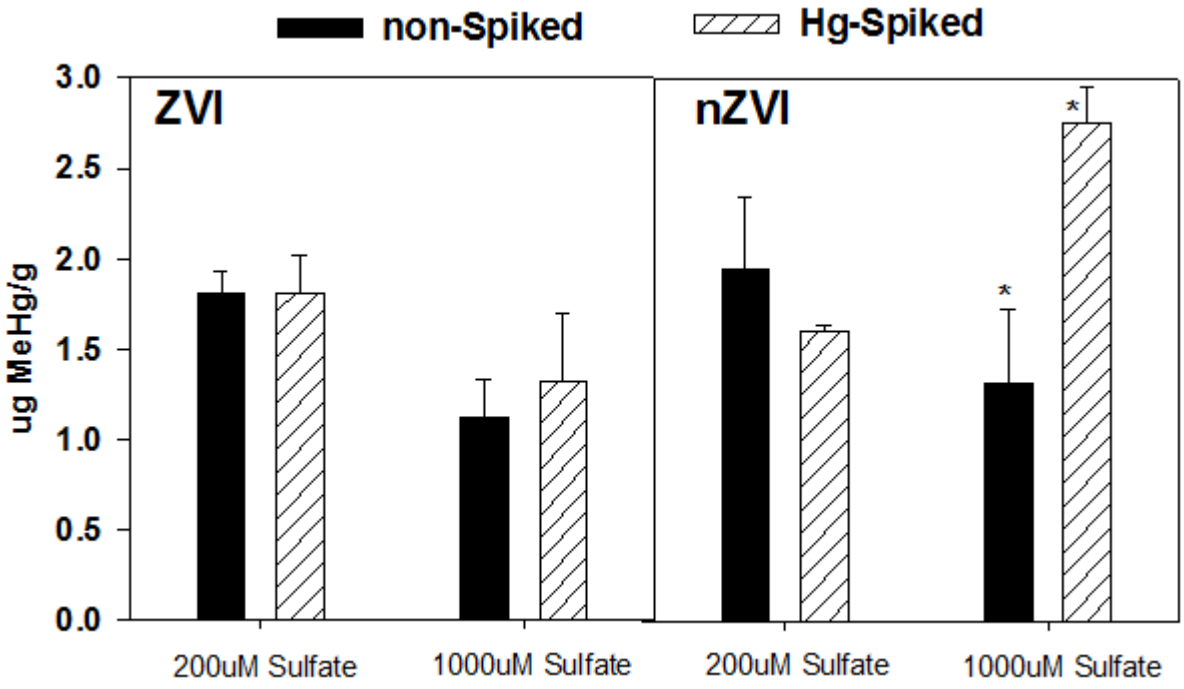

Figure 5-5. Methyl-Hg produced in sediment slurries spiked and non-spiked with Hg and containing a fixed amount (0.02 g for ZVI and 0.01 g for nZVI) of iron particles but different sulfate concentrations (200 and 1000 mM). (*) represents significant difference at 95% confidence.

Discussion

Based on general knowledge of the biogeochemistry of Hg in aquatic systems and results on Hg-iron interactions presented in earlier chapters, at least three key parameters can help explain MeHg trends or lack of, seen in this study. First, the speciation of Hg naturally present in used sediments and its impact on the bioavailability and transformation processes that lead to MeHg production. Second, used experimental conditions (e.g. ratios of used components and redox conditions). Third, the potential impact of co-occurring methylation and demethylation processes and the significance of their potential rates.

Speciation of Mercury and its Methylation in Aquatic Sediments

The literature on the methylation of Hg in sediment is quite abundant. Although Hg methylation by chemical reactions not catalyzed by non-microbial processes (Eq. 5-3,4,5), its relative contribution to the overall pool of produced MeHg has been estimated to be negligible based on conditions required for such reactions to take place under most common natural conditions (Celo et al. 2006; Craig 1986; Gardfeldt et al. 2003; Gilmour and Henry 1991; Monperrus et al. 2007; Weber 1993)

$$MeCo(dmg)_2H_2O + Hg^{2+} \rightarrow MeHg^{+} + MeCo(dmg)_2(H_2O)_2^{+} \quad (5\text{-}3)$$

$$Me_3Sn(IV) + Hg(II) \rightarrow Me_2Sn(IV) + MeHg(II) \quad (5\text{-}4)$$

$$Hg_2^{2+} + MeI \rightarrow MeHg^{+} + HgI^{+} \quad (5\text{-}5)$$

In contrast, biotic methylation of Hg is known to dominate in aquatic sediments and sediments, particularly when conditions for microbial reduction of sulfate by SRB are prevalent. However, the exact mechanisms of Hg methylation are still not fully understood (Beijer and Jernelov 1979; Choi et al. 1994; Jay et al. 2002; Jensen and

Jernelov 1969; Pak and Bartha 1998). Besides Hg methylation by SRB, recent studies have also linked iron reducing bacteria (IRB) to MeHg production (Fleming et al. 2006; Han et al. 2008; Kerin et al. 2006). Regardless of the pathway, the biotic or abiotic conversion of inorganic Hg species to MeHg depends primarily on Hg speciation, which controls Hg availability to methylating agents. The results of Hg speciation in used sediments are presented in Figure 5-7.

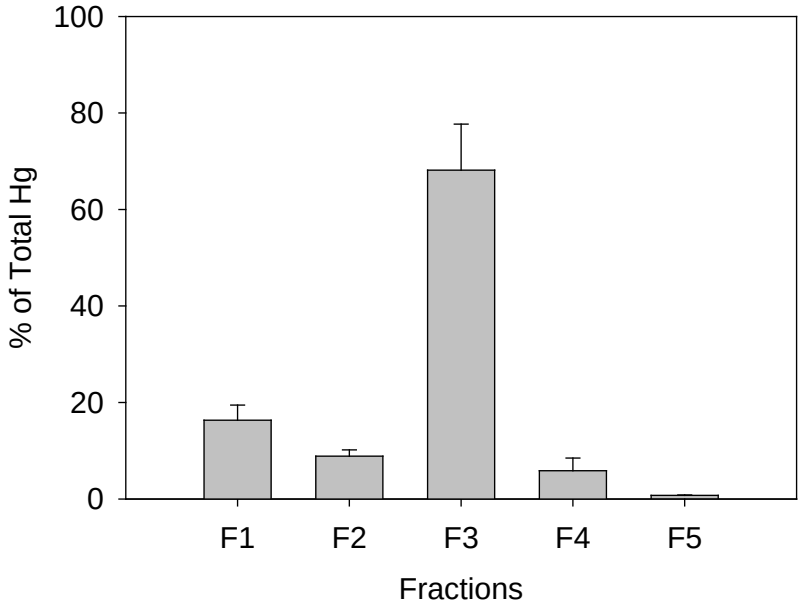

Figure 5-6. Percentage of Hg associated with different sediment fractions based on sequential selective extractions using a method adapted from Bloom et al. (2003). F1: Easily exchangeable Hg; F2: 'humic stomach acid' soluble; F3: organo chelated; F4: elemental Hg; and F5: mercuric sulfide.

From the results presented in Figure 5-6, Hg speciation in used sediments is primarily associated with the organic fraction (68%). The remaining fractions F1, F2, F4, and F5 accounted for 16%, 9%, 6% and <1%, respectively. Based on this Hg distribution among the different sediment organic and inorganic fractions, the extent of MeHg production is likely limited primarily due to the non-availability of sediment Hg. Complexation by sediment organic matter would therefore constitute a key limitation to

Hg bio-methylation. This observation would support the result trend shown in Figure 5-2. In fact, it appears that the Hg binding capacity of used sediments is so high that the use of Hg-spiked sediments produced MeHg levels that were similar in both control and Hg-spiked sediment slurries containing either ZVI or nZVI, and regardless of sulfate concentrations.

Effect of Specific Experimental Parameters

Sulfate

Sulfate concentrations can either inhibit or enhance MeHg production (Compeau and Bartha 1985; Gilmour and Henry 1991). Figure 5-7 shows a theoretically determined range for Hg methylation as a function of sulfate concentration, with a potential optimal Hg methylation supported by sulfate concentrations ranging from 200 to 500 μM. However, the optimum response within the above range is also dependent on a number other parameters such as pH, temperature, sediment porosity, and organic carbon content. Above this range it is hypothesized that reduction of sulfate will produce reduced sulfur species which on a molar ratio basis would likely precipitate most of the soluble ionic Hg as mercury sulfide. In contrast, sulfate concentrations <200μM would limit SRB activity and therefore Hg methylation (Gilmour and Henry, 1991)

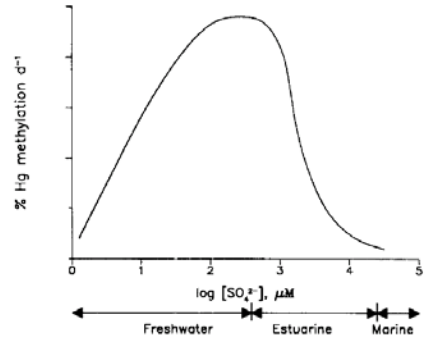

Figure 5-7. Sulfate concentration range for optimal mercury methylation rates in sediments (Gilmour and Henry 1991)

Published experimental data on the other hand do not necessarily agree with the above theoretical predictions, and due to the synergic effect of several environmental factors on the methylation process, the observed response to sulfate concentrations varies from site to site. For example, high MeHg production rates were found sulfate-rich salt marsh sediments (Compeau and Bartha 1984), low sulfate concentrations (about 92.9 μM) in a wetland microcosm study produced more MeHg than the highest tested sulfate concentration of 482 μM (Harmon et al. 2004).

Trends observed in this study follow those reported by Hamon et al (2004). At the lowest tested sulfate concentration (200 μM), for both ZVI and nZVI treated slurries, the amount of MeHg produced was the highest observed (Figure 5-2). While at the highest tested sulfate concentration (1000 μM), both ZVI and nZVI treated slurries produced low MeHg (Figure 5-2). This may be due to the formation of mercuric sulfide based on the hypothesis presented in Figure 5-7, as a sulfate concentration of 1000μM is outside the range of values that favor Hg methylation (Gilmour and Henry, 1991).

Organic carbon

It is believed that low rates of Hg methylation in systems containing reasonable sulfate levels (i.e. levels that stimulate Hg methylation) could be attributable to the non-availability of Hg to methylating microorganisms, and the strong association of Hg to sediment organic matter explains, at least partly, measured low Hg methylation rates (Harmon et al. 2004). The results of solid phase Hg speciation conducted in this study showed that approximately 68% of total Hg present in used sediments was organo-chelated, and therefore not directly available to microorganisms (Fraction 3, Table 5-1 and Figure 5-6).

Effect of iron addition to sediment slurries

Tables 5-5 and 5-6 show that Fe and sulfate do occur in measurable concentrations in both sediment and water samples used in this study. The use of iron particles would therefore increase Fe(II) levels in the slurries through reduction and dissolution of initially oxidized iron at the surface of the particles. Under sulfate reducing conditions, the presence of reduced iron could lead to the formation of iron sulfides, which in turn can co-precipitate Hg (Gilmour and Henry 1991). Reactions between water and iron particles (see chapter 2) and the interaction of Hg with such particles (chapter 3) show that Hg could be removed from solution through sorption onto iron particles as oxyhydroxides form on the surface of the iron particles and decrease Hg availability (Weisener et al. 2005). However, this formation is rather slower under anoxic conditions than in the presence of oxygen. An incubation time of 25 days used in this study may have given the iron particle enough time to undergo oxidation and then reduction, reactions which may help explain why sediment slurries with iron, sulfate, and no Hg addition had rather similar amount of produced MeHg (Figure 5-2).

The difference in the size of particles used (Figures 5-2 and 5-3) had apparently no effect on MeHg production. At the highest tested concentration of nZVI, the smallest amount of MeHg was produced while the highest produced amount of MeHg was measured in sediment slurries spiked with 0.01 g nZVI. The different trends seen between ZVI and nZVI, (Figure 5-4), can only be explained by the difference in SSA of used iron particles. However, the exact mechanisms as to why is not clear.

Methylation and Demethylation

MeHg produced in sediments is a net product of co-occurring Hg-methylation and MeHg-demethylation reactions. Measurements of potential rates of Hg methylation and

MeHg demethylation rates were beyond the scope of this study. Nevertheless, these potential rates commonly used to identify the tendency for a given sediment to produce and accumulate MeHg. For instance, when rates of Hg methylation (M) and MeHg demethylation (D) are equal, M/D would be equal to 1 and MeHg would not accumulate to measurable levels. Only when M/D>1 that MeHg builds up in the environment. Unfortunately, the accurate determination of these rates requires the use of stable Hg isotopes and ICP-MS, not available for this study due to fund limitation.

Conclusion

This study assessed the potential role of iron added in the metallic form and in different particle sizes to sediments on the biotransformation of both native and newly added Hg. The major findings can be summarized as follows:

- Relationship between the different fractions of Hg present in the solid phase and the amount of MeHg produced during the incubation of sediment slurries points to Hg speciation as a determinant factor in controlling the production of MeHg. In subsequent set of experiments using the same sediments, but spiked with Hg, no significant amount of MeHg was produced neither. This suggests that sediments used had a very high binding capacity for Hg which in turn controls the Hg availability and potential for methylation.
- The addition of metallic iron particles in sediments could impact the production of MeHg through two main mechanisms: (i) adsorption onto oxyhydroxides layers or (ii) release of Fe(II) which co-precipitates with Hg in iron sulfide minerals, depending on redox conditions. These processes would reduce the bioavailable fraction of Hg, and therefore, its methylation by sediment's microorganisms.

Ideally, measurements of potential rates of Hg methylation (M) and MeHg demethylation (D) would have been necessary to support the above conclusions. Further studies should consider (i) the concentration and types of organic carbon sources, (ii) M/D ratios, and (iii) kinetic aspects of MeHg production.

CHAPTER 6
CONCLUSION AND RECOMMENDATIONS

This research focused on the interaction of iron and mercury (Hg) in aquatic systems. With the ultimate goals of understanding the potential mechanism of such interactions and assessing the possibility of using identified biogeochemical processes in controlling Hg pollution issues. The rational behind this study is shown conceptually in Figure 6.1.

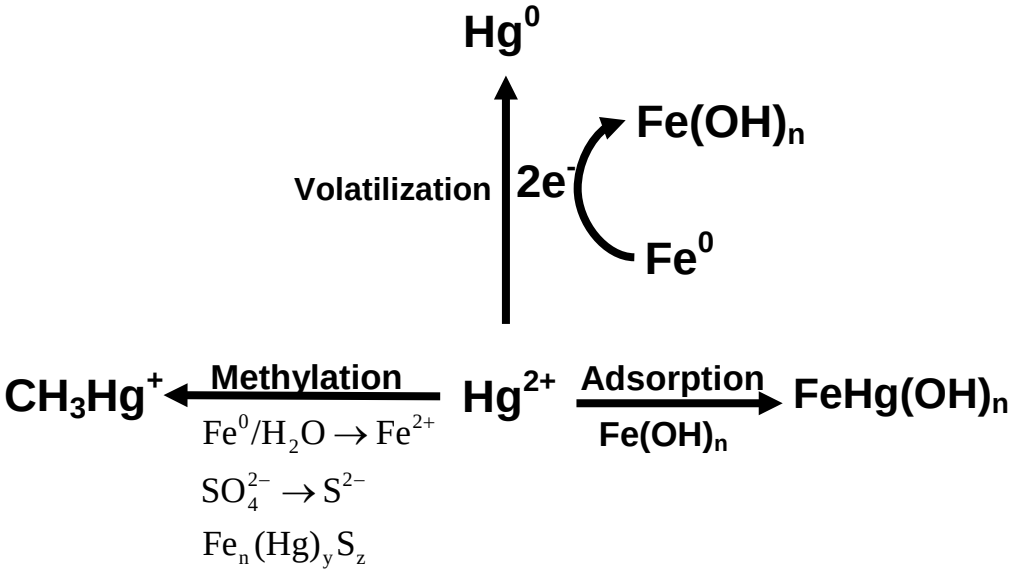

Figure 6-1: Hg-iron interactions investigated in this study.

Three different reaction pathways are anticipated to play a significant role in the fate of Hg in aqueous and sediment phases (Figure 6-1). First, Hg can be eliminated from the aqueous phase through volatilization following its interaction with metallic iron particles. This study showed that this specific process does not play a significant role with regard to the total mass of Hg removed from contaminated water matrixes. Second, corrosion of iron particles and the resulting formation of oxyhydroxide layers provide adsorption sites for removal of Hg from aqueous solution. Third, metallic iron impacts the bioavailability of inorganic Hg to methylating agents by (i) iron oxidation and Hg

adsorption and (ii) iron reduction and formation of Fe(II) which in combination with produced sulfides would co-precipitate dissolved Hg, hence limiting its availability for methylation.

The major findings based on lab experiments testing the above hypotheses are as follows:

- Batch experiments demonstrated that rates of Hg volatilization were impacted primarily by water chemistry (DI-water versus wastewater effluents (WW)), while the particle size of metallic iron seemed to play a minor role.
- Depending on how data are normalized (specific surface area (SSA) versus mass), kinetic studies show that rates of Hg adsorption are faster for nZVI when data are normalized by mass and the opposite when normalized by SSA.
- The faster rate of nZVI oxidation allows for early removal of aqueous Hg while ZVI would require a much longer time for oxidation and efficient removal of Hg.
- Experimental column studies have shown that the flow rate play a significant role in the efficiency of Hg removal by metallic iron particles. Unfortunately, good Hg removal is obtained at low rate such as 75 μl/min, while much higher flow rates such as 500 μl/min and up resulted in no Hg removal at all. Further studies are needed to improve Hg removal from columns using conditions that can be scaled up for industrial applications.
- The mass of nZVI that is necessary for an efficient removal of Hg is a parameter which needs to be considered. First, column entirely packed with nZVI could be expensive but at the same time result in clogging as observed by Weisner et al. (2003) using bulk ZVI.
- There is a need for a pretreatment of water due to the role of binding ligands such as dissolved organic matter, which limits Hg adsorption on oxyhydroxide layers.
- The presence of competitive cations did not significantly impact Hg adsorption and removal at tested concentrations. Further studies would be needed to test a much broader range of cation concentrations.
- Lab experiments adding iron particles to sediment slurries showed a potential for controlling Hg methylation in sediments. However, preliminary results obtained from this study need to be supplemented by further and more detailed investigations to validate this hypothesis.

Recommendations:

- All the volatilization experiments in this study were done in closed batch reactors, and further investigations are needed using open and column type conditions. However, the low rates of volatilization from batch experiments tend to suggest that this pathway may not be significant. In addition the effect of water chemistry on Hg volatilization should be investigated further as certain dissolved compounds such as humic substances can substantially increase rates of Hg volatilization (Alberts et al. 1974; Ravichandran 2004).

- Given the wide variety of chemical composition of WW, a study based on the types of WW samples would be necessary to validate the efficiency of nZVI technology.

- To efficiently account for the effect of SSA, methods should be developed to make sure that nZVI is not used as large aggregates, but well dispersed suspensions to take advantage of specific physical characteristics of nano size particles.

- Further research is needed on the release of Hg bound to complex organic constituents by use of different concentrations and types of oxidizing agents.

- Results from Hg methylation studies suggest that further research is needed to validate the hypothesis put forward in this study.

APPENDIX A
STATISTICAL ANALYSIS DATA

The statistical data for the methyl mercury experiments put forth in Chapter 5 are shown below. The t-test compares the means of two groups to assess whether there is a significant difference between the groups.

Group 1	Group 2	Pooled Standard Deviation sp	t statistic	Degrees of Freedom df	Alpha Level	Standard Table of Significance t value	Significant difference
Control	Control Trt 2	0.52	0.66	4	0.05	2.78	No
Control	Control ZVI	0.57	0.31	4	0.05	2.78	No
Control	Control nZVI	0.52	0.59	4	0.05	2.78	No
Control	Trt 1 ZVI	0.52	0.27	4	0.05	2.78	No
Control	Trt 1 nZVI	0.64	0.49	4	0.05	2.78	No
Control	Trt 2 ZVI	0.52	1.28	4	0.05	2.78	No
Control	Trt 2 nZVI	0.55	1.01	4	0.05	2.78	No
Control	Trt 3 ZVI	0.56	1.23	4	0.05	2.78	No
Control	Trt 3 nZVI	0.65	0.71	4	0.05	2.78	No
ZVI 0.5 g	ZVI 0.2 g	0.32	0.59	4	0.05	2.78	No
ZVI 0.5 g	ZVI 0.1 g	0.14	7.98	4	0.05	2.78	Yes
nZVI 0.01 g	nZVI 0.02 g	0.46	2.81	4	0.05	2.78	Yes
nZVI 0.01 g	nZVI 0.05 g	0.47	1.66	4	0.05	2.78	No
ZVI Trt 5	ZVI Trt 6	0.66	0.90	4	0.05	2.78	No
ZVI Trt 1	ZVI Trt 5	0.50	0.01	4	0.05	2.78	No
ZVI Trt 3	ZVI Trt 6	0.66	0.37	4	0.05	2.78	No
nZVI Trt 5	nZVI Trt 6	0.43	3.32	4	0.05	2.78	Yes
nZVI Trt 1	nZVI Trt 5	0.57	0.74	4	0.05	2.78	No
nZVI Trt 3	nZVI Trt 6	0.61	2.90	4	0.05	2.78	Yes

LIST OF REFERENCES

Aberg, B., Ekman, L., Falk, R., Greitz, U., Persson, G., and Snihs, J. O. (1969). "Metabolism of Methyl Mercury (203hg) Compounds in Man - Excretion and Distribution." *Archives of Environmental Health*, 19(4), 478-&.

Adams, N., Caroll, D., Madalinski, k., Rock, S., Wilson, T., and Pivetz, B. (2000). "Introduction to Phytoremediation." National Risk Management Research Laboratory. Office of Reasearch and Development.US Environmental Protection/600/R-99/107.

Alberts, J. J., Schindle.Je, Miller, R. W., and Nutter, D. E. (1974). "Elemental Mercury Evolution Mediated by Humic Acid." *Science*, 184(4139), 895-896.

Alkorta, I., and Garbisu, C. (2001). "Phytoremediation of organic contaminants in soils." *Bioresource Technology*, 79(3), 273-276.

Alowitz, M. J., and Scherer, M. M. (2002). "Kinetics of nitrate, nitrite, and Cr(VI) reduction by iron metal." *Environmental Science & Technology*, 36(3), 299-306.

Alvarez, P. J., and Illman, W. A. (2006). *Bioremediation and Natural Attenuation: Process Fundamentals and Mathematical Models*, John Wiley & Sons, Inc, Hoboken, NJ.

Amyot, M., Gill, G. A., and Morel, F. M. M. (1997). "Production and loss of dissolved gaseous mercury in coastal seawater." *Environmental Science & Technology*, 31(12), 3606-3611.

Amyot, M., Mierle, G., Lean, D. R. S., and McQueen, D. J. (1994). "Sunlight-Induced Formation of Dissolved Gaseous Mercury in Lake Waters." *Environmental Science & Technology*, 28(13), 2366-2371.

Anirudhan, T. S., Senan, P., and Unnithan, M. R. (2007). "Sorptive potential of a cationic exchange resin of carboxyl banana stem for mercury(II) from aqueous solutions." *Separation and Purification Technology*, 52(3), 512-519.

Astrup, T., Stipp, S. L. S., and Christensen, T. H. (2000). "Immobilization of chromate from coal fly ash leachate using an attenuating barrier containing zero-valent iron." *Environmental Science & Technology*, 34(19), 4163-4168.

Atia, A. A., Donia, A. M., and Elwakeel, K. Z. (2005). "Selective separation of mercury (II) using a synthetic resin containing amine and mercaptan as chelating groups." *Reactive and Functional Polymers*, 65(3), 267-275.

Atkins, P. (1994). *Physical Chemistry*, Oxford Univeristy Press.

Atwood, D. A., and Zaman, M. K. (2006). "Mercury removal from water." Recent Developments in Mercury Science, 163-182.

Bartzas, G., Komnitsas, K., and Paspaliaris, I. (2006). "Laboratory evaluation of Fe0 barriers to treat acidic leachates." *Minerals Engineering Selected papers from Processing and Disposal of Minerals Industry Wastes '05*, 19(5), 505-514.

Beijer, K., and Jernelov, A. (1979). "Methylation of mercury in aquatic environments." The Biogeochemistry of Mercury in the Environment, J. O. Nriagu, ed., Elsevier/North-Holland Biomendical Press, Amsterdam, 203-210.

Bennicelli, R., Stepniewska, Z., Banach, A., Szajnocha, K., and Ostrowski, J. (2004). "The ability of Azolla caroliniana to remove heavy metals (Hg(II), Cr(III), Cr(VI)) from municipal waste water." *Chemosphere*, 55(1), 141-146.

Benoit, J. M., Gilmour, C. C., Heyes, A., Mason, R. P., and Miller, C. L. (2003). "Geochemical and biological controls over methylmercury production and degradation in aquatic ecosystems." Biogeochemistry of Environmentally Important Trace Elements, 262-297.

Berger, C. M., Geiger, C. L., Clausen, C. A., Billow, A. M., Quinn, J. W., and Brooks, K. B. (2006). "Evaluating trichloroethylene degradation using differing nano- and micro-scale iron particles." Remediation of chlorinated and recalcitrant compounds, 2006. Proceedings of the fifth international conference on remediation of chlorinated and recalcitrant compounds, Monterey, California, 22-25 May, 2006, Battelle Press, Colombus USA, C-23.

Biernat, R. J., and Robins, R. G. (1972). "High-Temperature Potential/Ph Diagrams for Iron-Water and Iron-Water-Sulfur Systems." *Electrochimica Acta*, 17(7), 1261-&.

Bloom, N. (1989). "Determination of Picogram Levels of Methylmercury by Aqueous Phase Ethylation, Followed by Cryogenic Gas-Chromatography with Cold Vapor Atomic Fluorescence Detection." *Canadian Journal of Fisheries and Aquatic Sciences*, 46(7), 1131-1140.

Bloom, N. S. (1992). "On the Chemical Form of Mercury in Edible Fish and Marine Invertebrate Tissue." *Canadian Journal of Fisheries and Aquatic Sciences*, 49(5), 1010-1017.

Blowes, D. W., Ptacek, C. J., Benner, S. G., McRae, C. W. T., Bennett, T. A., and Puls, R. W. (2000). "Treatment of inorganic contaminants using permeable reactive barriers." *Journal of Contaminant Hydrology*, 45(1-2), 123-137.

Blowes, D. W., Ptacek, C. J., and Jambor, J. L. (1997). "In-situ remediation of Cr(VI)-contaminated groundwater using permeable reactive walls: Laboratory studies." *Environmental Science & Technology*, 31(12), 3348-3357.

Boening, D. W. (2000). "Ecological effects, transport, and fate of mercury: a general review." *Chemosphere*, 40(12), 1335-1351.

Boffetta, P., Garcia-Gomez, M., Pompe-Kirn, V., Zaridze, D., Bellander, T., Bulbulyan, M., Caballero, J. D., Ceccarelli, F., Colin, D., Dizdarevic, T., Espanol, S., Kobal, A., Petrova, N., Sallsten, G., and Merler, E. (1998). "Cancer occurrence among European mercury miners." *Cancer Causes & Control*, 9(6), 591-599.

Boffetta, P., Merler, E., and Vainio, H. (1993). "Carcinogenicity of Mercury and Mercury-Compounds." *Scandinavian Journal of Work Environment & Health*, 19(1), 1-7.

Bonzongo, J. C. J., Heim, K. J., Chen, Y. A., Lyons, W. B., Warwick, J. J., Miller, G. C., and Lechler, P. J. (1996). "Mercury pathways in the Carson River-Lahontan reservoir system, Nevada, USA." *Environmental Toxicology and Chemistry*, 15(5), 677-683.

Bostick, W. D., Shoemaker, J. L., Osborne, P. E., and Evansbrown, B. (1990). "Treatment and Disposal Options for a Heavy-Metals Waste Containing Soluble Tc-99." *Acs Symposium Series*, 422, 345-367.

Boussahel, R., Harik, D., Mammar, M., and Lamara-Mohamedl, S. (2007). "Degradation of obsolete DDT by Fenton oxidation with zero-valent iron." *Desalination*, 206(1-3), 369-372.

Cantrell, K. J., Kaplan, D. I., and Wietsma, T. W. (1995). "Zero-Valent Iron for the in-Situ Remediation of Selected Metals in Groundwater." *Journal of Hazardous Materials*, 42(2), 201-212.

Celo, V., Lean, D. R. S., and Scott, S. L. (2006). "Abiotic methylation of mercury in the aquatic environment." *Science of The Total Environment Selected papers from the 7th International Conference on Mercury as a Global Pollutant, Ljubljana, Slovenia June 27 - July 2, 2004*, 368(1), 126-137.

Chen, W., Westerhoff, P., Leenheer, J. A., and Booksh, K. (2003). "Fluorescence excitation - Emission matrix regional integration to quantify spectra for dissolved organic matter." *Environmental Science & Technology*, 37(24), 5701-5710.

Chen, Y., Bonzongo, J. C. J., Lyons, W. B., and Miller, G. C. (1997). "Inhibition of mercury methylation in anoxic freshwater sediment by group VI anions." *Environmental Toxicology and Chemistry*, 16(8), 1568-1574.

Chingombe, P., Saha, B., and Wakeman, R. J. (2005). "Surface modification and characterisation of a coal-based activated carbon." *Carbon*, 43(15), 3132-3143.

Choe, S., Chang, Y. Y., Hwang, K. Y., and Khim, J. (2000). *Chemosphere*, 41(null), 1307.

Choi, S. C., Chase, T., and Bartha, R. (1994). "Metabolic Pathways Leading to Mercury Methylation in Desulfovibrio-Desulfuricans Ls." *Applied and Environmental Microbiology*, 60(11), 4072-4077.

Clever, H. L., Johnson, S. A., and Derrick, M. E. (1985). "The Solubility of Mercury and Some Sparingly Soluble Mercury Salts in Water and Aqueous-Electrolyte Solutions." *Journal of Physical and Chemical Reference Data*, 14(3), 631-681.

Compeau, G., and Bartha, R. (1984). "Methylation and Demethylation of Mercury under Controlled Redox, Ph, and Salinity Conditions." *Applied and Environmental Microbiology*, 48(6), 1203-1207.

Compeau, G. C., and Bartha, R. (1985). "Sulfate-Reducing Bacteria - Principal Methylators of Mercury in Anoxic Estuarine Sediment." *Applied and Environmental Microbiology*, 50(2), 498-502.

Craig, P. (1986). "Organometallic Compounds in the Environment: Principles and Reactions." Organomercury Compounds in the Environment, P. Craig and H. Longman, eds., Chap 2, 65-110.

Cundy, A. B., Hopkinson, L., and Whitby, R. L. D. (2008). "Use of iron-based technologies in contaminated land and groundwater remediation: A review." *Science of The Total Environment*, In Press, Corrected Proof.

Deng, L., Fu, D. F., and Deng, N. S. (2009). "Photo-induced transformations of mercury(II) species in the presence of algae, Chlorella vulgaris." *Journal of Hazardous Materials*, 164(2-3), 798-805.

Di Natale, F., Lancia, A., Molino, A., Di Natale, M., Karatza, D., and Musmarra, D. (2006). "Capture of mercury ions by natural and industrial materials." *Journal of Hazardous Materials*, 132(2-3), 220-225.

Dong, W. M., Liang, L. Y., Brooks, S., Southworth, G., and Gu, B. H. (2009). "Roles of dissolved organic matter in the speciation of mercury and methylmercury in a contaminated ecosystem in Oak Ridge, Tennessee." *Environmental Chemistry*, 7(1), 94-102.

Dujardin, M. C., Caze, C., and Vroman, I. (2000). "Ion-exchange resins bearing thiol groups to remove mercury.: Part 1: synthesis and use of polymers prepared from thioester supported resin." *Reactive and Functional Polymers*, 43(1-2), 123-132.

Farrell, J., Kason, M., Melitas, N., and Li, T. (2000). "Investigation of the long-term performance of zero-valent iron for reductive dechlorination of trichloroethylene." *Environmental Science & Technology*, 34(3), 514-521.

Farrell, J., Wang, J. P., O'Day, P., and Conklin, M. (2001). "Electrochemical and spectroscopic study of arsenate removal from water using zero-valent iran media." *Environmental Science & Technology*, 35(10), 2026-2032.

Fendorf, S., Eick, M. J., Grossl, P., and Sparks, D. L. (1997). "Arsenate and chromate retention mechanisms on goethite .1. Surface structure." *Environmental Science & Technology*, 31(2), 315-320.

Feng, N., Bitton, G., Yeager, P., Bonzongo, J. C., and Boularbah, A. (2007). "Heavy metal removal from soils using magnetic separation: 1. Laboratory experiments." *Clean-Soil Air Water*, 35, 362-369.

Fleming, E. J., Mack, E. E., Green, P. G., and Nelson, D. C. (2006). "Mercury methylation from unexpected sources: Molybdate-inhibited freshwater sediments and an iron-reducing bacterium." *Applied and Environmental Microbiology*, 72(1), 457-464.

Gabriel, M. C., and Williamson, D. G. (2004). "Principal biogeochemical factors affecting the speciation and transport of mercury through the terrestrial environment." *Environmental Geochemistry and Health*, 26(4), 421-434.

Gao, J., Youn, S., Hovsepyan, A., Llaneza, V. L., Wang, Y., Bitton, G., and Bonzongo, J. C. J. (2009). "Dispersion and Toxicity of Selected Manufactured Nanomaterials in Natural River Water Samples: Effects of Water Chemical Composition." *Environmental Science & Technology*, 43(9), 3322-3328.

Gardfeldt, K., Munthe, J., Stromberg, D., and Lindqvist, O. (2003). "A kinetic study on the abiotic methylation of divalent mercury in the aqueous phase." *The Science of The Total Environment Pathways and processes of mercury in the environment. Selected papers presented at the sixth International Conference on Mercury as Global Pollutant, Minamata, Japan, Oct. 15-19, 2001*, 304(1-3), 127-136.

Gavaskar, A. R. (1999). "Design and construction techniques for permeable reactive barriers." *Journal of Hazardous Materials*, 68(1-2), 41-71.

Gillham, R. W., and Ohannesin, S. F. (1994). "Enhanced Degradation of Halogenated Aliphatics by Zero-Valent Iron." *Ground Water*, 32(6), 958-967.

Gilmour, C. C., and Henry, E. A. (1991). "Mercury Methylation in Aquatic Systems Affected by Acid Deposition." *Environmental Pollution*, 71(2-4), 131-169.

Gilmour, C. C., and Henry, E. A. (1992). "Mercury Methylation by Sulfate-Reducing Bacteria - Biogeochemical and Pure Culture Studies." *Abstracts of Papers of the American Chemical Society*, 203, 140-GEOC.

Givelet, N., Roos-Barraclough, F., Goodsite, M. E., Cheburkin, A. K., and Shotyk, W. (2004). "Atmospheric mercuty accumulation rates between 5900 and 800 calibrated years BP in the high Artic of Canada recorded by peat hummocks." *Environmental Science & Technology*, 38(19), 4964-4972.

Gomez-Serrano, V., Macias-Garcia, A., ESPINOSA-MANSILLA, A., and VALENZUELA-CALAHORRO, C. (1998). "Adsorption of mercury, cadmium and lead from aqueous solution on heat treated and sulphurized activated carbon." *Water Research*, 32(1), 1-4.

Gu, B., Liang, L., Dickey, M. J., Yin, X., and Dai, S. (1998). "Reductive precipitation of uranium(VI) by zero-valent iron." *Environmental Science & Technology*, 32(21), 3366-3373.

Gu, B., Phelps, T. J., Liang, L., Dickey, M. J., Roh, Y., Kinsall, B. L., Palumbo, A. V., and Jacobs, G. K. (1999). "Biogeochemical dynamics in zero-valent iron columns: Implications for permeable reactive barriers." *Environmental Science & Technology*, 33(13), 2170-2177.

Gustin, M. S., Chavan, P. V., Dennett, K. E., Donaldson, S., Marchand, E., and Fernanadez, G. (2006). "Use of constructed wetlands with four different experimental designs to assess the potential for methyl and total Hg outputs." *Applied Geochemistry Mercury: Distribution, Transport, and Geochemical and Microbial Transformations from Natural and Anthropogenic Sources*, 21(11), 2023-2035.

Hagare, P., Thiruvenkatachari, R., and Ngo, H. H. (2001). "A feasibility study of using hematite to remove dissolved organic carbon in water treatment." *Separation Science and Technology*, 36(11), 2547 - 2559.

Han, S., Obraztsova, A., Pretto, P., Deheyn, D. D., Gieskes, J., and Tebo, B. M. (2008). "Sulfide and iron control on mercury speciation in anoxic estuarine sediment slurries." *Marine Chemistry*, 111(3-4), 214-220.

Hanlon, J. (2007). "Analytical Methods for Mercury in National Pollutant Discharge Elimination Systems (NPDES) Permits." O. o. W. Management, ed., US EPA.

Harmon, S. M., King, J. K., Gladden, J. B., Chandler, G. T., and Newman, L. A. (2004). "Methylmercury formation in a wetland mesocosm amended with sulfate." *Environmental Science & Technology*, 38(2), 650-656.

Harmon, S. M., King, J. K., Gladden, J. B., and Newman, L. A. (2007). "Using sulfate-amended sediment slurry batch reactors to evaluate mercury methylation." *Archives of Environmental Contamination and Toxicology*, 52(3), 326-331.

Hawkins, W. B., Rodgers, J. H., Gillespie, W. B., Dunn, A. W., Dorn, P. B., and Cano, M. L. (1997). "Design and Construction of Wetlands for Aqueous Transfers and Transformations of Selected Metals." *Ecotoxicology and Environmental Safety*, 36(3), 238-248.

Hepler, L. G., and Olofsson, G. (1975). "Mercury - Thermodynamic Properties, Chemical-Equilibria, and Standard Potentials." *Chemical Reviews*, 75(5), 585-602.

Hinton, J. J., Veiga, M. M., and Beinhoff, C. (2003). "Women, mercury and artisanal gold mining: Risk communication and mitigation." *Journal De Physique Iv*, 107, 617-620.

Hoch, L. B., Mack, E. J., Hydutsky, B. W., Hershman, J. M., Skluzacek, I. M., and Mallouk, T. E. (2008). "Carbothermal synthesis of carbon-supported nanoscale zero-valent iron particles for the remediation of hexavalent chromium." *Environmental Science & Technology*, 42(7), 2600-2605.

Hovsepyan, A., and Bonzongo, J. C. J. (2009). "Aluminum drinking water treatment residuals (Al-WTRs) as sorbent for mercury: Implications for soil remediation." *Journal of Hazardous Materials*, 164(1), 73-80.

Hsu-Kim, H., and Sedlak, D. L. (2005). "Similarities between inorganic sulfide and the strong Hg(II) - Complexing ligands in municipal wastewater effluent." *Environmental Science & Technology*, 39(11), 4035-4041.

Huang, Y. H., and Zhang, T. C. (2005). "Effects of dissolved oxygen on formation of corrosion products and concomitant oxygen and nitrate reduction in zero-valent iron systems with or without aqueous Fe2+." *Water Research*, 39(9), 1751-1760.

Huang, Y. H., Zhang, T. C., Shea, P. J., and Comfort, S. D. (2003). "Effects of oxide coating and selected cations on nitrate reduction by iron metal." *Journal of Environmental Quality*, 32(4), 1306-1315.

Hylander, L. D., Grohn, J., Tropp, M., Vikstrom, A., Wolpher, H., de Castro e Silva, E., Meili, M., and Oliveira, L. J. (2006). "Fish mercury increase in Lago Manso, a new hydroelectric reservoir in tropical Brazil." *Journal of Environmental Management Mercury cycling in contaminated tropical non-marine ecosystems*, 81(2), 155-166.

Jay, J. A., Murray, K. J., Gilmour, C. C., Mason, R. P., Morel, F. M. M., Roberts, A. L., and Hemond, H. F. (2002). "Mercury methylation by Desulfovibrio desulfuricans ND132 in the presence of polysulfides." *Applied and Environmental Microbiology*, 68(11), 5741-5745.

Jensen, S., and Jernelov, A. (1969). "Biological Methylation of Mercury in Aquatic Organisms." *Nature*, 223(5207), 753-&.

Jing, Y. D., He, Z. L., and Yang, X. E. (2007). "Effects of pH, organic acids, and competitive cations on mercury desorption in soils." *Chemosphere*, 69(10), 1662-1669.

Junyapoon, S. (2005). "Use of Zero-Valent Iron for Wastewater Treatment." *KMITL Sci. Tech. J.*, 5(3), 587-595.

Kamal, M., Ghaly, A. E., Mahmoud, N., and Cote, R. (2004). "Phytoaccumulation of heavy metals by aquatic plants." *Environment International*, 29(8), 1029-1039.

Kanel, S. R., Greneche, J. M., and Choi, H. (2006). "Arsenic(V) removal kom groundwater using nano scale zero-valent iron as a colloidal reactive barrier material." *Environmental Science & Technology*, 40(6), 2045-2050.

Kanel, S. R., Manning, B., Charlet, L., and Choi, H. (2005). "Removal of arsenic(III) from groundwater by nanoscale zero-valent iron." *Environmental Science & Technology*, 39(5), 1291-1298.

Kenneke, J. F., and McCutcheon, S. C. (2003). "Use of pretreatment zones and zero-valent iron for the remediation of chloroalkenes in an oxic aquifer." *Environmental Science & Technology*, 37(12), 2829-2835.

Kerin, E. J., Gilmour, C. C., Roden, E., Suzuki, M. T., Coates, J. D., and Mason, R. P. (2006). "Mercury methylation by dissimilatory iron-reducing bacteria." *Applied and Environmental Microbiology*, 72(12), 7919-7921.

Khudenko, B. M., and Garciapastrana, A. (1987). "Temperature Influence on Absorption and Stripping Processes." *Water Science and Technology*, 19(5-6), 877-888.

Kim, J. P. (1995). "Methylmercury in Rainbow-Trout (Oncorhynchus-Mykiss) from Lakes Okareka, Okaro, Rotomahana, Rotorua and Tarawera, North-Island, New-Zealand." *Science of the Total Environment*, 164(3), 209-219.

King, J. K., Harmon, S. M., Fu, T. T., and Gladden, J. B. (2002). "Mercury removal, methylmercury formation, and sulfate-reducing bacteria profiles in wetland mesocosms." *Chemosphere*, 46(6), 859-870.

Koeber, R., Welter, E., Ebert, M., and Dahmke, A. (2005). "Removal of arsenic from groundwater by zerovalent iron and the role of sulfide." *Environmental Science & Technology*, 39(20), 8038-8044.

Krauskopf, K. B., and Bird, D. K. (1995). *Introduction to Geochemistry, 3rd*, McGraw Hill.

Lalonde, J. D., Amyot, M., Orvoine, J., Morel, F. M. M., Auclair, J. C., and Ariya, P. A. (2004). "Photoinduced oxidation of Hg-0 (aq) in the waters from the St. Lawrence estuary." *Environmental Science & Technology*, 38(2), 508-514.

Leonhauser, J., Rohricht, M., Wagner-Dobler, I., and Deckwer, W. D. (2006). "Reaction engineering aspects of microbial mercury removal." *Engineering in Life Sciences*, 6(2), 139-148.

Li, L., Fan, M. H., Brown, R. C., Van Leeuwen, J. H., Wang, J. J., Wang, W. H., Song, Y. H., and Zhang, P. Y. (2006a). "Synthesis, properties, and environmental applications of nanoscale iron-based materials: A review." *Critical Reviews in Environmental Science and Technology*, 36(5), 405-431.

Li, S. J., Li, T. L., Xiu, Z. M., and Jin, Z. H. (2008). "Reduction and immobilization of chromium(VI) by nano-scale Fe-0 particles supported on reproducible PAA/PVDF membrane." *Journal of Environmental Monitoring*, 12(5), 1153-1158.

Li, X. Q., Elliott, D. W., and Zhang, W. X. (2006b). "Zero-valent iron nanoparticles for abatement of environmental pollutants: Materials and engineering aspects." *Critical Reviews in Solid State and Materials Sciences*, 31(4), 111-122.

Lien, H.-L., and Wilkin, R. T. (2005a). "High-level arsenite removal from groundwater by zero-valent iron." *Chemosphere*, 59(3), 377-386.

Lien, H. L., and Wilkin, R. T. (2005b). "High-level arsenite removal from groundwater by zero-valent iron." *Chemosphere*, 59(3), 377-386.

Lin, C. J., and Pehkonen, S. O. (1998). "Oxidation of elemental mercury by aqueous chlorine (HOCl/OCl-): Implications for tropospheric mercury chemistry." *Journal of Geophysical Research-Atmospheres*, 103(D21), 28093-28102.

Lin, C. J., and Pehkonen, S. O. (1999). "The chemistry of atmospheric mercury: a review." *Atmospheric Environment*, 33(13), 2067-2079.

Loux, N. T. (2004). "A critical assessment of elemental mercury air/water exchange parameters." *Chemical Speciation and Bioavailability*, 16(4), 127-138.

Majewski, P. (2006). "Nanomaterials for Watertreatment." Nanomaterials-Toxicity, Health, and Environmetal Issues, C. S. S. R. Kumar, ed., Wiley-VCH Verlag GmbH & Co, Weinheim, 211-233.

Manning, B. A., Kiser, J. R., Kwon, H., and Kanel, S. R. (2007). "Spectroscopic investigation of Cr(III)- and Cr(VI)-treated nanoscale zerovalent iron." *Environmental Science & Technology*, 41(2), 586-592.

Matheson, L. J., and Tratnyek, P. G. (1994). "Reductive Dehalogenation of Chlorinated Methanes by Iron Metal." *Environmental Science & Technology*, 28(12), 2045-2053.

McRae, C. W. T., Blowes, D. W., and Ptacek, C. J. (1997). "Laboratory-scale investigation of As and Se using iron oxides." *Proc. Sixth Symposium and Exhibition on Groundwater and Soil Remediation*, 167-168.

Mehrotra, A., and Sedlak, D. (2005). "Decrease in Net Mercury Methylation Rates Following Iron Amendment to Anoxic Wetland Sediment Slurries." *Environmental Science & Technology*, 39(8), 2564-2570.

Miller, C. L., Mason, R. P., Gilmour, C. C., and Heyes, A. (2007). "Influence of dissolved organic matter on the complexation of mercury under sulfidic conditions." *Environmental Toxicology and Chemistry*, 26(4), 624-633.

Miller, C. L., Southworth, G., Brooks, S., Liang, L. Y., and Gu, B. H. (2009). "Kinetic controls on the complexation between mercury and dissolved organic matter in a contaminated environment." *Environmental Science & Technology*, 43(22), 8548-8553.

Mohapatra, M., Rout, K., Gupta, S. K., Singh, P., Anand, S., and Mishra, B. K. (2010). "Facile synthesis of additive-assisted nano goethite powder and its application for fluoride remediation." *Journal of Nanoparticle Research*, 12(2), 681-686.

Mondal, K., Jegadeesan, G., and Lalvani, S. B. (2004). "Removal of selenate by Fe and NiFe nanosized particles." *Industrial & Engineering Chemistry Research*, 43(16), 4922-4934.

Monperrus, M., Tessier, E., Point, D., Vidimova, K., Amouroux, D., Guyoneaud, R., Leynaert, A., Grall, J., Chauvaud, L., Thouzeau, G., and Donard, O. F. X. (2007). "The biogeochemistry of mercury at the sediment-water interface in the Thau Lagoon. 2. Evaluation of mercury methylation potential in both surface sediment and the water column." *Estuarine, Coastal and Shelf Science Biogeochemical and contaminant cycling in sediments from a human-impacted coastal lagoon*, 72(3), 485-496.

Moraci, N., and Calabro, P. S. (2010). "Heavy metals removal and hydraulic performance in zero-valent iron/pumice permeable reactive barriers." *Journal of Environmental Management*, 91(11), 2336-2341.

Morrison, S. J., Metzler, D. R., and Carpenter, C. E. (2001). "Uranium precipitation in a permeable reactive barrier by progressive irreversible dissolution of zerovalent iron." *Environmental Science & Technology*, 35(2), 385-390.

Mulligan, C. N., Yong, R. N., and Gibbs, B. F. (2001). "An evaluation of technologies for the heavy metal remediation of dredged sediments." *Journal of Hazardous Materials*, 85(1-2), 145-163.

Nabais, J. V., Carrott, P. J. M., Carrott, M. M. L. R., Belchior, M., Boavida, D., Diall, T., and Gulyurtlu, I. (2006). "Mercury removal from aqueous solution and flue gas by adsorption on activated carbon fibres." *Applied Surface Science*, 252(17), 6046-6052.

Narr, J., Viraraghavan, T., and Jin, Y. C. (2007). "Applications of nanotechnology in water/wastewater treatment: A review." *Fresenius Environmental Bulletin*, 16(4), 320-329.

Niu, S.-F., Liu, Y., Xu, X.-H., and Lou, Z.-H. (2005). "Removal of hexavalent chromium from aqueous solution by iron nanoparticles." *J Zhejiang Univ Sci B*, 6(10), 1022-7.

Noubactep, C. (2008). "A critical review on the process of contaminant removal in Fe-0-H2O systems." *Environmental Technology*, 29(8), 909-920.

Nriagu, J. O. (1988). "A Silent Epidemic of Environmental Metal Poisoning." *Environmental Pollution*, 50(1-2), 139-161.

Nurmi, J. T., Tratnyek, P. G., Sarathy, V., Baer, D. R., Amonette, J. E., Pecher, K., Wang, C. M., Linehan, J. C., Matson, D. W., Penn, R. L., and Driessen, M. D. (2005). "Characterization and properties of metallic iron nanoparticles: Spectroscopy, electrochemistry, and kinetics." *Environmental Science & Technology*, 39(5), 1221-1230.

Oh, Y. J., Song, H., Shin, W. S., Choi, S. J., and Kim, Y. H. (2007). "Effect of amorphous silica and silica sand on removal of chromium(VI) by zero-valent iron." *Chemosphere*, 66(5), 858-865.

Pak, K. R., and Bartha, R. (1998). "Mercury methylation by interspecies hydrogen and acetate transfer between sulfidogens and methanogens." *Applied and Environmental Microbiology*, 64(6), 1987-1990.

Paquette, K. E., and Helz, G. R. (1997). "Inorganic speciation of mercury in sulfidic waters: The importance of zero-valent sulfur." *Environmental Science & Technology*, 31(7), 2148-2153.

Pearson, R. G. (1963). "Hard and Soft Acids and Bases." *Journal of the American Chemical Society*, 85(22), 3533-&.

Penichecovas, C., Alvarez, L. W., and Arguellesmonal, W. (1992). "The Adsorption of Mercuric Ions by Chitosan." *Journal of Applied Polymer Science*, 46(7), 1147-1150.

Phillips, D. H., Gu, B., Watson, D. B., Roh, Y., Liang, L., and Lee, S. Y. (2000). "Performance evaluation of a zerovalent iron reactive barrier: Mineralogical characteristics." *Environmental Science & Technology*, 34(19), 4169-4176.

Ponder, S. M., Darab, J. G., Bucher, J., Caulder, D., Craig, I., Davis, L., Edelstein, N., Lukens, W., Nitsche, H., Rao, L. F., Shuh, D. K., and Mallouk, T. E. (2001). "Surface chemistry and electrochemistry of supported zerovalent iron nanoparticles in the remediation of aqueous metal contaminants." *Chemistry of Materials*, 13(2), 479-486.

Ponder, S. M., Darab, J. G., and Mallouk, T. E. (2000). "Remediation of Cr(VI) and Pb(II) aqueous solutions using supported, nanoscale zero-valent iron." *Environmental Science & Technology*, 34(12), 2564-2569.

Powell, R. M., Puls, R. W., Hightower, S. K., and Sabatini, D. A. (1995). "Coupled Iron Corrosion and Chromate Reduction - Mechanisms for Subsurface Remediation." *Environmental Science & Technology*, 29(8), 1913-1922.

Puls, R. W., Paul, C. J., and Powell, R. M. (1999). "The application of in situ permeable reactive (zero-valent iron) barrier technology for the remediation of chromate-contaminated groundwater: a field test." *Applied Geochemistry*, 14(8), 989-1000.

Rangsivek, R., and Jekel, M. R. (2005). "Removal of dissolved metals by zero-valent iron (ZVI): Kinetics, equilibria, processes and implications for stormwater runoff treatment." *Water Research*, 39(17), 4153-4163.

Raposo, R. R., Melendez-Hevia, E., and Spiro, M. (2000). "Autocatalytic formation of colloidal mercury in the redox reaction between Hg2+ and Fe2+ and between Hg22+ and Fe2+." *Journal of Molecular Catalysis A: Chemical*, 164(1-2), 49-59.

Ravichandran, M. (2004). "Interactions between mercury and dissolved organic matter - a review." *Chemosphere*, 55(3), 319-331.

Reynolds, R. L., Fishman, N. S., Wanty, R. B., and Goldhaber, M. B. (1990). "Iron Sulfide Minerals at Cement Oil-Field, Oklahoma - Implications for Magnetic Detection of Oil-Fields." *Geological Society of America Bulletin*, 102(3), 368-380.

Ritter, K., Odziemkowski, M. S., Simpgraga, R., Gillham, R. W., and Irish, D. E. (2003). "An in situ study of the effect of nitrate on the reduction of trichloroethylene by granular iron." *Journal of Contaminant Hydrology*, 65(1-2), 121-136.

Rumbold, D. G., and Fink, L. E. (2006). "Extreme spatial variability and unprecedented methylmercury concentrations within a constructed wetland." *Environmental Monitoring and Assessment*, 112(1-3), 115-135.

Sanchez, I., Stuber, F., Font, J., Fortuny, A., Fabregat, A., and Bengoa, C. (2007). "Elimination of phenol and aromatic compounds by zero valent iron and EDTA at low temperature and atmospheric pressure." *Chemosphere*, 68(2), 338-344.

Sanemasa, I. (1975). "Solubility of Elemental Mercury-Vapor in Water." *Bulletin of the Chemical Society of Japan*, 48(6), 1795-1798.

Sarathy, V., Salter, A. J., Nurmi, J. T., Johnson, G. O., Johnson, R. L., and Tratnyek, P. G. (2010). "Degradation of 1,2,3-Trichloropropane (TCP): Hydrolysis, Elimination, and Reduction by Iron and Zinc." *Environmental Science & Technology*, 44(2), 787-793.

Sarkar, D., Essington, M. E., and Misra, K. C. (2000). "Adsorption of mercury(II) by kaolinite." *Soil Science Society of America Journal*, 64(6), 1968-1975.

Sayles, G. D., You, G. R., Wang, M. X., and Kupferle, M. J. (1997). "DDT, DDD, and DDE dechlorination by zero-valent iron." *Environmental Science & Technology*, 31(12), 3448-3454.

Schluter, K. (2000). "Review: evaporation of mercury from soils. An integration and synthesis of current knowledge." *Environmental Geology*, 39(3-4), 249-271.

Schnoor, J. (1997). "Phytoremediation, Technology Evaluation Report." *Groundwater Remediation Technologies Analysis Center*, TE-98-01, 1-30.

Schroeder, W., Lindqvist, O., Munthe, J., and Xiao, Z. F. (1992). "Volatilization of Mercury from Lake Surfaces." *Science of the Total Environment*, 125, 47-66.

Service, R. F. (1998). "Superstrong nanotubes show they are smart, too." *Science*, 281(5379), 940-942.

Sharma, A., Verma, N., Sharma, A., Deva, D., and Sankararamakrishnan, N. (2010). "Iron doped phenolic resin based activated carbon micro and nanoparticles by milling: Synthesis, characterization and application in arsenic removal." *Chemical Engineering Science*, 65(11), 3591-3601.

Shon, H. K., Vigneswaran, S., and Snyder, S. A. (2006). "Effluent organic matter (EfOM) in wastewater: Constituents, effects, and treatment." *Critical Reviews in Environmental Science and Technology*, 36(4), 327-374.

Simon, F. G., Segebade, C., and Hedrich, M. (2003). "Behaviour of uranium in iron-bearing permeable reactive barriers: investigation with U-237 as a radioindicator." *Science of the Total Environment*, 307(1-3), 231-238.

Skinner, K., Wright, N., and Porter-Goff, E. (2007). "Mercury uptake and accumulation by four species of aquatic plants." *Environmental Pollution*, 145(1), 234-237.

Skogerboe, R. K., and Wilson, S. A. (1981). "Reduction of ionic species by fulvic acid." *Analytical Chemistry*, 53(2), 228-232.

Slowey, A. J., and Brown, J., Gordon E. (2007). "Transformations of mercury, iron, and sulfur during the reductive dissolution of iron oxyhydroxide by sulfide." *Geochimica et Cosmochimica Acta*, 71(4), 877-894.

Steffen, A., Douglas, T., Amyot, M., Ariya, P., Aspmo, K., Berg, T., Bottenheim, J., Brooks, S., Cobbett, F., Dastoor, A., Dommergue, A., Ebinghaus, R., Ferrari, C., Gardfeldt, K., Goodsite, M. E., Lean, D., Poulain, A. J., Scherz, C., Skov, H., Sommar, J., and Temme, C. (2008). "A synthesis of atmospheric mercury depletion event chemistry in the atmosphere and snow." *Atmospheric Chemistry and Physics*, 8(6), 1445-1482.

Stumm, W., and Morgan, J. J. (1996). "Aquatic Chemistry-Chemical Equilibria and Rates in Natural Waters." Wiley Interscience, New York, Ch 10.

Su, C. M., and Puls, R. W. (2001). "Arsenate and arsenite removal by zerovalent iron: Kinetics, redox transformation, and implications for in situ groundwater remediation." *Environmental Science & Technology*, 35(7), 1487-1492.

Su, C. M., and Puls, R. W. (2003). "In situ remediation of arsenic in simulated groundwater using zerovalent iron: Laboratory column tests on combined effects of phosphate and silicate." *Environmental Science & Technology*, 37(11), 2582-2587.

Till, B. A., Weathers, L. J., and Alvarez, P. J. J. (1998). "Fe(0)-supported autotrophic denitrification." *Environmental Science & Technology*, 32(5), 634-639.

Uchimiya, M., and Stone, A. T. (2009). "Reversible redox chemistry of quinones: Impact on biogeochemical cycles." *Chemosphere*, 77(4), 451-458.

Ullrich, S. M., Tanton, T. W., and Abdrashitova, S. A. (2001). "Mercury in the aquatic environment: A review of factors affecting methylation." *Critical Reviews in Environmental Science and Technology*, 31(3), 241-293.

US.EPA. (1997). "Mercury Study Report to Congress." US EPA, Washington DC.

US.EPA. (2005). "Clean Air Mercury Rule." US EPA.

Valenzuela, A., and Ftyas, K. (2002). "Mercury Management in Small-Scale Mining." *Minig Environmental Management*, 6(10).

W.H.O. (1990). "Environmental Criteria 101: Methylmercury." World Health Organization, Geneva, Switzerland.

W.H.O. (1991). " Inorganic Mercury. Environmental Health Criteria. ." World Health Organization Geneva, Switzerland.

Wang, Q., Kim, D., Dionysiou, D., Sorial, G., and Timberlake, D. (2004). "Sources and Remediation for Mercury Contamination in Aquatic Systems - A Literature Review." *Environmental Pollution*, 131, 323-336.

Warner, K. A., Bonzongo, J.-C. J., Roden, E. E., Ward, G. M., Green, A. C., Chaubey, I., Lyons, W. B., and Arrington, D. A. (2005). "Effect of watershed parameters on mercury distribution in different environmental compartments in the Mobile Alabama River Basin, USA." *Science of The Total Environment*, 347(1-3), 187-207.

Warner, K. A., Roden, E. E., and Bonzongo, J. C. (2004). "Microbial mercury transformation in anoxic freshwater sediments under iron-reducing and other electron-accepting conditions (vol 37, pg 2153, 2003)." *Environmental Science & Technology*, 38(1), 352-352.

Watras, C. J., Bloom, N. S., Claas, S. A., Morrison, K. A., Gilmour, C. C., and Craig, S. R. (1995). "Methylmercury Production in the Anoxic Hypolimnion of a Dimictic Seepage Lake." *Water Air and Soil Pollution*, 80(1-4), 735-745.

Weber, J. H. (1993). "Review of possible paths for abiotic methylation of mercury(II) in the aquatic environment." *Chemosphere*, 26(11), 2063-2077.

Weisener, C. G., Sale, K. S., Smyth, D. J. A., and Blowes, D. W. (2005). "Field column study using zerovalent iron for mercury removal from contaminated groundwater." *Environmental Science & Technology*, 39(16), 6306-6312.

Westerhoff, P., and James, J. (2003). "Nitrate removal in zero-valent iron packed columns." *Water Research*, 37(8), 1818-1830.

Wilkin, R. T., and McNeil, M. S. (2003). "Laboratory evaluation of zero-valent iron to treat water impacted by acid mine drainage." *Chemosphere*, 53(7), 715-725.

Wilkin, R. T., Su, C. M., Ford, R. G., and Paul, C. J. (2005a). "Chromium-removal processes during groundwater remediation by a zerovalent iron permeable reactive barrier." *Environmental Science & Technology*, 39(12), 4599-4605.

Wilkin, R. T., Su, C. M., Ford, R. G., and Paul, C. J. (2005b). "Long-term geochemical behavior of a zerovalent iron permeable reactive barrier for the treatment of hexavalent chromium in groundwater." *Geochimica Et Cosmochimica Acta*, 69(10), A264-A264.

Xu, Y. H., and Zhao, D. Y. (2007). "Reductive immobilization of chromate in water and soil using stabilized iron nanoparticles." *Water Research*, 41(10), 2101-2108.

Yang, G. C. C., and Lee, H. L. (2005). "Chemical reduction of nitrate by nanosized iron: Kinetics and pathways." *Water Research*, 39(5), 884-894.

Yin, C. Y., Aroua, M. K., and Daud, W. M. A. W. (2007). "Review of modifications of activated carbon for enhancing contaminant uptakes from aqueous solutions." *Separation and Purification Technology*, 52(3), 403-415.

Yuan, C., and Lien, H. L. (2006). "Removal of arsenate from aqueous solution using nanoscale iron particles." *Water Quality Research Journal of Canada*, 41(2), 210-215.

Zavoda, J., Cutright, T., Szpak, J., and Fallon, E. (2001). "Uptake, selectivity, and inhibition of hydroponic treatment of contaminants." *Journal of Environmental Engineering-Asce*, 127(6), 502-508.

Zhang, H., Jin, Z. H., Han, L., and Qin, C. H. (2006). "Synthesis of nanoscale zero-valent iron supported on exfoliated graphite for removal of nitrate." *Transactions of Nonferrous Metals Society of China*, 16, S345-S349.

Zhang, H., and Lindberg, S. E. (2001). "Sunlight and iron(III)-induced photochemical production of dissolved gaseous mercury in freshwater." *Environmental Science & Technology*, 35(5), 928-935.

Zhang, W. X. (2003). "Nanoscale iron particles for environmental remediation: An overview." *J. Nanopart. Res.*, 5(null), 323.

BIOGRAPHICAL SKETCH

Julianne D Vernon was born in the Bronx, NY USA in 1981. She received her bachelor's degree at The City College of New York in chemical engineering. After which she worked for the New York City Department of Environmental Protection as a Process Engineer in the Bureau of Wastewater. After which, she received her doctorate of philosophy in Environmental Engineering at the University of Florida under the guidance of Dr. Jean Claude Bonzongo in Spring 2010.